

Thesis in the master's course Biotechnology, presented to the
Universidade do Algarve, Faculdade de Ciências e Tecnologia
in cooperation with Necton S.A.

**Environmental and nutritional parameters
influencing the growth of *Skeletonema* cultures
and optimization of the large-scale production
in photobioreactors**

Sarah Josenhans, 60163

Supervised by Prof. Sara Raposo

and Dr. Hugo Pereira

SARAH JOSEHANS 60163

**Environmental and nutritional parameters influencing
the growth of *Skeletonema* sp. cultures and
optimization of the large-scale production
in photobioreactors**

Master's course Biotechnology

The work was supervised by

Prof. Sara Raposo and Dr. Hugo Pereira



UNIVERSIDADE DO ALGARVE

Faculdade de Ciências e Tecnologia

in cooperation with Necton S.A.

Lecture year 2018-19

**ENVIRONMENTAL AND NUTRITIONAL PARAMETERS INFLUENCING THE GROWTH OF
SKELETONEMA SP. CULTURES AND OPTIMIZATION OF THE LARGE-SCALE PRODUCTION
IN PHOTOBIOREACTORS**

Declaração de autoria de trabalho

Declaro ser o autor deste trabalho, que é original e inédito. Autores e trabalhos consultados estão devidamente citados no texto e constam da listagem de referências incluída.

Copyright

A Universidade do Algarve reserva para si o direito, em conformidade com o disposto no Código do Direito de Autor e dos Direitos Conexos, de arquivar, reproduzir e publicar a obra, independentemente do meio utilizado, bem como de a divulgar através de repositórios científicos e de admitir a sua cópia e distribuição para fins meramente educacionais ou de investigação e não comerciais, conquanto seja dado o devido crédito ao autor e editor respetivos.

Acknowledgements

Soli Deo Gloria

This work was not possible without the help of many people, who I appreciate a lot. I'd like to acknowledge my supervisors first. Professora Sara Raposo prepared my degree well with her lecture and helped me to make this a well-constructed work. Hugo Pereira elaborated the experimental design and through his comments and critic I could improve a lot. The whole team of Necton supported my research and made me e good time during the internship by being open for my questions and always having some jokes, no matter how hard or green the work was. A special attention I want to give to Ana and Tânia, from whom I learned immensely in the lab. Mariana and Hélia were a great scientific backup. The biochemical analyses were supported by Ana and Brigida (CIMA-UAlg), as well as the lab of the CCMAR. This thesis wasn't possible without Inês, who introduced me to the work, explained software, organized material, was an example in her working attitude that I never came up to and answered my questions without hesitation from the first to the last moment during the whole year.

I am glad for the whole experience and the privilege to take a master course at the UAlg in Portugal. My classmates made me a good company. My professors had a positive attitude towards me, what encouraged me from the first semester until handing in this thesis.

Outside of the university in the GBU and the IEB Loulé I found real friends like a family, making it possible to enjoy the stay far from home. I believe that their prayers supported me in intense phases of work and study.

My German friends, family and fiancé waited for me patiently and gave me the freedom I needed.

Abstract

Microalgae have a large variety of applications and their biomass can be produced in a sustainable way. The diatom genus *Skeletonema* comprises a unique biochemical composition and is already widely used in the cultivation of shrimps and molluscs. The biomass of *Skeletonema* strains is rich in essential biomolecules, including fucoxanthin and polyunsaturated fatty acids and hold a high market demand. However, the large-scale production of this species is still challenging and needs to be optimised. In this context, different trials were conducted from lab- to industrial-scale and the growth of *Skeletonema* sp. cultures was observed and evaluated. In the laboratory, using Algem[®] photobioreactors (PBRs), obtained results revealed that autumn conditions are favourable over winter conditions, and cultures with lower inoculum concentrations show a higher specific growth rate. In addition, an initial silicate concentration of at least 0.11 mM favours the growth of the culture and the species growth is tolerant to pH values within 7.0 to 8.5. After the lab-scale optimization, cultures were successfully scaled-up under outdoor conditions, using flat panel PBRs of 100 - 1000 L and later to tubular PBRs up to 19000 L. In the production PBRs, it was found that nutrient starvation impairs the physiological state of cultures and diluted cultures suffer from photoinhibition by radiation maxima of 1500 $\mu\text{mol m}^{-2} \text{s}^{-1}$. A maximal daily growth rate of 0.331 d^{-1} was observed in a tubular PBR, exposed to an average radiation and temperature of 521 $\mu\text{mol m}^{-2} \text{s}^{-1}$ and 15.24 °C, respectively. The average macronutrient composition of *Skeletonema* sp. biomass as percentage of dry weight was 20.88 % carbohydrates, 31.52 % proteins and 18.14 % lipids. Overall, the lab-scale optimization and large-scale production of *Skeletonema* was successfully achieved and the biochemical composition of the biomass seems favourable for the nutrition of aquaculture organisms.

Keywords

Microalgae, diatom, large-scale production, fluorometry, biochemical composition, nutraceutical

Resumo

Microalgas são os produtores primários e essenciais nos ecossistemas aquáticos. São organismos fotossintéticos eficientes. A sua biomassa tem uma variedade de aplicações e pode ser produzida de maneira sustentável. Dentro das microalgas existe o grupo único das diatomáceas, caracterizado pelo frústula de sílica. A espécie de diatomácea *Skeletonema* tem uma composição bioquímica única e é bastante usada na nutrição dos moluscos em cativeiro (por exemplo ostras), crustáceos e *Artémia*, que por sua vez são usados como fonte de alimento na aquicultura. A biomassa da estirpe *Skeletonema* é rica em biomoléculas valiosas como fucoxantina e ácidos gordos não saturados, de importância nutricional. A biomassa é importante comercialmente para a indústria cosmética e na área da medicina para o tratamento do cancro e doenças neurológicas. Algumas espécies de microalgas já são produzidas a grande escala, mas a produção da *Skeletonema* ainda demonstra dificuldades.

Dentro deste tópico, foram realizados diferentes ensaios, de escala laboratorial e outros de escala industrial, com o objetivo de otimizar a produção da biomassa da *Skeletonema* sp. O crescimento das culturas de *Skeletonema* sp. foi observado e avaliado por diferentes parâmetros, nomeadamente densidade ótica, peso seco e concentração celular. A medida de densidade ótica com uso de um espectrofotómetro é um método com protocolo bem estabelecido e rápido. Mas com algumas imprecisões, que se pode dever á pouca homogeneização da cultura ou as modificações fisiológicas da célula. O peso seco tem interesse industrial, pois representa a concentração da biomassa na cultura. Obtém-se através da filtração e secagem de um volume da cultura. A obtenção da concentração celular através da densidade ótica é uma medida mais precisa, pois só a espécie de cultivo é contada. Este método também pode medir sem precisão o peso seco quando o tamanho celular é variável. O estado fisiológico das células foi monitorizado através da observação ao microscópio e por fluorometria. A microscopia revelou que as células demonstravam estar em condição saudável, também foi observado de maneira direta a mudança na aparência. A habilidade fotossintética duma célula é avaliada pela fluorometria. O método é baseado na determinação do movimento dos eletrões durante os processos de oxidação e redução no fotossistema da célula. Após o recobro no escuro as células são expostas a uma intensidade de luz e pulso definido que ativam os aparatos fotossintéticos das células. Os parâmetros determinados foram a fluorescência mínima F_0 , que representa as células fotossintéticas ativas e a eficiência

do fotossistema II F_v/F_m , um indicador de stress da cultura. A observação por fluorometria mostra o estado fisiológico de uma célula de maneira rápida e quantitativa.

No laboratório, diferentes parâmetros de cultura foram testados com o uso de sistema de Algem[®], para inferir sobre o crescimento em condições específicas da estirpe *Skeletonema* sp. Foram testados duas estirpes específicas com as condições de temperatura e radiação da estação de outono e inverno. Num ensaio foi testado diferentes concentrações iniciais de inóculo valores de $2 \cdot 10^5$, $4 \cdot 10^5$, $6 \cdot 10^5$ e $1 \cdot 10^6$ células mL⁻¹. Concentrações de silicatos no meio testadas foram desde 0.05, 0.11, 0.22 a 0.43 mM. Os valores fisiológicos de pH de interesse foram entre o 7.0 e 8.5. Os resultados demonstraram que diferentes estirpes têm diferentes padrões de crescimento, e que a condição mais favorável para o crescimento foi o outono. Uma cultura com um valor de inóculo mais baixo mostrou um valor de crescimento específico maior. O valor F_v/F_m numa cultura com 0.05 mM de silicatos no meio, foi significativamente mais baixo, indicando falta deste elemento criando stress na cultura de células, visto que a sílica é essencial para o crescimento das diatomáceas. Uma concentração inicial de pelo menos 0.11 mM favoreceu o crescimento das culturas. A estirpe demonstrou tolerância a valores de pH entre 7.0 e 8.5.

Apos uma otimização de escala laboratorial, as culturas de *Skeletonema* sp. foram testadas com sucesso numa grande escala em condições ao ar livre, em fotobioreatores de painéis lisos de 100-1000 L. O processo de aumento para grande escala incluiu vários destes painéis, este processo demorou 28 a 73 dias. A biomassa foi produzida num fotobioreactor tubular de 10000L a 19000 L e foram armazenados em renovações semi-contínuas de meio de cultura. As culturas cresceram nos fotobioreatores tubulares até ao máximo 33 dias.

O crescimento da *Skeletonema* sp. em fotobioreatores ao ar livre foi medida através da densidade ótica e do peso seco. A observação fluorométrica deu uma avaliação exata das culturas, mostrando enfraquecimento na função de aparatos fotossintéticos das células, equivalente ao stress da cultura. No aumento da escala e na produção em fotobioreatores, o valor F_v/F_m foi reduzido na falta de nutrientes ou quando culturas mais diluídas foram expostas a valores máximos de radiação de $1500 \mu\text{mol m}^{-2} \text{s}^{-1}$. Culturas, que cresceram durante alguns dias em fotobioreatores ao ar livre não mostraram uma redução no valor F_v/F_m quando expostas a radiação, porém as culturas transferidas de laboratório há pouco tempo tendem a

sofrer mais pela radiação súbita. A observação indicou a habilidade da *Skeletonema* sp. possui para se adaptar às condições de radiação.

Um valor máximo de crescimento específico de 0.331 d^{-1} , observado num fotobioreator tubular, durante uma radiação de $521 \mu\text{mol m}^{-2} \text{ s}^{-1}$ e temperatura de $15.24 \text{ }^\circ\text{C}$. Este valor máximo foi similar aos valores médios de crescimento específico observado no sistema Algem[®]. A produtividade foi avaliada da seguinte forma: a biomassa recolhida é dividida pelo total por o tempo da produção e o volume do reator ou a sua área da produção. A média da produtividade volumétrica foi $0.034 \text{ g L}^{-1} \text{ d}^{-1}$ e a da produtividade por área é de $1.447 \text{ g m}^2 \text{ d}^{-1}$. Os valores foram parecidos aos valores de um relatório sobre a cultura da *Skeletonema* sp. na escala piloto ao ar livre. Valores da produtividade máxima foram calculados baseados na determinação diário do crescimento. A análise revelou uma grande variabilidade no próprio fotobioreator e entre os fotobioreatores conduzidos durante a época examinada. Em geral, as condições climáticas no local da produção suportaram o crescimento da *Skeletonema* sp. Em dias de radiação extremamente alta, as culturas devem ser sombreadas e arrefecidos com o objetivo de reduzir o efeito da fotoinibição. Por outro lado, o crescimento foi reduzido nos dias de baixa radiação. A produção de *Skeletonema* sp. tem de ser gerida da melhor forma para otimizar a produção da sua biomassa.

A composição média dos macronutrientes da biomassa de *Skeletonema* sp., dado em percentagem do peso seco, foi 20.88 % carboidratos, 31.52 % proteínas e 18.14 % lípidos. A espécie pode ser considerada como um alimento rico na aquacultura. Seguido a literatura, *Skeletonema* sp. contem pigmentos e ácidos gordos com aplicações importantes. A microalga tem atividade anticancerígena e neuro-protetiva. Estes factos mostraram o potencial de aplicações de alto valor.

Em suma, a otimização em ensaios laboratoriais e a produção em grande escala de *Skeletonema* sp. foi realizada com sucesso e a composição bioquímica da biomassa mostrou benefícios na alimentação e para a saúde de organismos aquáticos.

Palavras chave

Microalgas, diatomácea, produção em larga escala, fluorometria, composição bioquímica, nutracêutica

Contents

Declaração de autoria de trabalho.....	i
Copyright	ii
Acknowledgements	iii
Abstract	iv
Keywords	iv
Resumo.....	v
Palavras chave	vii
List of figures	x
List of tables	xiii
Abbreviations	xiv
1. Introduction.....	1
1.1 Microalgae.....	1
1.2 The diatom <i>Skeletonema</i>	2
1.3 Optimization of growth and biochemical composition by changed culture conditions	5
1.4 Considerations of large-scale production	8
1.5 Growth monitoring of microalgal cultures.....	11
1.6 Pulse amplitude modulated fluorometry.....	11
2. Objective of the work.....	15
3. Material and methods.....	16
3.1 Species.....	16
3.2 Medium	16
3.3 Experimental Culture Units - Algems®	16
3.4 Production Units.....	18
3.5 Growth parameter determination	20
3.6 Fluorometric measurements.....	21
3.7 Nitrate concentration.....	22
3.8 Biochemical Analysis of the Biomass.....	22
3.9 Quantitative productivity evaluation	24
3.10 Statistical Analysis	25
4. Results and Discussion	26
4.1 Laboratory trials in the Algem® system.....	26
4.2 <i>Skeletonema</i> sp. in outdoor cultivation	41
4.3 Large-scale production of <i>Skeletonema</i> sp. in tubular PBRs	44
4.4 Fluorometry evaluation of the large-scale production	48
4.5 Biochemical evaluation of large-scale production	53

5.	Conclusion and final remarks	56
5.1	Knowledge gain from laboratory trials.....	56
5.2	Experiences in outdoor production.....	56
5.3	Value of <i>Skeletonema</i> sp. biomass	56
5.4	Open questions	56
5.5	Suggestions for future research	57
5.6	Summary.....	57
6.	References.....	58
7.	Additional data	66
7.1	Chapter 4.1 Results Algem® trials	66
7.2	Chapter 4.2 <i>Skeletonema</i> sp. in outdoor cultivation.....	67
7.3	Chapter 4.3 Large-scale production of <i>Skeletonema</i> sp. in tubular photobioreactors.....	70
7.4	Chapter 4.4 Fluorometer evaluation of the large-scale production	71
7.5	Chapter: biochemical analysis	76

List of figures

Figure 3.1 Microscopic picture of <i>Skeletonema</i> sp. cells. Magnification: 40x. Single cells as well as pairs of cells after division are visible. In the separate picture the typical chain formation is displayed...	16
Figure 3.2 The Algem® system: two shaken growth chambers containing Erlenmeyer flasks, with air mixed with CO ₂ supply, probes for pH and optical density.	17
Figure 3.3 1: Flat panel photobioreactors of 100 L, 2: CO ₂ supply and air-sparkling machinery.....	19
Figure 3.4 Four tubular systems of photobioreactors. Microalgal culture is pumped through the horizontal tube. The photobioreactor at the left is without culture, the others contain culture of different species and densities.	20
Figure 3.5 Retention tanks and pumps of tubular photobioreactors. The towers at the left and right side contain the operated culture. The tank in the middle serves to hold harvested culture before being transferred through a pipeline to a centrifuge.	20
Figure 4.1 Conditions of light and temperature, set by the Algem® photobioreactor and culture growth, represented by optical density. Strains: <i>Skeletonema</i> sp. SKC0218 and SKM0118. ‘Autumn’ and ‘winter’ refer to the different profiles applied in the trial.	27
Figure 4.2 Growth rates of <i>Skeletonema</i> sp. SKC0218 and SKM0118 cultures under autumn and winter season conditions. Significant differences are indicated with different letters.....	28
Figure 4.3 Average growth of two experiments testing different inoculum concentrations on the growth of <i>Skeletonema</i> sp. The daily radiation and temperature variation are shown.	29
Figure 4.4 Overview of different fluorometry values and nitrate concentration in the medium in the first trial regarding the inoculum concentration <i>Skeletonema</i> sp. SKC0218. Samples were taken at the first and seventh day, analyses were also done at the start and the end of the experiment, after eight days.....	30
Figure 4.5 Impaired cells of <i>Skeletonema</i> sp. sampled from the Algem® system. The cells are not clearly defined, the colour is rather pale, and the cells are sticking together in an aggregate. Magnification: 40x.	31
Figure 4.6 Average growth rates of <i>Skeletonema</i> sp. in two experiments regarding the inoculum concentration. Significant differences are marked with different letters.....	33
Figure 4.7 Final dry weight of <i>Skeletonema</i> sp. cultures with different inoculum concentrations. Average of two experiments. The letters indicate no statistical differences.....	33
Figure 4.8 Average growth of <i>Skeletonema</i> sp. SKC0218 by optical density from two trials regarding initial silicate concentration, showing light and temperature profile conditions.	34
Figure 4.9 Different parameters recorded at the start, second, fourth and seventh day in the experiment regarding the silicate concentration. The graphs represent average values from two experiments. Species: <i>Skeletonema</i> sp. SKC0218.....	35
Figure 4.10 Growth rate of <i>Skeletonema</i> sp. SKC0218 cultures grown with different initial silicate concentrations. The values are calculated from the optical density and show average results from two experiments. The letters indicate no significant differences.	36
Figure 4.11 The final dry weight of <i>Skeletonema</i> sp. SKC0218 cultures growing at different initial silicate concentrations, showing average of two experiments. The letters indicate no significant differences.	36

Figure 4.12 Growth by optical density of <i>Skeletonema</i> sp. SKC0218 cultures maintained at different pH setpoints, showing light and temperature profile conditions. The graph represents the average of two experiments.	38
Figure 4.13 Different parameters recorded at the fourth, sixth, eighth and eleventh day and at the end of the experiment regarding the pH setpoint. Species: <i>Skeletonema</i> sp. SKC0218	39
Figure 4.14 Growth rate of <i>Skeletonema</i> sp. SKC0218 cultures grown at different pH setpoints. Average results from two experiments are shown. The letters indicate no significant differences.	40
Figure 4.15 Final dry weight of <i>Skeletonema</i> sp. SKC0218 cultures, grown under different pH conditions. The values show an average of two experiments. Different letters indicate significant differences.	40
Figure 4.16 Growth of <i>Skeletonema</i> sp. SKC0218 in flat panel photobioreactors (FP), used for the inoculation of a tubular photobioreactor (PBR #1). Meteorological data during the scale-up process is shown. Timespan: 20.11.2018 – 22.01.2019. Arrows indicate a culture renewal of 2000 and 5000 L, respectively.	42
Figure 4.17 Left: a <i>Ciliophora</i> and right: <i>Tetraselmis</i> sp. found as contaminants in a <i>Skeletonema</i> sp. culture.	43
Figure 4.18 Overview of the large-scale production of <i>Skeletonema</i> sp. SKC0218 in tubular photobioreactors. Timespan: 20.12.2018-26.04.2019. Thick arrows indicate culture harvest, thin arrows indicate addition of medium, explanation can be read in the additional data in Table 7.3. Augmentation of reaction volume and volume renewal was always done with sterilized seawater and medium in the same ratio as used for inoculation. Meteorological data is shown in parallel.	45
Figure 4.19 Flat panel photobioreactor, inoculated from laboratory culture at the 18.03.2019, volume 100 L. Transfer to 1000 L photobioreactor after seven days. At the seventeenth day, volume for the inoculation of another photobioreactor was used and renewed. Meteorological and fluorometry data are shown parallel with culture parameters and growth. Timespan: 18.03.-18.04.2019; Strain: <i>Skeletonema</i> sp. SKC0119.	49
Figure 4.20 Growth development of <i>Skeletonema</i> sp. SKC0218 in relation to culture parameters and fluorometry evaluation, displayed with meteorological data. Tubular photobioreactor #3, 12.02.-13.03.2019, arrows indicate addition of 500 and 2500 L medium, respectively.	52
Figure 4.21 Lyophilized biomass from <i>Skeletonema</i> sp. SKC0218 in large scale production. All samples were harvested in March, stored and lyophilized under the same conditions.	54
Figure 7.1 Overview of different fluorometry values and nitrate concentration in the medium in the second trial regarding the inoculum concentration. Analyses were done at the second, fourth and seventh day, at the end of the experiment. Species: <i>Skeletonema</i> sp. SKC0218.	66
Figure 7.2 Different parameters recorded at the second, fourth, and eighth day (the end) of the second experiment testing different pH setpoints on the growth of <i>Skeletonema</i> sp. SKC0218.	67
Figure 7.3 Meteorological data and growth of <i>Skeletonema</i> sp. in flat panel photobioreactors with 100 L volume. Timespan: 21.09.-4.10.2019, strains of <i>Skeletonema</i> sp: FP 1A: SKM0118, FP 1B: SKM0116.	68
Figure 7.4 Scale-up process of <i>Skeletonema</i> sp. SKC0218 in a tubular photobioreactor. Growth of flat panel and tubular photobioreactors in dry weight, meteorological observations are displayed in parallel. Timespan: 14.12.2018-21.02.2019. Arrows refer to operational changes and are listed in Table 7.3.	69

Figure 7.5 Growth and culture parameters of *Skeletonema* sp. SKC0119 between 5. and 16.04.2019 in a 1000 L flat panel photobioreactors. Meteorological and fluorometry values are shown in parallel. 72

Figure 7.6 Growth observations, culture parameters and fluorometry results shown in parallel with meteorological data. In both flat panel photobioreactors *Skeletonema* sp. SKC0119 was grown. Timespan: 16.-29.04.2019. FP 12: 1000 L flat panel photobioreactor, inoculated with culture of another outdoor photobioreactor. FP 13B: 100 L flat panel photobioreactor, inoculated with laboratory culture..... 74

Figure 7.7 Growth development of *Skeletonema* sp. SKC0218 in a tubular photobioreactor. Culture growth and fluorometer parameters are shown as well as meteorological data. Timespan: 11.-20.3.2019 76

Figure 7.8 Carbohydrate content in *Skeletonema* sp. SKC0218 biomass expressed as percentage of dry weight. The samples were all collected from tubular photobioreactors during the season 2018/19, kept under the same culture conditions The label indicates a sequential number of the sample, a second number refers to the batch of centrifugation, a third number to the batch of lyophilization. The growth stage of the culture in the moment of sampling is indicated: exp.: exponential phase, stat.: stationary phase, decl.: decline phase..... 77

Figure 7.9 Protein content in percentage of dry weight in *Skeletonema* sp. SKC0218 biomass. Significant differences are expressed with different letters. The label indicates a sequential number of the sample, a second number refers to the batch of centrifugation, a third number to the batch of lyophilization. The growth stage of the culture in the moment of sampling is indicated: exp.: exponential phase, stat.: stationary phase, decl.: decline phase..... 78

Figure 7.10 Lipid content in *Skeletonema* sp. SKC0218 biomass, harvested from cultures in outdoor production. The label indicates a sequential number of the sample, a second number refers to the batch of centrifugation, a third number to the batch of lyophilization. The growth stage of the culture in the moment of sampling is indicated: exp.: exponential phase, stat.: stationary phase, decl.: decline phase. FP: the sample derives from flat panel photobioreactors. There are no significant differences between the values. 78

Figure 7.11 The total ashes (inorganic matter) in the biomass of *Skeletonema* sp. SKC0218 is expressed in percentage of dry weight. The label indicates a sequential number of the sample, a second number refers to the batch of centrifugation, a third number to the batch of lyophilization. The growth stage of the culture in the moment of sampling is indicated: exp.: exponential phase, stat.: stationary phase, decl.: decline phase. FP: the sample derives from flat panel photobioreactors. There are no significant differences between the values. 79

List of tables

Table 3.1 NutriBloom plus medium elemental composition	16
Table 4.1 Productivity evaluation of <i>Skeletonema</i> sp. SKC0218 in the tubular photobioreactor #1, production from 20.12.18-22.01.19.	43
Table 4.2 Summary of the scale-up processes and harvests of <i>Skeletonema</i> sp. SKC0218 during the season 2018/29. Dates of the scale-up process as well as duration of the production in the tubular system are included. The harvested volume is the volume extracted during the production time and the final volume of the reactor.....	44
Table 4.3 Specific growth rate and productivity of all operated tubular photobioreactors with <i>Skeletonema</i> sp. SKC0218 and average values of for the season 2018/19. The volume indicates the maximum volume of an operated reactor.	46
Table 4.4 Macronutrient content in the biomass of <i>Skeletonema</i> sp. SKC0218, grown in large-scale. Average values and standard deviation from all collected samples during the season are calculated.	53
Table 7.1 Operations in production management of tubular photobioreactor #2.....	70
Table 7.2 Yielded biomass, specific growth rate and productivity parameters from the a tubular photobioreactor. The productivity parameters were calculated from the harvest yield in the production period. Species: <i>Skeletonema</i> sp. SKC0218.....	70
Table 7.3 Changes in operation management in tubular photobioreactors, referring to arrows in figure 4.18.....	71
Table 7.4 Origin of <i>Skeletonema</i> sp. SKC0218 biomass samples in biochemical analysis. A consecutive number was given to the samples, the date of harvest and originating photobioreactor are given, the growth stage of the culture at the time of harvest was estimated according to growth development.....	77

Abbreviations

DW	Dry weight, measure of biomass concentration, given in g L^{-1}
F_0	Minimum fluorescence at the dark-adapted state, fluorometric measure of the biomass
FP	Flat panel photobioreactor, supported plastic bag for microalgae cultivation
F_v/F_m	Maximum photochemical yield or efficiency of photosystem II, measure for the physiological state of a culture
OD	Optical density, measure of biomass by absorbance at a wavelength to define
PAM	Referring to pulse amplitude modulated fluorometry, a tool for the quantitative evaluation of photosynthetic processes in a cell
PAR	Photosynthetically active radiation
PBR	Photobioreactor, culture vessel in any design for phototrophic microalgal production
QY_{max}	Quantum yield, in the dark-adapted state an equivalent to F_v/F_m

1. Introduction

1.1 Microalgae

1.1.1 *Microalgae definition*

Microalgae are aquatic organisms of microscopic scale that comprise the ability of photosynthesis. This definition includes prokaryotic species such as cyanobacteria (blue-green-algae) and eukaryotic species, among others Chlorophyta (green algae), Rhodophyta (red algae), Dinoflagellata as protists and the class Bacillariophyta, that encompasses diatoms (Van Den Hoek, Mann and Jahns 1995). As primary producers they represent an essential part of the food chain in aquatic ecosystems. Several thousand species are identified and maintained in culture collections all over the world.

1.1.2 *Applications of microalgae*

The interest in this group is emerging, as microalgae can be applied in a variety of areas and produced in a sustainable manner. Since macroalgae make part of the diet in some cultures, microalgae have the potential to contribute to the nutrition of the world's population. An advantage over agriculture is that microalgae can be produced in an alternative way, not demanding arable land. The macronutrient composition allows to classify some species as good sources of carbohydrates, proteins or lipids. Regarding secondary metabolites, microalgae have a valuable fatty acid, vitamin and amino acid profile (Brown et al. 1997; Fabregas and Herrero 1986). The macro- and micronutrients contained, are beneficial for a human diet and promote animals' nutrition. A large established application of microalgae biomass is feedstock for aquaculture. They are essential for aquaculture hatcheries, as they constitute the feed for crustaceans and mollusks as well as for early larval stages of many fish, being used to enrich the live feeds traditionally used (Fabregas and Herrero 1986; Brown et al. 1997; Hannah, Mani and Ramasamy 2013). It was shown by alimending *Artemia* sp., a feedstock for shrimp and fish farming, with microalgal biomass, that the fatty acid and essential amino acid profile of their biomass was altered (Herawati, Hutabarat and Radjasa 2015).

Further, pigments from species such as *Porphyridium* and *Haematococcus* are already used as food colourings (Arad and Yaron 1992; Lorenz and Cysewski 2000). Due to the pigments and fatty acids content, microalgae or extracts of them find application in cosmetic and nutraceutical products (Stolz and Obermayer 2005). For example, phycocyanin from *Spirulina*

showed anti-oxidant and anti-viral activity (Pleonsil, Soogarun and Suwanwong 2013; Shih et al. 2003), while an ethanolic extract from *Amphora* sp. displayed antibacterial activity (Boukhris et al. 2017).

Microalgae are implemented in environmental biotechnology, reducing the nutritional charge of effluents and improving sustainability of related processes. *Chlorella* was effectively used to reduce remaining ammonia, phosphate and colour from a textile wastewater by biosorption (Lim, Chu and Phang 2010). *Chlamydomonas* was used for bioremediation of a toxic pyrolysis acetic acid-rich product and simultaneous lipid production (Liang et al. 2013). Further, working on the global aim of reducing greenhouse gases, microalgae attribute to CO₂ sequestration. Microalgal cultures can be used to fix CO₂ from flue gas, providing its compensation (Watanabe and Hall 1996). At the same time, the flue gas represents an alternative source of CO₂ (Olofsson et al. 2015). A feasibility assessment emphasizes, that only the valorization of by-products might improve the economics of the CO₂ mitigation process using microalgae (Ono and Cuello 2006).

The microalgal biomass is suitable for fermentation and as biodiesel feedstock, in this manner contributing to fulfil the increasing demand for fuel. Again, microalgae can be produced without reducing the agricultural area and so the food-or-fuel debate can be avoided. Some strains produce a significant amount of fatty acids and triacylglycerides (TAG), that can be upgraded to biodiesel (Slocombe et al. 2015). Fermentation provides methane, methanol and ethanol, that after refining or distillation can serve as biogas or bioethanol (de Farias Silva and Bertucco 2016).

1.2 The diatom *Skeletonema*

1.2.1 General information about the species *Skeletonema*

Diatoms are a eukaryotic class of microalgae with the distinct characteristic of an outer silicate frustule. It is composed of a lower and upper part, enclosing the cell like a box with a lid. Diatoms contribute to the geochemical silicate cycle in the environment: the cells take up silicate from silicate-rich water and fixate it in their frustule, residues of dead cells make up the silicate fraction of sediments. Diatoms appear with frustules in innumerable variations, which serves as an identifying feature between the different species. The reproduction of diatoms is generally asexual, whereby the new part of the shell is built up inside the mother cell, before the cells separate. The new cell is constituted of one old and one newly composed

half of the frustule. Like this, the descendant cell will be smaller after every division. At a point where no division is possible, the cell will enter a spore form and change to a sexual reproduction cycle (Godhe, Kremp and Montresor 2014). As a rough grouping, there exist pennate and centric diatoms, the criterion is a longitudinal or circular axis of cell symmetry, respectively.

Skeletonema is a cosmopolitan genus of centric diatoms, like other groups abundant in all kinds of waterbodies. These include brackish water and estuaries, *Skeletonema* sp. as euryhaline organisms tolerate a large range of salinity values (Hevia-Orube et al. 2016; Brand 1984). The species first gained attention as a being dominant in harmful algal bloom (HAB) events (Song et al. 2016). Within the genus, there are over 200 strains and 13 approved species, distinguished by details in the frustule and genetic marker in the large subunit ribosomal DNA (Sarno et al. 2005; Kooistra et al. 2008; Yamada et al. 2013; Hasle and Evensen 1976; Makarova and Proshkina-Lavrenko 1964; Sarno et al. 2007). The cells of the marine species *S. costatum* and *S. marinoi* are longish and connected to chains of up to eight cells. The size ranges from 2-5 μm in width and 5-25 μm in length (Olenina et al. 2006). The frustule is rather fragile, which needs to be considered when cultivated (Stoermer and Julius 2003). The cells' colour is brown or appears greenish at times. The species depends on a symbiotic community of bacteria, producing for example the essential vitamin B12 (Croft et al. 2005).

1.2.2 Applications of *Skeletonema* biomass according to biochemical properties and constituents

The biomass of *Skeletonema* is relatively rich in proteins, for *S. marinoi* and *S. costatum* 21-28 % and 23.3 % of dry weight (DW) are given, respectively (Olofsson et al. 2015; Houcke et al. 2017). Carbohydrates are as well high, namely 30 % and 26.4 % of DW for the two different species. The lipid content is lower, found to be 16-28 % and 16.2 % of DW, respectively. Another study about *S. costatum* reports 5-15 % lipids of DW, dependent on the growth phase (Schwenk et al. 2013). A higher value was given with 24.4 % of DW in a pilot-scale outdoor cultivation (Pérez et al. 2017).

Especially the lipid fraction of *Skeletonema* sp. is of high value, the fatty acid profile is similar to fish oil and should be seen as an alternative source for essential fatty acids (Sijtsma and De Swaaf 2004). Unsaturated fatty acids account for 82.8 % of the total fatty acid content (Houcke et al. 2017). In specific, *Skeletonema* was reported to present 41 and 7 % as percentage of the

lipids of eicosapentaenoic and docosahexaenoic acids, respectively (Servel et al. 1994). Unsaturated fatty acids are essential constituents of cell membranes and show a health benefit against cardiovascular diseases (Gill and Valivety 1997). Fatty acids with a chain length of more than ten have found to be antibacterial (Galbraith and Miller 1973).

The cells of *Skeletonema* sp. contain carotenoids, chlorophyll *a* and *c* in their chloroplast (Gao et al. 2018; Wu, Gao, and Wu 2009). For example, 0.02 % of the DW of *S. costatum* was found to be carotenoids (Pennington, Guillard and Liaaen-Jensen 1988). One valuable molecule of the carotenoids in *S. costatum* with a relevant abundance is fucoxanthin, making up 49 % to 90 % of the carotenoids or 31 $\mu\text{g (mg C)}^{-1}$ (Pennington, Guillard and Liaaen-Jensen 1988; Gilstad, Johnsen and Sakshaug 1993). Fucoxanthin, isolated from a brown algae, was shown to have anti-cancer activity (Chung et al. 2013). In an *in vitro* assay, fucoxanthin revealed antioxidant and neuroprotective activities (Alghazwi et al. 2019). Other carotenoids contained in *S. costatum* are β - β -Carotene, Diatoxanthin and Diadinoxanthin, with 8 %, 16 % and 27 % of the total carotenoids, respectively (Pennington, Guillard and Liaaen-Jensen 1988).

Vibrio, a common pathogen in fish aquaculture, is inhibited by *Skeletonema* species (Olofsson et al. 2013). An ethanolic extract from *S. costatum* effectively inhibits several *Vibrio* species (Naviner et al. 1999). A potential pharmaceutical application was shown in a zebrafish-bioassay. The nucleoside inosine in extracts from *S. marinoi* showed to be a neuroactive molecule (Brillatz et al. 2018). Further, organic extracts from *S. costatum* showed anti-tuberculosis activity (Lauritano et al. 2018).

High-grade life feed is the basis for the quality of the derived aquaculture products. Feeding *Artemia* sp., applied as aquaculture feed, with *S. costatum* increased the protein, lipid and carbohydrate content (Hannah, Mani and Ramasamy 2013). Feeding *Artemia* with *S. costatum* revealed a favourable highly unsaturated fatty acid content and essential amino-acid profile (Herawati, Hutabarat and Radjasa 2015).

Microalgae are not only feed for aquaculture, some species are applied in oyster refining. Diets containing *S. costatum* successfully altered the fatty acid profile, constituting aroma precursors, and the sensory consumer evaluation was changed (Houcke et al. 2017; Pennarun et al. 2003). The weight of oysters, due to an increased fattening index, could be augmented by a *S. costatum* supply (Soletchnik et al. 2001).

1.3 Optimization of growth and biochemical composition by changed culture conditions

Each microalgal species has individual requirements for optimal growth, regarding environmental factors, nutrient supply and cultivation conditions like mixing and aeration. Present studies about *Skeletonema* sp. cultivation cover a range of factors, define conditions for an optimal growth rate, productivity and even report altered biochemical composition of the biomass. Monitoring the photosynthesis activity allows considerations about the physiological state and optimizing the operation (Malapascua et al. 2014). If the photosynthetic apparatus of the microalgae works in an ideal way, optimal growth and productivity can be assumed.

The existence and metabolism of microalgae is based on photosynthesis. The organisms use photosynthetically active radiation (PAR), which is light at a wavelength between 400 and 700 nm. Around 45 % of the sunlight reaching the earth, constitutes the PAR fraction. The solar irradiation is expressed as power per area (W m^{-2}) and can be converted into the photon flux in $\mu\text{mol photons m}^{-2} \text{s}^{-1}$, which is relevant for photosynthesis. The light strength, composition and time of light exposure differs with the season and between geographic locations. Radiation values in the range of 400-2000 $\mu\text{mol m}^{-2} \text{s}^{-1}$ were recorded, varying between days and during the daily cycle (Masojídek et al. 2011).

S. costatum cultivated at 75 $\mu\text{mol m}^{-2} \text{s}^{-1}$ with a 12:12h light:dark cycle, shows a growth rate of 0.56 d^{-1} (Gilstad, Johnsen and Sakshaug 1993). In another study 430 $\mu\text{mol m}^{-2} \text{s}^{-1}$ were sufficient to grow laboratory cultures indoors, whereas outdoor cultures exposed to 1294 $\mu\text{mol m}^{-2} \text{s}^{-1}$ as an average value, had a growth rate of up to 0.25 d^{-1} (Pérez et al. 2017). Growth and effective quantum yield of photosystem II are negatively affected by UV-B radiation, the experiment indicates, that sunlight irradiation is only beneficial to a certain level (Wu, Gao and Wu 2009). In treatments with only UV-A or without UV radiation, the growth showed a lag phase of two days, referring to the capability of the culture to adapt with a photoprotective mechanism to given light conditions. Optimal and harmful irradiance for *S. costatum* were quantified earlier: whereas up to 2.5 doublings per day were observed at 460-630 $\mu\text{mol m}^{-2} \text{s}^{-1}$, the growth was reduced by 50 % at 2000 $\mu\text{mol m}^{-2} \text{s}^{-1}$ (Sakshaug and Andresen 1986). In another study, an irradiation with $1.6 \cdot 10^{16}$ quanta $\text{s}^{-1} \text{cm}^{-1}$ was found as optimal for *S. costatum* (Tian, Mingjiang and Peiyuan 2002).

Next to radiation, the temperature is a main influence factor on physiology of photosynthetic organisms and enzyme activity in general. Laboratory experiments were conducted at 21 °C (Bertozzini et al. 2013). In combination with other cultivation factors, 25 °C were found to be optimal (Tian, Mingjiang and Peiyuan 2002). The temperature for laboratory cultures was maintained at 24±2 °C, whereas 25±9 °C were measured for the outdoor cultivation (Pérez et al. 2017). The difference and higher deviation points to uncontrollable circumstances, regarding the temperature.

In one study, *S. costatum* grew better at 15-20 ‰ salinity than at a higher value of 25-30 ‰ (Laing 1985). In combination with different temperature and irradiance, a salinity range of 18-35 ppt was found optimal for the growth of *S. costatum* (Tian, Mingjiang and Peiyuan 2002). For another cultivation, the used sea water had a salinity of 40 psu (Pérez et al. 2017). This reflects the large tolerance regarding the salinity, that a euryhaline species carries, and makes it possible to use abundant seawater, a possibility to reduce production costs.

The pH value in microalgae cultures influences enzyme activity and in specific carbon acquisition of the culture. At low pH, CO₂ enters the cell by diffusion, at neutral pH values, CO₂ can be actively incorporated and at a higher pH and low CO₂ concentration, bicarbonate can be ingested (Colman and Rotatore 1995; Goldman 1999; Colman and Balkos 2005; Balkos and Colman 2007). Microalgae grow at physiological pH values, the optimal pH value for *S. costatum* is around 8 (Blanchemain, Grizeau and Guary 1994). In a pilot-scale production of the same species, the pH was regulated by CO₂ injection to maintain a value between 8 and 8.2 (Pérez et al. 2017). In a simultaneous experiment without CO₂ injection, the pH rose due to photosynthetic activity close to 9.5, which was considered as no drastic change.

Microalgae gain their nutrients from the culture medium. General requirements can be estimated, optimal conditions must be studied for *Skeletonema* species in specific. The nitrogen source is of enormous relevance, structural and functional biomolecules like enzymes are built of it. Commonly, nitrate (NO₃²⁻) as an inorganic source is provided. In an experiment regarding various nitrate levels it was shown, that the growth rate was 27 % higher at a nitrate level of 25 µM compared to 1-5 µM (Gao et al. 2018). It was further increased by levels of up to 100 µM but raising the nitrate level to 250 µM did not show a significant increase in the growth rate. A reduced nitrogen level combined with reduced light availability has influence on enzyme activity in *S. costatum* (Smith, Zimmerman and Alberte 1992).

Silicate limitation has a severe impact on gene expression (Lauritano et al. 2015) and enzyme activity in *Skeletonema* species (Wang et al. 2017). The growth rate of *S. marinoi* was reported as 0.88 d^{-1} under laboratory conditions (Lauritano et al. 2015). In this study, the silicate level of $107 \text{ }\mu\text{M}$ was considered as normal, reduction or complete removal lead to decreased growth rates of 0.76 and 0.16 d^{-1} , respectively. Silicate enrichment from 5-10 to 15-30 mg Si L^{-1} significantly improved *S. costatum* growth in 200 L scale experiments (Laing 1985). In a laboratory experiment with *S. marinoi*, with a high silicate treatment of $109.5 \text{ }\mu\text{M}$ silicate, a 1.5 times higher cell density was achieved compared to a medium silicate concentration of $32.5 \text{ }\mu\text{M}$. The culture with the high silicate treatment decreased in cell number after day 7, when the silicate concentration decreased to around $40 \text{ }\mu\text{M}$, which is still higher than the initial concentration in the medium silicate treatment. The cell number in the medium silicate treatment declined after day 7 as well, as the concentration was at around $3 \text{ }\mu\text{M}$. The culture in a low silicate treatment with an initial concentration of $2.5 \text{ }\mu\text{M}$ grew despite this low value for six days, but never showed as high cell numbers as the other experiments. It can be assumed, that a silicate concentration even below $2.5 \text{ }\mu\text{M}$ is sufficient to allow *Skeletonema sp.* growth, but the group comments, that silicate is the limiting factor in this case (Wang et al. 2017).

The culture conditions influence the percentage and constitution of the contained macronutrients in microalgal biomass (Taraldsvik and Mykkestad 2000; Orefice et al. 2016). In the same way, nutrient stress alters the production of secondary metabolites, such as carotenoids or vitamins (Goiris et al. 2015; Yongmanitchai and Ward 1991; Lai et al. 2011). The biochemical composition defines the quality of the microalgae biomass for specific applications. For aquaculture feedstock, it means the composition of macronutrients, the percentage of distinct essential fatty acids or the carbohydrate species in the microalgal biomass influence growth and development of the feeding animals (Leonardos and Lucas 2000; D'Souza and Loneragan 1999; Houcke et al. 2017).

The presence of highly valuable molecules in *Skeletonema sp.* biomass with an abundance of health promoting applications for human and animals motivates to improve the production of this rarely cultivated species. The production of microalgae not only needs to be augmented in terms of biomass, but to be optimized regarding the biochemical profile, as this determines the value of the product.

1.4 Considerations of large-scale production

1.4.1 *Microalgae production*

Microalgae are produced in so called photobioreactors (PBRs) of manifold design. Basic requirements of microalgae are an aquatic culture medium with adequate salinity and pH value. Essential nutrients are carbon, nitrogen and phosphorus; for diatoms as well silicate. Culture media recipes are applied for a long time to grow different species and some formula are commercialized (Guillard and Ryther 1962; Harrison, Waters and Taylor 1980). Still, the macro- and micronutrient composition can be adapted for individual species. The form of the carbon source depends on the metabolism of the species. For photoautotrophic species it is most common to supply the culture with CO₂ together with the aeration, less common is to provide dissolved bicarbonate. Heterotrophic organisms can be fed with different organic carbon molecules.

A major motivation for microalgae production is the utilization of the natural and abundant sunlight. The photosynthetic organisms use the energy input by irradiation for growth and metabolism. The PBRs are constructed in a way to expose them to sunlight and provide movement of the culture (Silva Benavides et al. 2013; Vejrazka et al. 2012; Chini Zittelli, Rodolfi and Tredici 2003). In a homogenous suspension, sufficient gas exchange, nutrient and light availability is given. Microalgal cultures can be shaken, mixed by air bubbles, baffles or pumps. The manner and force of mixing the culture must consider fragility of species (Tredici et al. 2016). Highly concentrated cultures impair photosynthetic activity, whereas diluted cultures are less productive. Optimization of microalgae production is complex, as the species have individual preferences. This includes the ability to grow at reduced sunlight input or a tolerance to high irradiation. Some will suffer easily from photoinhibition and different temperatures are preferred by different species.

A delicate step is the scale-up process, when a microalgal culture cultivated in the laboratory is transferred to an outdoor PBR. Later, the volume is increased and eventually the design of the PBRs changed. Conditions cannot be maintained identical in different systems. It must be observed, if a certain species requires constant renewal of medium or the culture vessel to avoid the accumulation of residues or bacteria. Some species are well suitable for continuous production, for other reasons the batch mode will be recommended in some cases. Outdoor

cultivation is not sterile. Other aquatic microorganisms compete for nutrients and sunlight and there are predator species of the cultivated microalgae.

Later considerations of microalgae cultivation include the downstream processing, this means the harvesting and preservation processes. Most common is a concentration of the biomass by centrifugation or ultrafiltration. In alternative, some species are suitable for sedimentation, after a time extracted from the PBR the biomass settles down, which reduces the centrifugation costs immensely. The biomass can be directly stored frozen in form of a wet paste, or later dried using processes such as freeze-drying (lyophilization), spray- or drum-drying.

1.4.2 General requirements on microalgae species

Despite the large variety of existing species, microalgae need to comprise certain characteristics to be used in a commercial large-scale production. This can be generally paraphrased as a basic robustness, tolerance against changing environmental factors and the possibility to be easily harvested (Tredici 2010).

1.4.3 The scale-up process

Rising a microalgal culture from a small volume in the algal collection to a production volume is challenging. Cultures are kept in volumes smaller than 0.5 L and are stepwise grown until approximately 5 L indoors. Pilot-scale PBRs in the scale of hundreds of liters are used to rise the required volume for the inoculation of a production unit with several 1000 L. Even if many successful attempts are described, each step in every system inhabits individualities. Outdoor PBRs cannot be controlled in the same way as in the laboratory, concerning especially the temperature and irradiance. Noting the light conditions, with increasing depth of the culture shading of the cells increases. The fluid dynamics differs in every system. The microalgae might show different behaviour in growth in different scales of cultivation systems, so each stage must be evaluated separately and results from laboratory experiments or pilot plants must be applied with care to production units.

1.4.4 Photobioreactor design for microalgae cultivation

A variety in design of PBRs was developed for the growth of microalgae. They differ in cost, the ease of use and possibility of controlling parameters and sterility. There are different systems and methods that guarantee adequate agitation and aeration of the culture. In a homogenous suspension, sufficient gas-exchange, nutrient and light availability is given. In a

lab-scale airlift-reactors, shaking flasks or aerated balloons are used. Air-lift reactors are characterized by a high surface to volume ratio (Lee and Bazin 1990). The microalgae *Chaetocerus gracilis* and *S. costatum* were grown in cylindrical PBR of 5 or 80 L, in which the stirring was conducted by air injection, supplemented with CO₂ (Pérez et al. 2017).

The first operated outdoor production system were open ponds, having the advantages of being simple to set up and operate (Tredici 2007). The culture is moved through the reservoir, paddle wheels can serve to this purpose. The integration of baffles for a throughout mixing is suitable. Such production units are used for species that are robust and tolerant to contamination, for example *Nannochloropsis* is grown in open raceway ponds (Crowe et al. 2012). Another open setup is the thin layer cascade, where the culture is directed over a flat surface. This system was described for a *Chlorella* cultivation (Masojídek et al. 2011). The culture was pumped through thin sloping planes with a height of 6 mm and an area of 24 m² for the experimental unit and 224 m² in the production unit. Both setups were held outside and therefore exposed to sunlight as natural light source. Thin layer cascades are characterized by a high surface to volume ratio, high areal productivity, easy heat up by solar radiation and a good light utilization, leading to a higher culture density as for example open ponds. Generally, open systems have a lower capital expenditure and operational costs (Jorquera et al. 2010). Due to the exposure to the environment, production for human consumption might be problematic. Therefore, closed systems, such as airlift and flat panel (FP) reactors and tubular systems, were developed. Airlift-reactors are constituted of a column, the injection of air serves to circulate the culture (Chini Zittelli, Rodolfi and Tredici 2003). FPs can be made of glass in a steel frame or supported plastic bags (Tredici et al. 2016; Kaspar et al. 2014). Air-sparging provides mixing of the culture and CO₂ supply.

PBRs such as the thin layer cascade, cylindrical or column PBR and a vertical flat-plate PBR with a volume of about 100 L were tested in pilot-scale (Malapascua et al. 2014). In case of tubular reactors, the culture is pumped from a retention vessel through a system of transparent tubes (Silva Benavides et al. 2013). The tubes can be made of glass or plastic and constitute the area of a photosynthetic active culture. The mixing effect can be supported by inert particles added to the culture, for example plastic balls or pieces. This helps avoiding the built-up of a biofilm on the reactor walls or big clusters of microalgal cells.

Production units can work in a batch, semi-continuous or continuous mode. For some species it might be advantageous to grow the culture to a certain density and harvest the whole volume at once. In a semi-continuous production, a defined culture volume is extracted according to a given pattern and substituted by culture medium. In the latter case, culture volume is taken from the system constantly and harvested, the system is filled with water and nutrients at the same time. Batch systems are easier to handle and therefore cheaper, as the complete culture is taken out, they are less susceptible to contamination. Continuous production systems offer the possibility to regulate the density of the culture, costs can be saved as less inocula are required and while the production unit is running, there is no necessity of a new laborious setup.

1.5 Growth monitoring of microalgal cultures

To observe the biomass and growth of a culture, an easy, quick and non-invasive method is desired. The measurement of the optical density (OD) has advantages of being fast and simple. The pigments contained in the cells will absorb light at a certain wavelength, which is detected by a spectrophotometer. The absorbance is given in arbitrary units. For every species, an optimal wavelength for the measurement needs to be defined, depending on the pigment composition (Sathyendranath, Lazzara and Prieur 1987). In the literature, *Skeletonema* cultures are measured at wavelengths between 665 and 750 nm (Pérez et al. 2017; Latała, Marcin and Stepnowski 2009). Big vacuoles and other contained components can distort the results; hence a changed metabolism can change the OD, despite an unaltered biomass concentration. The DW measurement is especially relevant for the commercial production, because it directly reflects the mass of the desired product. A rather large volume (about 30 mL) and more time is needed to perform it, compared to other techniques. The cell count is advantageous in that sense, that selectively the cells of the observed species are considered. Next to these rather classical methods, fluorometry offers an alternative, the parameter minimum fluorescence at dark-adapted stage F_0 represents the biomass. The fluorometry measurement is extensive and quick, simple to perform and requires a small sample volume.

1.6 Pulse amplitude modulated fluorometry

1.6.1 Basic understanding of fluorometry

The pulse amplitude modulated (PAM) fluorometry is used to describe the state of a culture with different parameters, referring to photosynthesis. The basic principle of photosynthesis

is the transformation of light energy into chemical energy, in the form of ATP usable for the cells. Light energy is imported by photons that induce the movement of electrons through the photosynthetic apparatus, reductive and oxidative reactions are taking place and create an electrochemical potential. A proton-gradient is established and used: Protons, flowing down their gradient, activate ATP-synthase complexes, that convert ADP to ATP. By PAM-fluorometry, the fluorescence of the photoactive compounds, the pigments, and the electron transfer and redox potentials within the photosynthetic apparatus, are measured. The results provide information about the photosynthetic capacity and efficiency of the examined culture. As the present work applies PAM fluorometry to suspended microalgae cells, in the following only the term *culture* is used, when any type of sample can be examined.

1.6.2 Methodology of fluorometry

After a dark adaption time of 10-15 minutes, the culture is excited with light of defined strength and light pulses in specific intervals, that produce an output of fluorescence. After the time of dark adaption, all reaction centers of the photosystem are said to be “open”, in this conformation they are ready to work, this means to receive electrons. There are three light intensities to distinguish: weak measuring light, actinic light and a strong saturating pulse. The measuring light has generally less than $0.5 \mu\text{mol m}^{-2} \text{s}^{-1}$ and does not activate the components of the photosystems. It measures the minimum fluorescence of the culture in the dark-adapted state F_0 . This parameter can be used to measure the growth of a culture. Actinic light activates the photosystem and induces an electron flow. When a saturating pulse of up to $10000 \mu\text{mol m}^{-2} \text{s}^{-1}$ is applied, all the reaction centers are excited and a maximum fluorescence F_m is measured. The device used in the present study applies a strength of $1000 \mu\text{mol m}^{-2} \text{s}^{-1}$ for the actinic light and $3000 \mu\text{mol m}^{-2} \text{s}^{-1}$ as a saturating pulse. In the following, protocols and applications of PAM fluorometry are described.

1.6.3 OJIP curves

OJIP measurement reveals the chlorophyll *a* fluorescence induction (Malapascua et al. 2014; Strasser, Tsimilli-Michael and Srivastava 2004). The results are presented in dependence of the time. The name is an acronym for the results of the OJIP graph, appearing after intervals of micro- and milliseconds. The “O” (origin) state is the minimal value, induced by the measuring light, which equates the beforementioned F_0 . Then the sample is exposed to actinic light. The curve shows a local maximum and the first inflection, designated as “J”. This state

represents the reduction of the quinone Q_A , the first electron acceptor in the photosystem II. At the second inflection state “I” the quinones (Q_A and Q_B) are differently reduced, present in different redox states. The valley between the I and the J state is explained by the movement of electrons from one quinone to another. The part of the curve between I and P is called thermal phase. The “P” (peak) state is the absolute maximum of the graph, representing the maximum fluorescence F_m . In this state, all reaction centers of the photosystem are closed and the quinone pool is fully reduced.

1.6.4 Efficient quantum yield

The difference between F_0 and F_m is defined as the variable fluorescence F_v . The quantum efficiency or yield of photosystem II F_v/F_m is an important parameter, that helps to estimate the qualitative state of a culture and gives information about the photosynthetic capacity. It is derived by the formula $(F_m - F_0)/F_m$. The derived values are species and (for higher plants) tissue specific, maximum values between 0.7 and 0.8 are reported. *Skeletonema* shows typical values around 0.6 (Fouqueray et al. 2007); decrease of this value implies stress (Bouchard and Purdie 2011; White, Anandraj and Bux 2011).

1.6.5 Light regimes in phototrophic cultures

By evaluating the photosynthetic efficiency, the light regime that a culture is experiencing can be determined (Tredici 2010). At a very low light intensity, photosynthetic reactions do not compensate energy requirements of respiration. At distinctly higher intensities, a culture can work under suboptimal conditions, where all the irradiance is used in a highly efficient manner. As the overall photosynthetic rate does not reach a maximum here, a light-limited condition is described. At a light intensity, designated as E_k , a maximum rate of photosynthesis P_{max} is observed (Cosgrove and Borowitzka 2010). By this marker, a light-saturated condition can be defined, that allows efficient photosynthesis. With increasing light intensity, photosynthesis might be down-regulated. This is due to photoprotection, the condition is then called light-inhibited (Masojídek, Vonshak, and Torzillo 2010).

1.6.6 Application of growth monitoring and fluorometry parameters

The photosynthetic efficiency of a culture describes its physiological state. F_v/F_m is a suitable parameter to observe stress in a culture. In an experiment with reduced phosphorous or nitrate concentration in the medium, the cell number declined parallel with the F_v/F_m in both experiments compared to a control culture (Kang, Tsui and Chang 2012). The referring nutrient

might be depleted at that time of the cultivation. This assessment combined with tracking the growth of a culture lays the basis to detect negative influences, evaluate growth parameters and optimise the production accordingly.

2. Objective of the work

The present work aimed to optimise the cultivation of *Skeletonema* sp. biomass in laboratory to large-scale production systems. In order to achieve this main goal, in the laboratory, different experiments were conducted in Algem[®] photobioreactors to define the optimum production season, initial inoculum concentration, silicate concentration and pH-setpoint. After the laboratory trials, the scale-up to outdoor conditions and large-scale production was targeted. Therefore, the volumetric and areal productivities for the biomass production of *Skeletonema* sp. in large-scale was evaluated. Another objective was to assess, if fluorometry could be effectively implemented as a technique to evaluate the physiological state of cultures. Finally, an evaluation of the biochemical composition of produced biomass regarding the proximate composition of macronutrients (carbohydrates, proteins, lipids) and ashes was performed and the potential biotechnological applications discussed.

3. Material and methods

3.1 Species

The species used in the experimental trials were the two strains *Skeletonema* sp. with the internal sign SKC0218 and SKM0118 (figure 3.1). In the large-scale units were produced among these *Skeletonema* sp. SKC0118 and SKC0119. The strains originated from the RCC (Roscoff Culture Collection, France).

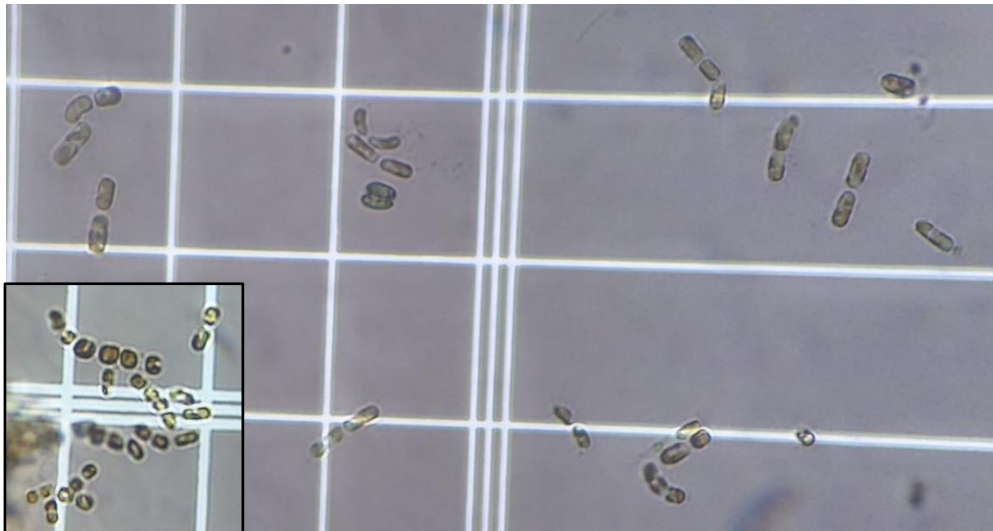


Figure 3.1 Microscopic picture of *Skeletonema* sp. cells. Magnification: 40x. Single cells as well as pairs of cells after division are visible. In the separate picture the typical chain formation is displayed.

3.2 Medium

Cultures were grown in autoclaved sea water with 35 psu, supplied with NutriBloom plus culture medium (Table 3.1).

Table 3.1 NutriBloom plus medium elemental composition

Macronutrients	Metals	Vitamins
2.8 % N	0.112 % Fe	0.0035 % Thiamine
0.31 % P	0.014 % Zn	0.0005 % Biotin
(resulting in an N:P ratio of 1:9)	0.01 % Mo	0.0003 % B12
	0.005 % Mg	
	0.001 % Co	
	0.001 % Cu	

If not indicated differently, silicate was supplied by 2 mL L⁻¹ of a 23 g L⁻¹ sodium metasilicate pentahydrate solution or 0.108 M silica; resulting in 0.216 mM silicate in the medium.

3.3 Experimental Culture Units - Algems®

The experimental trials were done in a setup of four 1 L Erlenmeyer flasks with a working volume of 500 mL. These were aerated with a shaft releasing air at the bottom of the flasks, had a sterile air-outlet, constantly shaken at 120 rpm, the pH was maintained at 8 by a CO₂

injection; and the temperature was externally controlled. Illumination was performed by LEDs; the light intensity and daily cycle was controlled by a profile provided from the Algem® software. The flasks were contained in a box, preventing any irradiation but the controlled illumination (*Figure 3.2*). The profile settings were defined by a month and the geographic position of the production plant: 37.03 °N, 7.87 °W. If not indicated differently, the profile was set for *October*, including the setting of a maximum PAR of 708 $\mu\text{mol m}^{-2} \text{s}^{-1}$, sun fraction of 0.38, a daylength of 9h 58 min, T_{min} 12.0 °C, T_{max} 18.5 °C. The initial OD of the trials was 0.08 a.u. at 740 nm. NutriBloom plus medium was given after nitrate analysis of the inoculum culture to achieve a concentration of 4 mM in the newly inoculated culture and silicate was supplied by 2 mL L⁻¹ of a 0.108 M silicate solution, giving 0.216 mM silicate in the cultures. The OD at 740 nm was measured continuously by the Algem® system.

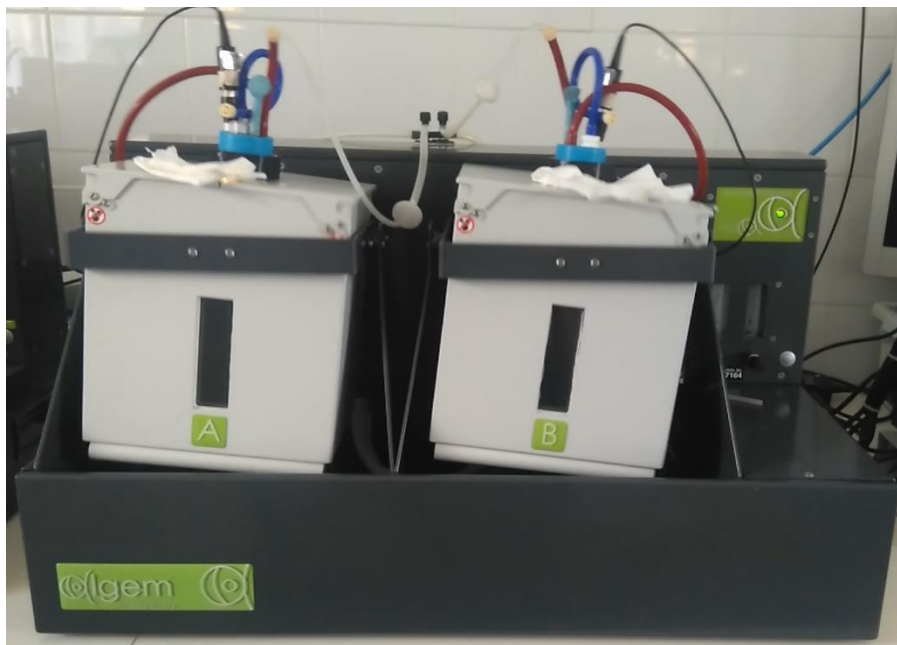


Figure 3.2 The Algem® system: two shaken growth chambers containing Erlenmeyer flasks, with air mixed with CO₂ supply, probes for pH and optical density.

The trials were run until a plateau phase was reached. Samples were taken every two days; 10 mL were sampled from each flask under sterile conditions.

The trials related to the inoculum concentration, silicate concentration and pH setpoint were performed in duplicates.

3.3.1 Strain selection and season

The different strains *Skeletonema* sp. SKC0218 and SKM0118 were tested at autumn and winter conditions. The Algem[®] profile was set to October and January, respectively. The Algem[®] profile *January* includes the setting of a maximum PAR of 653 $\mu\text{mol m}^{-2} \text{s}^{-1}$, sun fraction of 0.35, a daylength of 9h 43 min, T_{min} 7.8 °C, T_{max} 13.8 °C.

3.3.2 Inoculum concentration

To test the optimal initial inoculum concentration, first a culture of *Skeletonema* sp. SKM0118 was used. The four flasks were inoculated with 5, 10, 20 and 30 % of the volume from the inoculum culture, resulting in ODs of 0.02, 0.04, 0.08 and 0.15 a.u. at a wavelength of 740 nm or cellular concentrations of $2 \cdot 10^5$, $4 \cdot 10^5$, $6 \cdot 10^5$ and $1 \cdot 10^6$ cells mL^{-1} , respectively. For every dilution, the demand of medium and silicate was calculated.

The trial was repeated with *Skeletonema* sp. SKC0218 and initial ODs of 0.03, 0.06, 0.10 and 0.17 at a wavelength of 740 nm.

3.3.3 Silicate concentration

Different silicate concentrations were tested using *Skeletonema* sp. SKC0218. The concentrated silicate solution was supplied by 0.5, 1.0, 2.0 or 4.0 mL L^{-1} resulting in initial concentrations of 0.05, 0.11, 0.22 or 0.43 mM silicate in the medium.

3.3.4 pH setpoint

Different pH setpoints were tested on *Skeletonema* sp. SKC0218. The chosen setpoints were 7.0, 7.5, 8.0 and 8.5.

3.4 Production Units

The production of *Skeletonema* sp. at Necton (Olhão, Portugal) started with cultures from an own culture collection. Cultures were grown indoors without artificial illumination at 25 °C in 5 L glass balloons. Newly inoculated cultures were provided with 2 mL L^{-1} of Nutribloom plus. In the production unit, the nutrients were supplied Mondays and Thursdays after nitrate analysis to reach a concentration of 4 mM nitrate. The scale up process was performed with FP PBRs with a volume from 100 to 1000 L (*figure 3.3*). They were aerated with a regulable air- CO_2 mixture to stabilize the pH of the culture. The pH value was measured daily at 8:30 h, according to the value, the CO_2 valve was adjusted manually. Tubular PBRs were inoculated

with 3000 to 4000 L culture from the FP PBRs. The tubular systems had a volume of 10000 to 19000 L, the culture was pumped with a velocity of $0.5\text{-}1\text{ m s}^{-1}$ from a retention tank through the system, plastic particles of $2\times 5\text{ mm}$ ensured a thorough mixing (*figure 3.4* and *figure 3.5*). The pH was regulated automatically by CO_2 injection. The PBRs were located outside were cooled by water sprinklers on demand. At the production facility, the sunlight radiation and temperature were recorded.

Culture to harvest was transported by a pipeline system to centrifuges. The concentrated biomass was stored frozen.

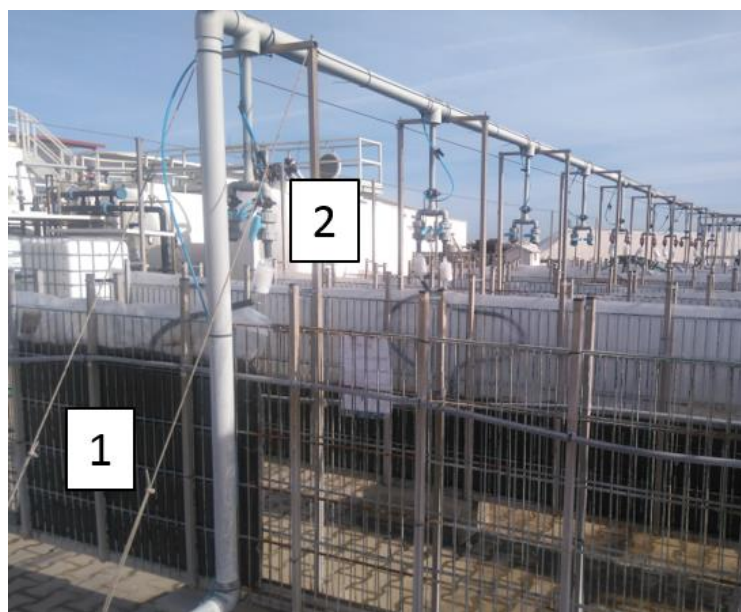


Figure 3.3 1: Flat panel photobioreactors of 100 L, 2: CO_2 supply and air-sparkling machinery



Figure 3.4 Four tubular systems of photobioreactors. Microalgal culture is pumped through the horizontal tube. The photobioreactor at the left is without culture, the others contain culture of different species and densities.

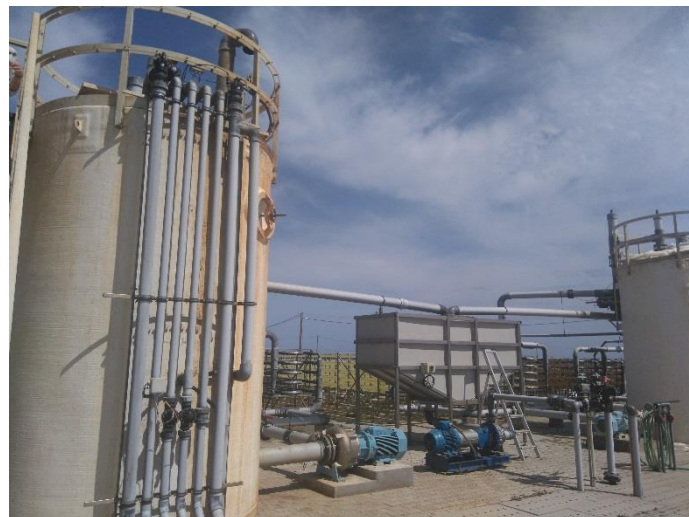


Figure 3.5 Retention tanks and pumps of tubular photobioreactors. The towers at the left and right side contain the operated culture. The tank in the middle serves to hold harvested culture before being transferred through a pipeline to a centrifuge.

3.5 Growth parameter determination

3.5.1 Optical density

The OD of the cultures was measured in the UV-mini-1240 UV/VIS spectrophotometer by Shimadzu (Kyoto, Japan). Plastic cuvettes were used, in case the culture reached an OD of 1, it was diluted in saltwater. For production cultures, the OD was recorded daily at a wavelength of 450 nm. The OD of each sample from the experimental trials was measured at 450 and 740 nm.

3.5.2 Dry weight

Glass microfiber filters (d=47 mm) with a retention particle size of 1.5 μm by VWR International (Leuven, Belgium) were used in a vacuum drying system. The filters were equilibrated with 20 mL of distilled water and 2 mL of ammonium formate (31.5 g L^{-1}). After drying at 60 °C for at least 24 hours, the filters were loaded with 8-10 mL of culture, washed with the same volume of ammonium formate and again dried for at least 24 hours.

The DW was correlated to the OD of the cultures in the FP and tubular PBRs measured at a wavelength of 450 nm; with a coefficient of determination of 0.9171 and 0.9214, respectively.

For the growth curves the DW was calculated according to the following equations:

$$\text{Dry weight}_{\text{flat panel PBR}} [\text{g L}^{-1}] = A_{450} \cdot 0.3125 + 0.2147$$

$$\text{Dry weight}_{\text{tubular PBR}} [\text{g L}^{-1}] = A_{450} \cdot 0.3031 + 0.2177$$

3.5.3 Cellular concentration

The cells in a culture sample were counted using a Neubauer haemocytometer with a chamber volume of 10^{-4} mL under a light microscope at a 40x magnification. Concentrated cultures were diluted in a proportion so that only up to 200 cells were counted in the field. The cellular concentration in cells mL^{-1} was then obtained by the formula:

$$\text{Cellular concentration} [\text{cells mL}^{-1}] = \text{number of counted cells} \cdot 10^4 \cdot \text{dilution factor}$$

3.6 Fluorometric measurements

The AquaPen-C 100 by Photon Systems Instruments (Drasov, Czech Republic) was used according to the manual. The culture was adapted in 3 mL cuvettes to the dark for 10-15 minutes and inserted to the device under dark conditions. The protocols of OJIP and NPQ1 were run, measuring a fluorescence induction curve and the non-photochemical quenching, respectively. Complete protocols are found in the manual. The samples were excited with actinic light, the settings of the device were chosen for a flash pulse at a strength of 25 % and the saturating pulse of 95 %. F_0 , the minimal fluorescence at the dark-adapted state, was applied as an indicator for the biomass concentration. The photochemical efficiency of the photosystem II is the ratio of the variable fluorescence F_v and maximum fluorescence F_m and refers to the health of the culture; it is defined by the equation:

$$F_v/F_m = \frac{F_m - F_0}{F_m}$$

F_v/F_m decreases if the culture suffers from stress. The maximum quantum yield of the photosystem II QY_{max} is in the dark-adapted state an equivalent to F_v/F_m .

3.7 Nitrate concentration

The nitrate concentration in the medium is determined by a spectrophotometric method. Briefly, 0.5 mL of supernatant from centrifuged cultures are transferred to a tube with 9.3 mL of a 35 g L⁻¹ NaCl solution and 200 μL HCl (83 mL L⁻¹). The absorbance at 220 and 275 nm was measured against a blank, constituted of 9.8 mL NaCl and 200 μL HCl, in duplicates. The nitrate concentration was determined by the following formula:

$$\text{Nitrate [mM]} = ((A_{220} - 2 \cdot A_{275}) \cdot 0.3051 + 0.0057) \cdot 20$$

3.8 Biochemical Analysis of the Biomass

3.8.1 Sample treatment and storage

The biomass of representative samples of harvested culture from the large-scale production was freeze-dried and analysed for the biochemical composition.

3.8.2 Total protein content

For protein determination, the Lowry protein assay (Lowry et al. 1951) modified by Herbert (Herbert, Phipps and Strange 1971) was used. Solutions of 5 % Na₂CO₃ and 1 % C₄H₄KNaO₆ · 4 H₂O were prepared. A 0.5 % CuSO₄ · 5 H₂O solution was prepared in the C₄H₄KNaO₆ · 4 H₂O solution. Just before use, 50 mL of the first and 2 mL of the second solution were mixed, after that referred as to reagent A. Folin-Ciocalteu reagent was 1:1 diluted with distilled water, and will be called reagent B in the following. A 1 mg mL⁻¹ bovine serum albumin (BSA) in 1 M NaOH solution served as a standard substance.

The samples were prepared by resuspending 20 mg lyophilized biomass in 2 mL 1M NaOH and boiled for 1 h in a water bath at 100 °C. After cooling down, the samples were centrifuged for 10 minutes at 3100 rpm. Each 100 μL were transferred to three tubes. To the sample, 400 μL 1 M NaOH and 300 μL distilled water were added. For the standard curve, amounts between 10 and 400 μL BSA (1 mg mL⁻¹) were filled up to 500 μL with 1 M NaOH and 300 μL distilled water were added. The blank was constituted of 500 μL 1 M NaOH and 300 μL water. The following procedure was applied to the standard preparations, samples and the blank.

To the each of the preparations, 2 mL of the reagent A were added, and the solution homogenized. After 10 minutes, 400 µL reagent B were added and mixed well. The samples were left for 30 minutes at room temperature. The absorbance at 750 nm was read. The amount of protein in the sample and as percentage of biomass was calculated each according to the calibration curve established at the same day.

The analysis was done for samples collected during the large-scale production. The analysis was done in triplicates.

3.8.3 Total lipid content

The lipids were extracted by a procedure derived from the method by Bligh and Dyer (Bligh and Dyer 1959). Therefore, 1-5 mg of lyophilized sample were transferred into a tube. The sample was left with 0.8 mL distilled water for at least 10 minutes at room temperature. Then, 2 mL methanol and 1 mL chloroform were added. The sample was homogenized for one minute on ice, using the Ultra Turrax T18 digital, IKA (Staufen, Germany) at 20000 rpm. Next, 1 mL chloroform was added, and the sample homogenized on ice, for 30 seconds. After that, 1 mL distilled water was added, and the sample again homogenized on ice, for 30 seconds. The sample was centrifuged at 25000 *g* for 10 minutes, 700 µL of the bottom fraction were transferred to a previously weighed tube and placed in a heat block, set to 60 °C. After the liquid evaporated, the dry tubes were weighed again. The lipid content as percentage of DW was calculated using the following formula:

$$\text{Lipids [\% of dry weight]} = \frac{(m_{\text{final}} - m_{\text{initial}}) \cdot V_{\text{total}}}{m_{\text{sample}} \cdot V_{\text{evap}}} \cdot 100$$

Hereby, m_{final} and m_{initial} refer to the weight of the glass tube, V_{total} is the volume of chloroform used (2 mL), V_{evap} the volume left for evaporation (0.7 mL) and m_{sample} the initially used weight of the dry sample. The lipid content was determined for the samples collected from the large-scale production. The analysis was carried out in duplicates.

3.8.4 Total ash content

In a previously weighed porcelain cup, 0.5-1 g of the lyophilized biomass was placed. The samples were dried at 80 °C over night, for the determination of the DW. After gradual heating over 2 hours, the biomass was burnt at 550 °C for 4 hours. The percentage of ashes in the samples can be determined using the following formula:

$$\text{Total ashes [\% of dry weight]} = \frac{m_{\text{burnt}} \cdot 100}{m_{\text{dry}}}$$

m_{dry} is the DW of the sample and m_{burnt} the weight remaining after burning the sample. The analysis was carried out in triplicates for the samples collected from the large-scale production.

3.8.5 Total carbohydrate content

The carbohydrate content was calculated by subtracting the lipid, protein and ash content from one hundred percent.

3.9 Quantitative productivity evaluation

The specific growth rate in the laboratory experiments and the large-scale production was determined based on the OD. The productivity in the tubular PBRs was evaluated quantitatively. Therefore, the parameters volumetric and areal productivity were calculated. The data is based on values measured as OD and converted to DW. In case of a declining growth, only positive values were used to determine an average.

3.9.1 Specific growth rate

The specific growth rate is calculated by dividing the difference of the natural logarithm of the biomass of the culture by the time of growth between two measurements, considering values during the exponential growth phase. Usually, the biomass of a culture is followed by a daily measurement of the OD.

$$\text{Growth rate}[d^{-1}] = \frac{\ln(X_2) - \ln(X_1)}{t_2 - t_1}$$

In the formula, X represents the biomass. For the Algem[®] experiments, the biomass was represented by the OD at 740 nm. In the large-scale production, the OD was recorded at 450 nm.

3.9.2 Total volumetric productivity

The volumetric productivity was calculated by dividing the gained biomass X from all harvests of a PBR in gram by the volume of the reactor V_R in L and the operated time t_R in days.

$$\text{Total volumetric productivity [g L}^{-1} \text{ d}^{-1}] = \frac{X}{\frac{V_R}{t_R}}$$

3.9.3 Total areal productivity

The tubular PBRs are built on an area of 340 m². To obtain the total areal productivity, the gained biomass X from all harvests of a PBR in g was divided by the area of the reactor a_R in m² and the operated time t_R.

$$\text{Total areal productivity [g m}^{-2} \text{ d}^{-1}] = \frac{X}{\frac{a_R}{t_R}}$$

3.9.4 Daily volumetric productivity

The maximal volumetric productivity was calculated using data of the daily measurement of the biomass concentration in a PBR. The daily volumetric productivity was calculated by dividing the difference in the biomass concentration in g L⁻¹ by the difference in time.

$$\text{Volumetric productivity [g L}^{-1} \text{ d}^{-1}] = \frac{X_2 - X_1}{t_2 - t_1}$$

3.9.5 Daily areal productivity

The maximal areal productivity was calculated using data of the daily measurement of the biomass concentration in a PBR. To obtain the daily areal productivity, the difference in the actual biomass present in the whole reactor was determined, multiplying the biomass X with the reactor volume V_R. This value was divided by the area of the reactor a_R and the difference in time.

$$\text{Maximal areal productivity [g m}^{-2} \text{ d}^{-1}] = \frac{(X_2 - X_1) \cdot V_R}{\frac{a_R}{t_2 - t_1}}$$

3.10 Statistical Analysis

The data was statistically analysed by a one-way ANOVA and a p-value of 0.05, using the software GraphPad Prism version 8.

4. Results and Discussion

4.1 Laboratory trials in the Algem® system

4.1.1 Strain selection and season

In a preliminary experiment, two strains, *Skeletonema* sp. SKC0218 and SKM0118, were used. The Algem® software was programmed with two different light and temperature conditions, that simulate the autumn and winter seasons at the production facility of Necton. Each of the two strains was grown once with the autumn and once with the winter settings.

The cultures of both species grew faster under autumn conditions, than under winter conditions (*figure 4.1*). For unknown reason, the *Skeletonema* sp. SKC0218 culture under autumn condition entered a stationary phase and declined already at about 80 h, whereas the *Skeletonema* sp. SKM0118 culture showed a stationary phase from 110 h without entering a death phase. The two cultures under winter conditions grew slower but entered a stationary phase only after 200 h, by this at the end of the experiment, the *Skeletonema* sp. SKC0218 culture under winter conditions had the highest OD of all. It can be noted, that due to the measurement of the growth by OD instead of cell count, the death phase might have started before a decrease in OD is visible (Maier 2009).

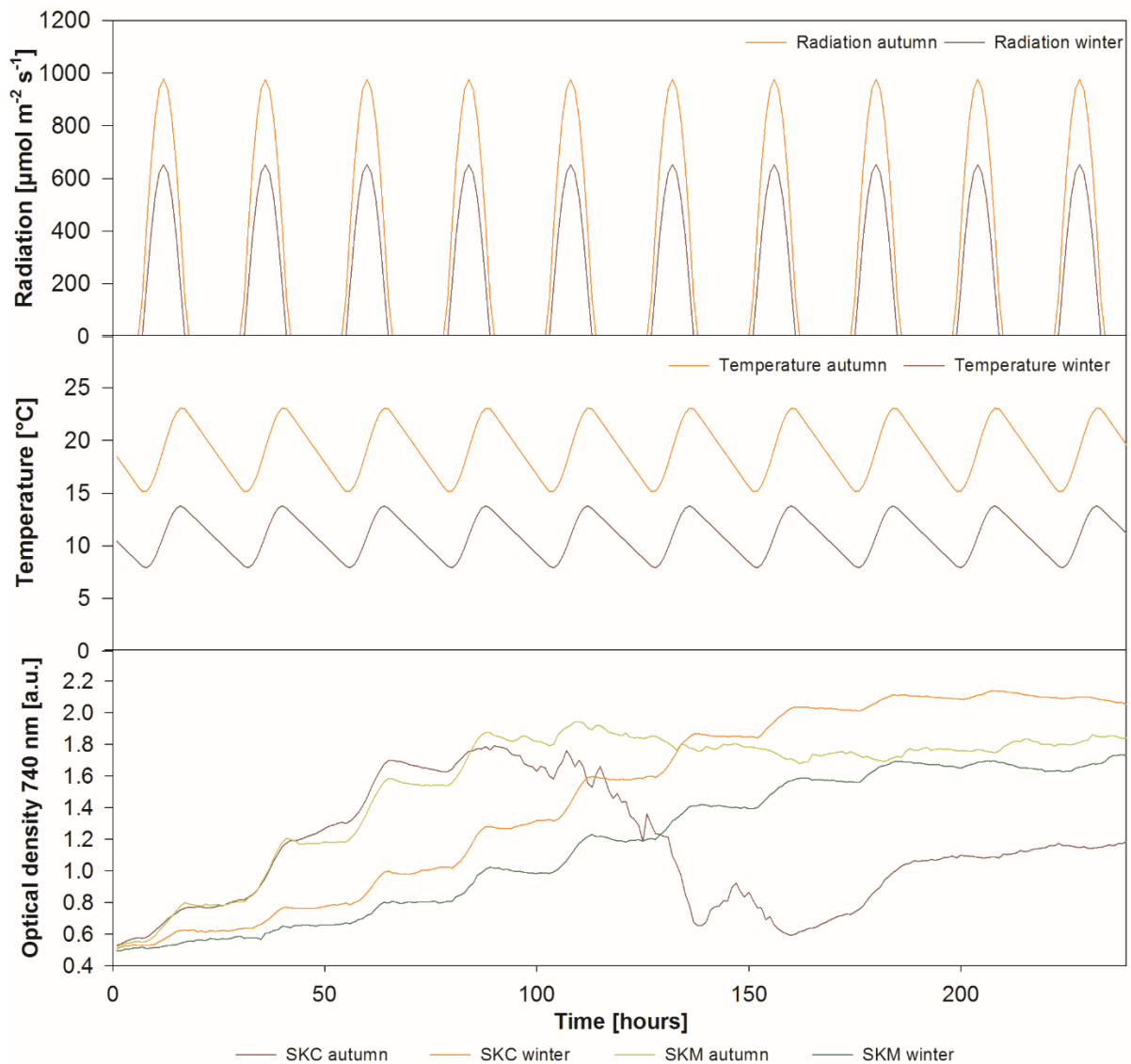


Figure 4.1 Conditions of light and temperature, set by the Algem[®] photobioreactor and culture growth, represented by optical density. Strains: *Skeletonema* sp. SKC0218 and SKM0118. 'Autumn' and 'winter' refer to the different profiles applied in the trial.

The average growth rate of the *Skeletonema* sp. SKM0118 culture under autumn conditions was significantly different from the same strain under winter conditions (0.36 ± 0.08 vs. $0.16 \pm 0.03 \text{ d}^{-1}$, figure 4.2). The difference between the seasons was not significant for the strain *Skeletonema* sp. SKC0218 (0.38 ± 0.10 vs $0.23 \pm 0.04 \text{ d}^{-1}$). Also, the growth in the same season for the different strains was not significantly different. The experiment showed that both the used species as well as the set conditions alter the growth of the culture, but one criterium per se does not have a significant influence. *Skeletonema* sp. SKM0118 seems to be more susceptible to changed environmental conditions.

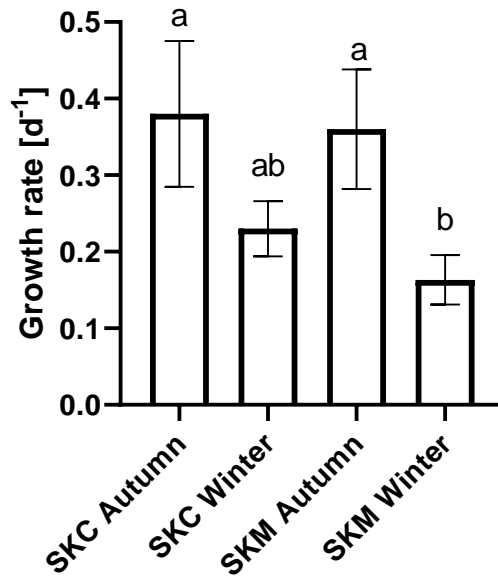


Figure 4.2 Growth rates of *Skeletonema* sp. SKC0218 and SKM0118 cultures under autumn and winter season conditions. Significant differences are indicated with different letters.

For a more efficient testing of other culture parameters, the strain *Skeletonema* sp. SKC0218 and the season condition for autumn were used in the following experiments.

4.1.2 Inoculum concentration

Skeletonema sp. cultures with different inoculum concentrations cultivated under standard conditions grew during five days to an OD of up to 1.7, for higher concentrated cultures (figure 4.3). Lower concentrated cultures showed a slightly longer lag phase (two instead of one day) and reached a final OD of 1.3.

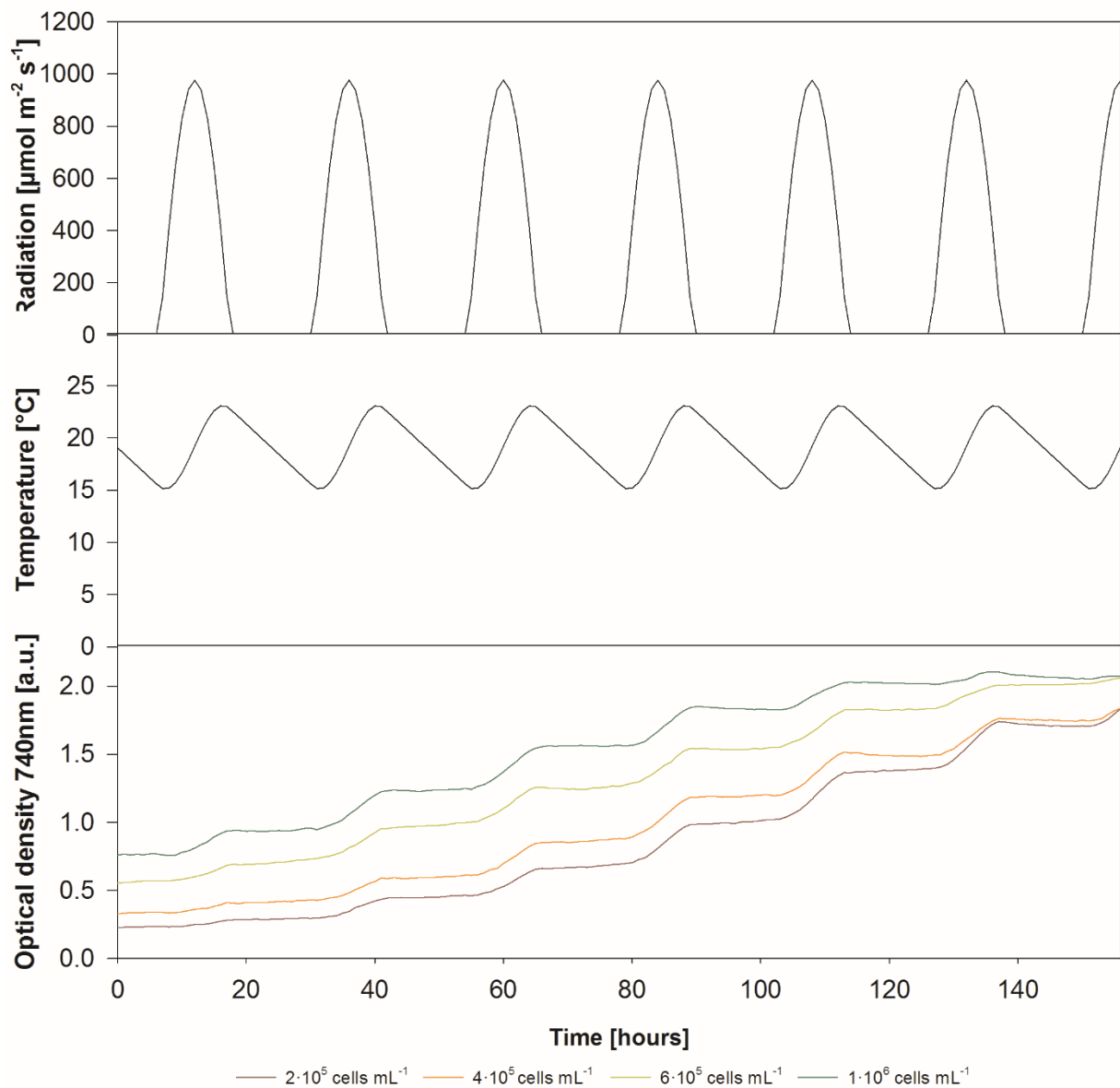


Figure 4.3 Average growth of two experiments testing different inoculum concentrations on the growth of *Skeletonema sp.* The daily radiation and temperature variation are shown.

According to the constant measurement of the OD in the Algems[®] (figure 4.3), it was assumed that after five days (120 hours) the growth slowed and after six days (about 140 hours) the

culture entered a stationary phase. By comparing different growth parameters (*figure 4.4*), the development was distinguished more precisely.

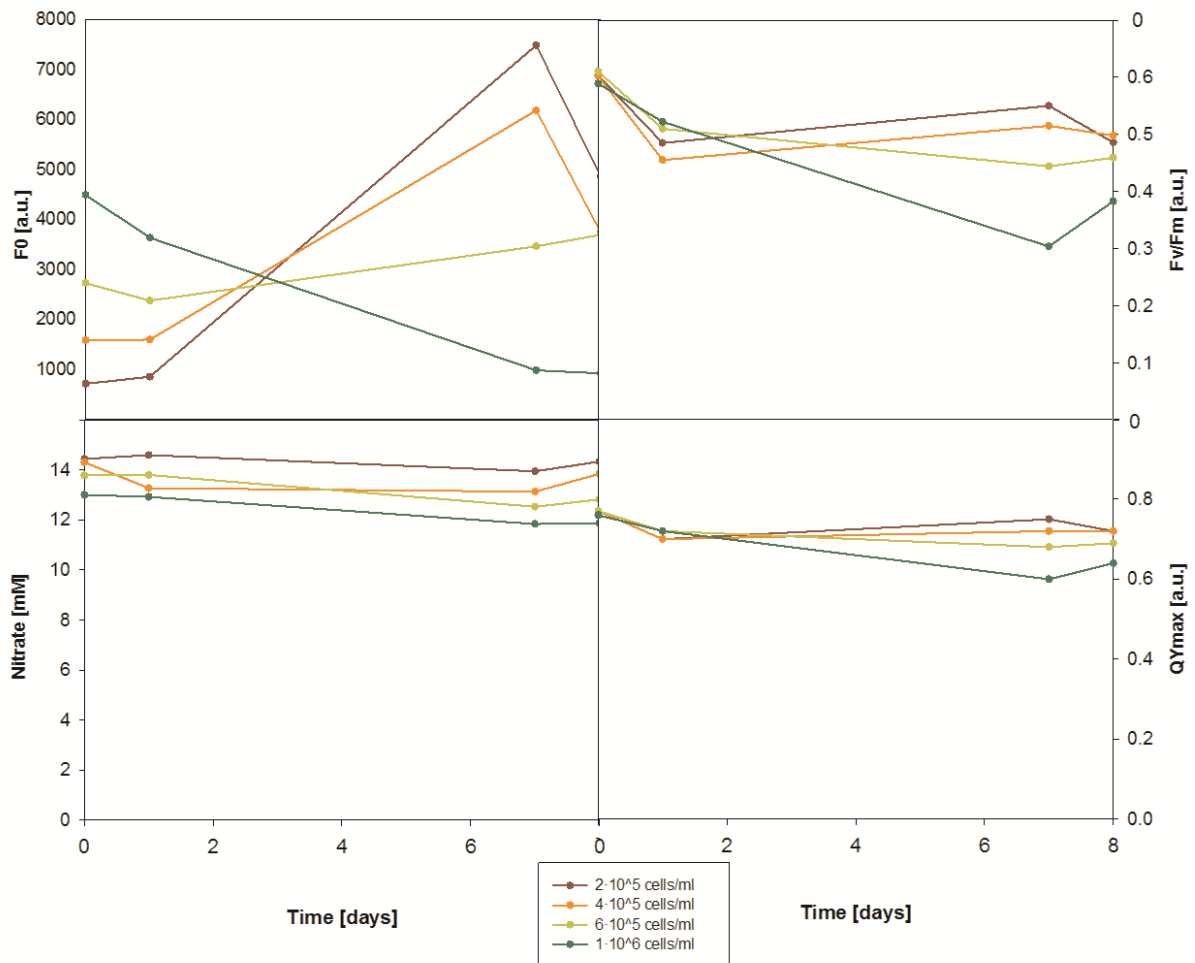


Figure 4.4 Overview of different fluorometry values and nitrate concentration in the medium in the first trial regarding the inoculum concentration *Skeletonema sp. SKC0218*. Samples were taken at the first and seventh day, analyses were also done at the start and the end of the experiment, after eight days.

F_0 for the three lower concentrated cultures increased until day 7. Between the last sample after seven days and the end of the experiment after eight days it suffered a decrease, referring to a decline in biomass or death phase and therefore supporting the observation by the OD measurement. For the culture with the highest initial inoculum concentration, F_0 decreased constantly, indicating that the minimum photosynthetic capacity of the cells in this culture was reduced. Similar to the first trial, for the culture with the highest inoculum concentration the F_0 value was decreasing between the fourth and the seventh day (*Figure 7.1*). This assumes a degradation of the cells, as the photosynthetic capacity was reduced, exemplarily shown in *figure 4.5*. The cultures with the lowest inoculum concentration showed the highest value of F_0 in the last sample. From this it can be concluded, that the biomass had

more photosynthetically active cells, despite the lower OD. Although F_0 was decreasing after a few days, the OD was constantly increasing.

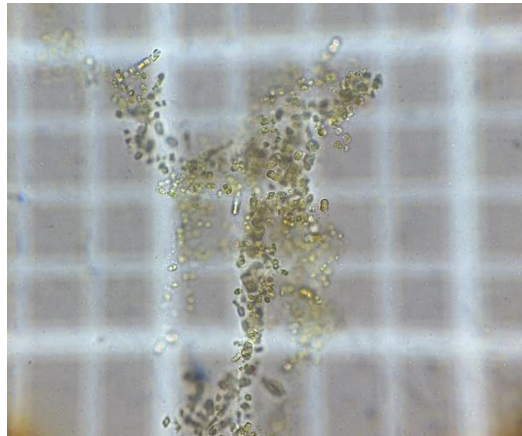


Figure 4.5 Impaired cells of Skeletonema sp. sampled from the Algem[®] system. The cells are not clearly defined, the colour is rather pale, and the cells are sticking together in an aggregate. Magnification: 40x.

The F_v/F_m value for the culture with the highest inoculum concentration suffered a remarkable drop at the time of the second sample after seven days down to 0.31, showing a culture suffering stress (*figure 4.4*). The F_v/F_m for the other three cultures was quite constant around 0.50, which is an average value. The same trend was supported by the QY_{max} measurement, that represents F_v/F_m under dark adapted conditions. In the second experiment (*Figure 7.1*), the F_v/F_m values did not show remarkable differences between the four cultures, it seemed as if none of them suffered severe stress. During the experiment, the value was decreasing in a similar manner for all cultures from initially 0.8, which was among the highest values observed, to 0.5, indicating a normal state of the culture. After entering an exponential phase, the quality of the cells decreased and consequently growth was inhibited. This was noticeable in the development of the maximum quantum yield of photosystem II, QY_{max} , in the second experiment testing the inoculum concentration. QY_{max} as well as F_v/F_m represent stress on the culture, the variables decreased with increasing stress. From the start of the experiment to the first sample, the value increased from 0.6 to 0.8, showing a well development of the culture. To the end of the trial, the value decreased to 0.7, still representing a well physiological state but indicating increasing stress. The value of F_v/F_m decreased constantly from 0.8 to 0.5. Generally, stress is provoked by nutrient starvation, too less or too much light or any unfavourable culture condition. In the present experiment, the pH, light and temperature conditions were the same for all cultures and must be excluded to explain the elevated stress level. In the first experiment, the nutrient level was very high throughout the

whole experiment, in the repetition of the experiment, the nitrate value went down to 0.56 mM for the culture with the lowest inoculum concentration and to 0.60 mM for the culture with the highest inoculum concentration. The other cultures had final nitrate values of over 1 mM, which is a value considered sufficient for growth of the culture. Because the F_v/F_m value decreased in a similar manner for all cultures, but the nitrate concentration differs, the nutrients were not considered of having been the stress trigger in the present case. Rather an unfavourable culture environment of a too high culture density might have impaired the physiological state of the cultures.

Comparing the biomass concentration of the different cultures, the OD of cultures with an initially high inoculum concentration was always higher than of cultures with a lower inoculum concentration. Still, the culture with the lowest initial inoculum concentration had a significantly higher specific growth rate ($0.36 \pm 0.08 \text{ d}^{-1}$) than the culture with the highest initial inoculum ($0.20 \pm 0.07 \text{ d}^{-1}$, *figure 4.6*). In other experiences, cultures with higher concentrated inocula showed faster growth, the opposite was observed in the present experiment. The nitrate concentration of all cultures in the first experiment was very high until the end and decreased in a similar manner for the four experimental conditions in the second experiment (*figure 4.4* and *Figure 7.1*). Because no differences in the nutrient supply between the four cultures were observed, starvation must be excluded to explain lower growth rates. The final DW of the cultures with higher inoculum concentration was higher than the other ones, still, the highest value was achieved with an inoculum concentration of $6 \cdot 10^5 \text{ cells mL}^{-1}$ (*Figure 4.7*). Eventually, the higher concentrated culture reached a density, that is unfavourable for further growth. This related to a much lower cellular concentration of *Skeletonema* sp. in natural environments, as found to be up to $10^4 \text{ cells mL}^{-1}$ (Saravanan and Godhe 2010) or $5 \cdot 10^4$ to $5 \cdot 10^5 \text{ cells mL}^{-1}$ in an induced bloom of a mixed culture in an open pond (De Pauw, Verboven and Claus 1983).

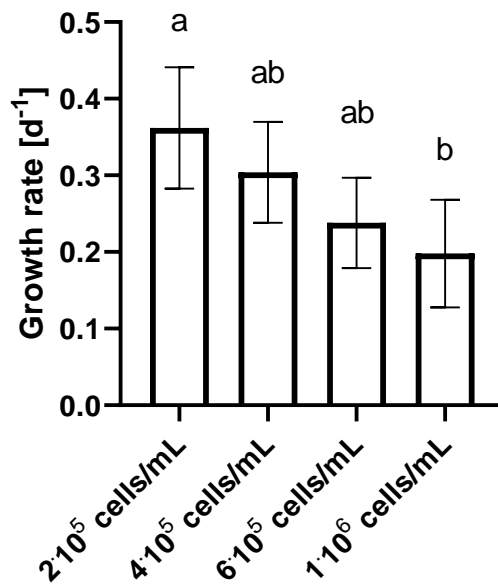


Figure 4.6 Average growth rates of *Skeletonema sp.* in two experiments regarding the inoculum concentration. Significant differences are marked with different letters.

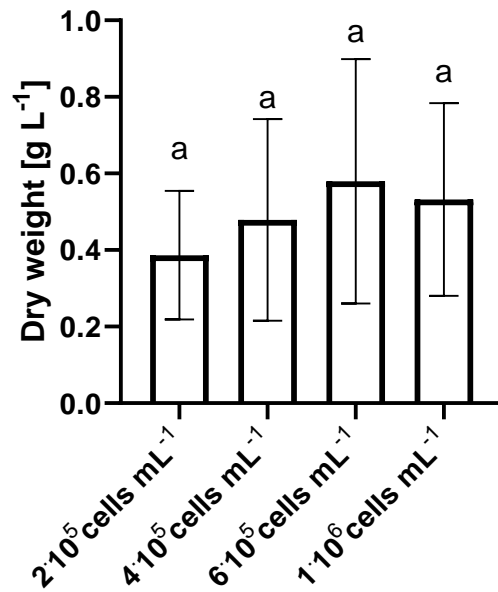


Figure 4.7 Final dry weight of *Skeletonema sp.* cultures with different inoculum concentrations. Average of two experiments. The letters indicate no statistical differences.

Another group working with a similar volume of 600 mL and an inoculum concentration of $2.5 \cdot 10^4$ cells mL⁻¹ observed senescence after two weeks (Bertozzini et al. 2013). In the present experiment it can be seen, that *Skeletonema sp.* entered a stationary phase already after a week. The cultures grew well with the given inoculum concentrations but entered a stationary phase earlier. This needs to be considered in large-scale production. Production cultures must

be operated in a way, for example by constant renewals of the culture medium, to maintain cultures in an exponential growth stage to avoid a trigger for aging.

4.1.3 Silicate concentration

To assess the effect of silicate concentration in the culture medium, four different initial concentrations (0.05, 0.11, 0.22 and 0.43 mM) were tested on the growth of *Skeletonema* sp. in duplicate. The four cultures in the experiments developed similarly, the growth of all but the culture supplied with the highest silicate concentration declined at the fifth day (figure 4.8). The two cultures provided with higher silicate concentrations showed a slightly longer exponential growth phase.

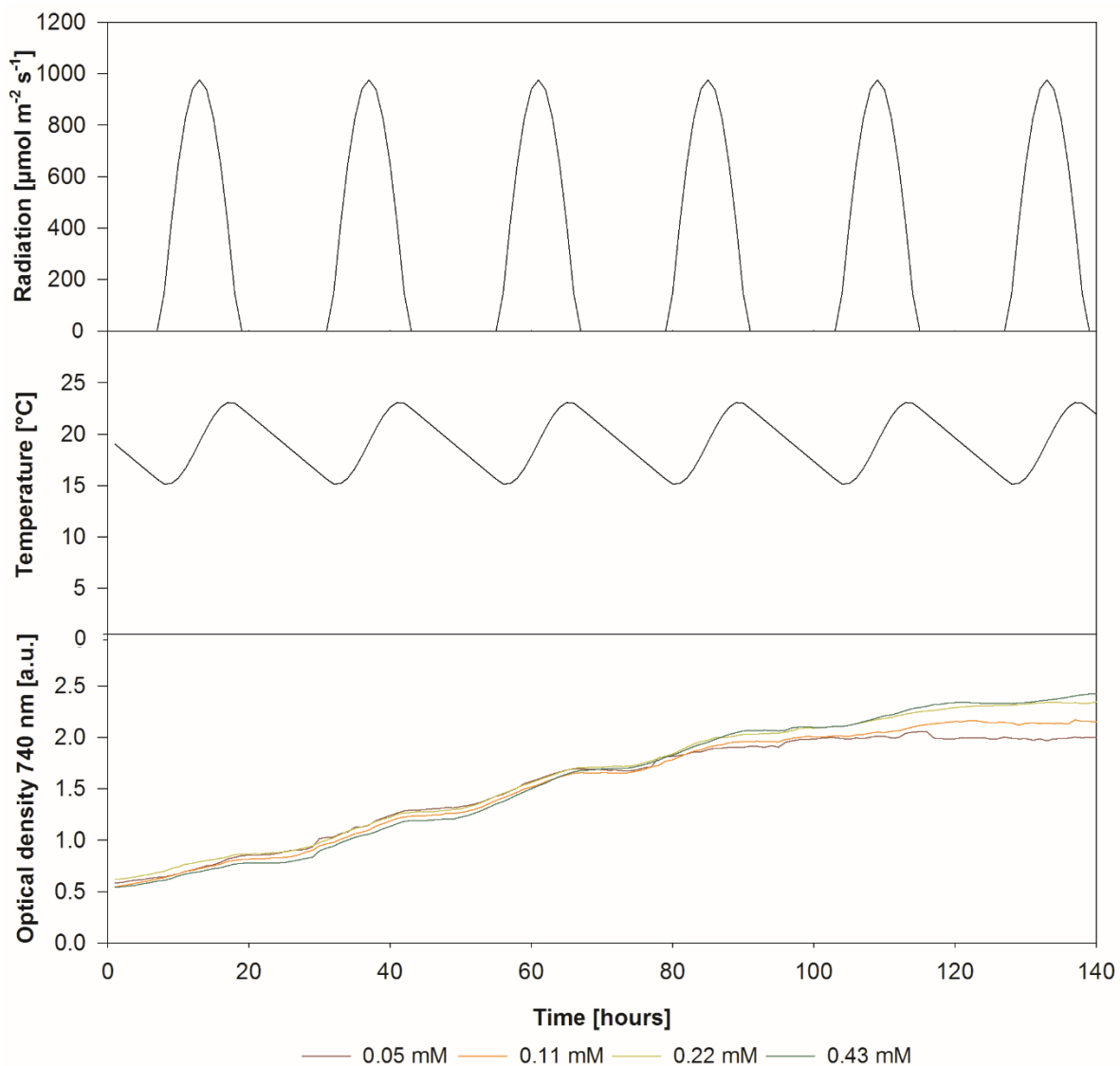


Figure 4.8 Average growth of *Skeletonema* sp. SKC0218 by optical density from two trials regarding initial silicate concentration, showing light and temperature profile conditions.

The growth of the cultures was followed by measuring the OD constantly in the Algem[®] system (figure 4.8), the fluorometry parameters F_0 and F_v/F_m as well as the culture parameter nitrate concentration in the medium were obtained for samples in between (figure 4.9).

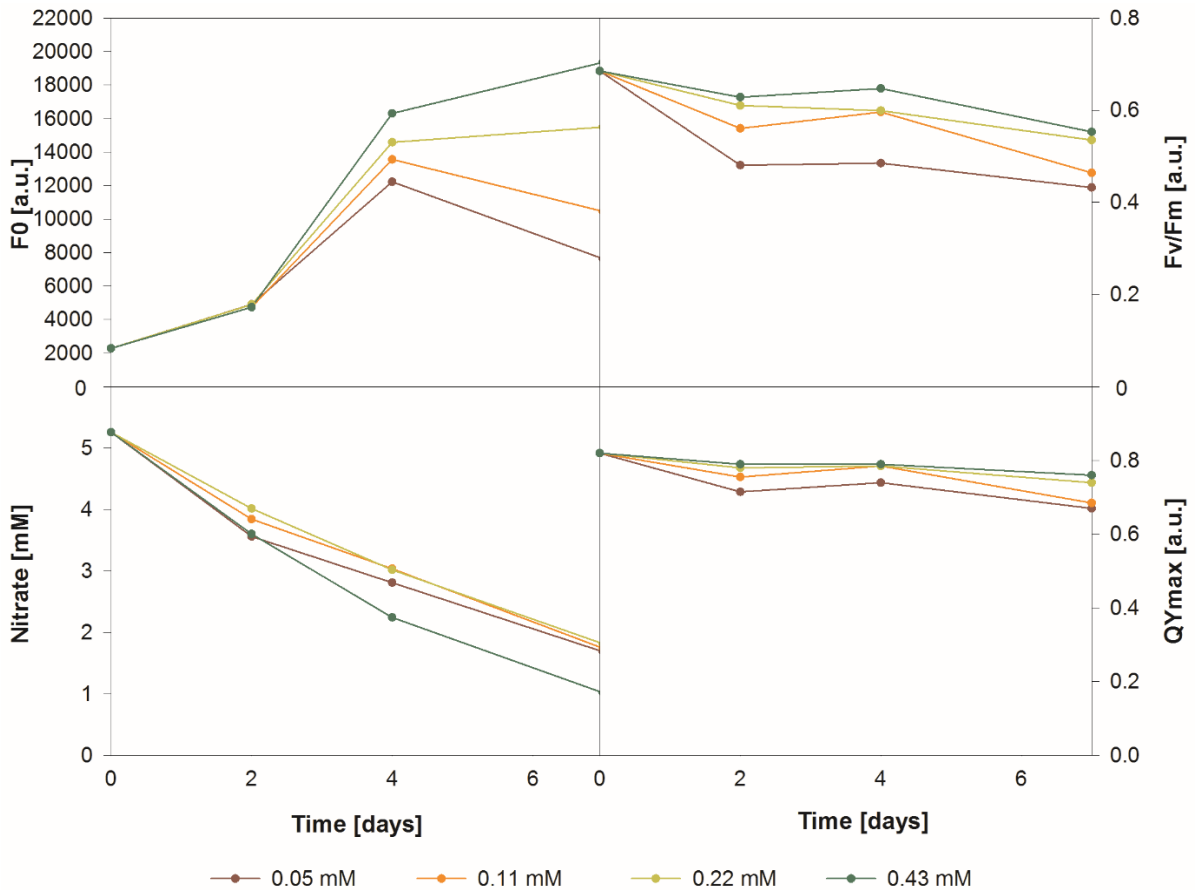


Figure 4.9 Different parameters recorded at the start, second, fourth and seventh day in the experiment regarding the silicate concentration. The graphs represent average values from two experiments. Species: *Skeletonema sp. SKC0218*.

The nitrate concentration decreased in a linear manner, assuming regular growth or consumption of the present cells. The nitrate consumed by the culture supplied with the highest silicate concentration was slightly higher. Despite an increasing OD, the F_0 value was stagnating or even decreasing between the third measurement and the end of the experiment, which represented an impairment of photosynthetically active cells. The OD of the culture supplied with the lowest silicate concentration did not rise from hour 100 onwards, the value of 1.99 was constant until the 144th hour and declined to 1.72 at the 155th hour. Interestingly, the F_v/F_m of the culture with 0.05 mM silicate was much lower than the other values at the first sample and stayed lower than of the other cultures throughout the experiment. The difference in the F_v/F_m between the culture provided with 0.05 mM (0.51±0.09) compared to 0.43 mM silicate (0.62±0.04) was significant. It can be concluded,

that this culture suffered silicate starvation which means nutrient stress for the culture, visible in a reduced value of F_v/F_m .

Although the cultures provided with 0.22 and 0.43 mM silicate achieved a higher growth rate and final DW than cultures with less silicate in the medium (figure 4.10 and figure 4.11), the differences were not statistically different.

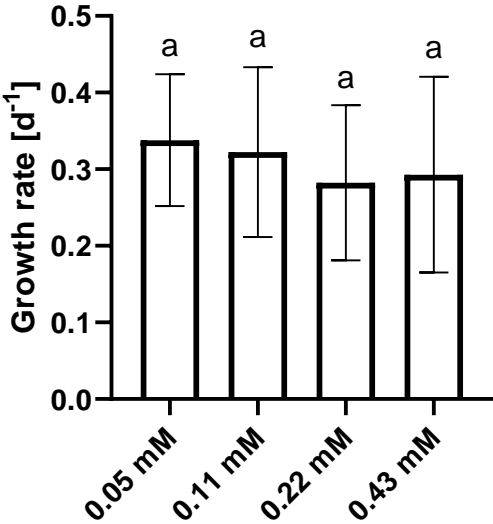


Figure 4.10 Growth rate of *Skeletonema sp. SKC0218* cultures grown with different initial silicate concentrations. The values are calculated from the optical density and show average results from two experiments. The letters indicate no significant differences.

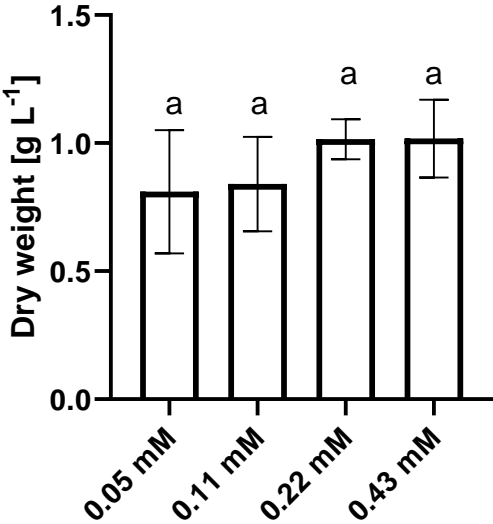


Figure 4.11 The final dry weight of *Skeletonema sp. SKC0218* cultures growing at different initial silicate concentrations, showing average of two experiments. The letters indicate no significant differences.

Skeletonema strains were investigated, using a medium provided with 0.08 mM silicate (Yamada et al. 2013). In other experiments, 0.11 mM silicate was considered as a high silicate concentration and served as the control condition, whereas the naturally present 2.5 μ M silicate in seawater served to simulate silicate starving conditions (Wang et al. 2017). The group used a concentration between these values of 0.03 mM as a medium silicate concentration. Viewing the cells under a transmission electron microscope revealed physiological differences and altered expression levels of programmed cell death-related genes in *Skeletonema* cultures between the high and low silicate conditions. In the presented trial, the provided silicate concentrations were rather high compared to the mentioned studies. The growth rates of the cultures supplied with different silicate concentrations did not show significant differences (*figure 4.10*). It was concluded that the silicate concentration provided in the tested range did not support a faster growth for any culture with a different silicate level. With exception of an initial silicate concentration of 0.05 mM, the silicate supply might have been saturated. The significantly lower F_v/F_m value of the culture with the lowest initial silicate concentration was an evidence for stress, supposedly by silicate starvation. It needs to be elucidated, in which manner it influences the physiology and biochemistry of the culture.

4.1.4 pH-setpoint

With the standard conditions, 0.11 mM silicate in the medium and light and temperature conditions defined by the autumn program of the Algem[®] software, four different pH setpoints were tested on the growth of *Skeletonema* sp. SKC0218 in duplicate. The pH values in the physiological range were 7.0, 7.5, 8.0 and 8.5.

By the observation of different culture parameters, the growth and physiological state of the microalgal culture was described in a differentiated way (*figure 4.13* and *Figure 7.2*). In the experiments, according to *figure 4.12*, the OD was constantly increasing, but it was assumed that at the end of the experiment the viability of the cells may have been compromised, as the cultures entered a stationary phase. This was confirmed by the development of F_0 , representing the fluorescent level of the cells, and by this the capacity of the photosynthetic apparatus. In the first experiment testing the different pH values, the nitrate concentration between the last two measurements (day 8 and day 11) stayed almost constant, in the duplicate of the experiment, the decrease and therefore consume between the day 4 and day

8 was not as strong as between day 2 and day 4, indicating decelerated growth. A lowered nutrient consume indicated a stagnating growth of the cultures. It must be noted, that the second experiment did not last as long as the first one (ten versus seven days). In the first experiment regarding the pH setpoint, lysis of cells was more extreme at the end of the experiment and the culture did not consume a significant amount of nitrate. A decreasing DW between the last two samples in the first experiment was an indicator of cell lysis. In *figure 4.15* the maximum DW is presented as the final DW.

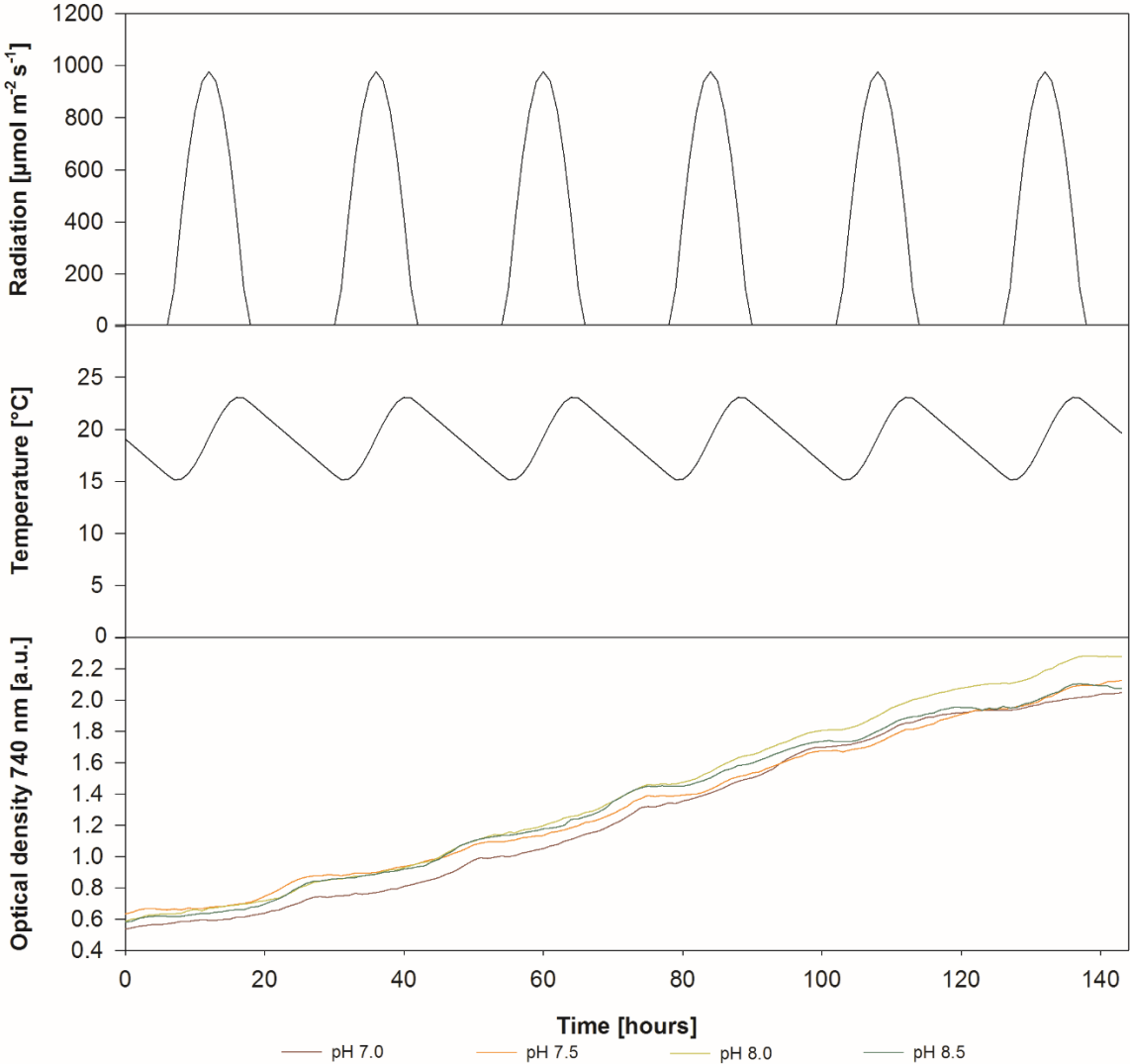


Figure 4.12 Growth by optical density of *Skeletonema sp. SKC0218* cultures maintained at different pH setpoints, showing light and temperature profile conditions. The graph represents the average of two experiments.

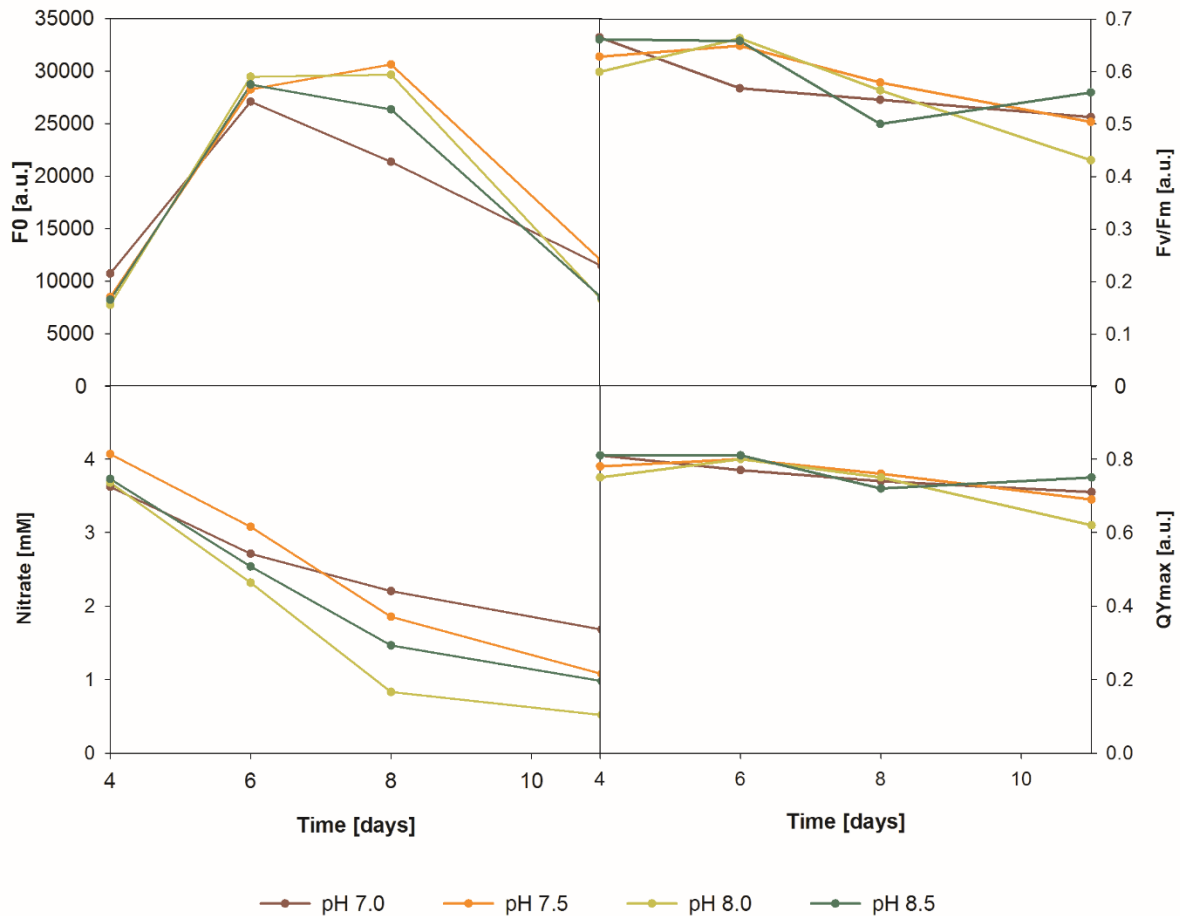


Figure 4.13 Different parameters recorded at the fourth, sixth, eighth and eleventh day and at the end of the experiment regarding the pH setpoint. Species: *Skeletonema sp. SKC0218*

The values of QY_{max} and F_v/F_m were stable until the sixth day in the first experiment and declined after this point of time; in the second experiment a remarkable decline was noticed from the fourth to the eighth day. It must be noted that a sample between these days would have been illuminative, as a decline of the culture is assumed in this time. The decline of these parameters indicated stress on the culture. The controlled culture conditions could be excluded to explain the stress, the final nitrate levels of above 1 mM did not indicate nutrient starvation. As the experiment was running for some days already, the cells might have suffered senescence.

Neither the values of the growth rate, nor of the final DW were significantly different for cultures grown at different pH setpoints (figure 4.14 and figure 4.15). These results were similar to another study, that found similar growth rates at pH values from 6.5 to 8.5. The growth rate of cultures grown at pH 9 or higher was found to be lower (Taraldsvik and Mykkestad 2000). In a study growing *Skeletonema* in 5 and 80 L PBRs, experiments were done

with and without pH regulation by CO₂ injection. In the latter case, the pH rose to a value of about 9, which impaired growth of the culture (Pérez et al. 2017). As such high values were not tested in the given experiment, it can be said that a pH in the physiological range supported *Skeletonema* sp. growth, and that the differences between the pH values did not impair the state of the culture. An impaired physiological state of all the cultures was observed after one week of growth.

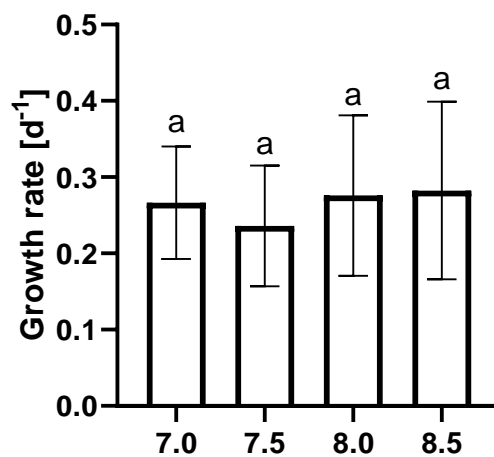


Figure 4.14 Growth rate of *Skeletonema* sp. SKC0218 cultures grown at different pH setpoints. Average results from two experiments are shown. The letters indicate no significant differences.

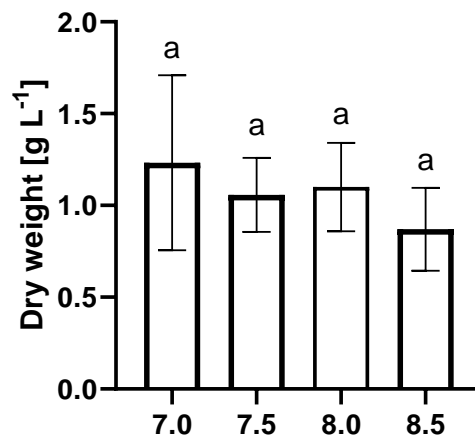


Figure 4.15 Final dry weight of *Skeletonema* sp. SKC0218 cultures, grown under different pH conditions. The values show an average of two experiments. Different letters indicate significant differences.

4.1.5 Conclusions from Algem[®] trials

In the Algem[®] system, influences on the growth of *Skeletonema* sp. by different culture parameters were tested under well-defined conditions. The strain *Skeletonema* sp. SKC0218 was identified to have stronger growth than *Skeletonema* sp. SKM0118 under the given

conditions. The light and temperature conditions, in the experimental units defined by a season profile, influenced the growth, the conditions with higher light and temperature was advantageous. For the tested species, a lower initial inoculum concentration resulted in significantly higher growth rates. Growth rates were not different for the different silicate concentrations under study. Still, a significantly lower F_v/F_m value indicated a silicate starvation of the culture with an initial silicate concentration of 0.05 mM. *Skeletonema* sp. growth was tolerant to the tested pH range of 7.0 to 8.5. The final DW could not be enhanced by any of the treatment.

4.2 *Skeletonema* sp. in outdoor cultivation

4.2.1 General procedure of a scale-up process

Scale-up processes are shown exemplarily (*figure 4.16* and *figure 7.4*). The process started generally with the transfer of about 25 L dense culture, growing in the laboratory, to inoculate an outdoor 100 L FP PBR, containing sterilized seawater and nutrients. The culture was then transferred to FP PBRs of larger volume (up to 1000 L), and later, 3000 to 4000 L culture was used to inoculate a tubular PBR of 8000 up to 19000 L. The volume of the PBR was frequently increased by adding culture medium, if the culture was harvested, the volume was substituted by the same medium.

4.2.2 Scale-up process and productivity of a tubular photobioreactor

In the scale-up process of the tubular PBR #1, first a 100 L FP PBR was inoculated and scaled up after eleven days to an 800 L FP PBR (*figure 4.16*). Originating from this, after ten more days two 1000 L FP PBRs were operated parallel and served to inoculate four 800 L FPs after four days. The 15000 L tubular PBR was inoculated after a scale-up process of 31 days with 3200 L culture volume.

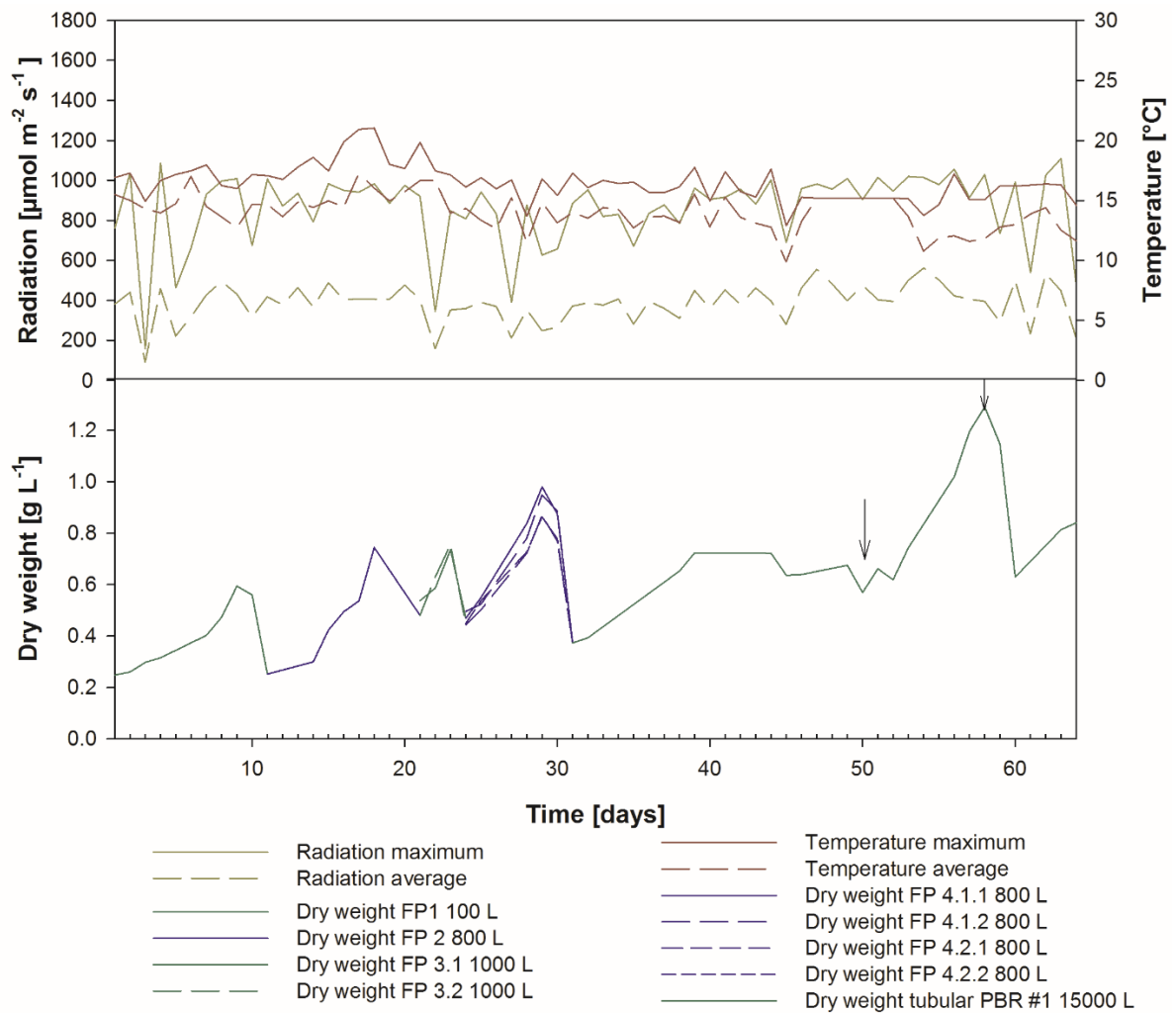


Figure 4.16 Growth of *Skeletonema sp. SKC0218* in flat panel photobioreactors (FP), used for the inoculation of a tubular photobioreactor (PBR #1). Meteorological data during the scale-up process is shown. Timespan: 20.11.2018 – 22.01.2019. Arrows indicate a culture renewal of 2000 and 5000 L, respectively.

The average radiation and temperature during the referred timespan were $387 \mu\text{mol m}^{-2} \text{s}^{-1}$ and $14 \text{ }^\circ\text{C}$, respectively, with maximum values of $1109 \mu\text{mol m}^{-2} \text{s}^{-1}$ and $21.02 \text{ }^\circ\text{C}$.

At the 51st and 59th day of the culture in total or the 20th and 28th day in the tubular reactor, 2000 L and 6000 L, respectively, were harvested and renewed by water and medium. The culture remained in the reactor for 33 days, before it was harvested completely. The overall biomass DW gained from these three harvests was 11.02 kg.

The productivity evaluation of the PBR in *table 4.1* is based on the daily measured OD, that was converted to DW. The values for this reactor differed a lot between the days and the standard variation was high. The average value of the growth rate 0.169 d^{-1} was among the lowest values observed in the Algem[®] system. The laboratory experiments were done using an autumn profile to regulate the light and temperature, the reactor was operated outdoors

in the winter with lower radiation. This might have reduced the growth of *Skeletonema* sp. in comparison to the laboratory trials. The values were slightly lower than the average growth rate of 0.217 d^{-1} , calculated for the complete production season.

Table 4.1 Productivity evaluation of *Skeletonema* sp. SKC0218 in the tubular photobioreactor #1, production from 20.12.18-22.01.19.

	Specific growth rate [d ⁻¹]	Volumetric productivity [g L ⁻¹ d ⁻¹]	Areal productivity [g m ⁻² d ⁻¹]
Average	0.169 ± 0.056	0.075 ± 0.053	3.330 ± 2.335
Maximum	0.270	0.176	7.756

4.2.3 Overview of scale-up processes during the season 2018/19

Several scale-up processes of *Skeletonema* sp. at Necton took place in the season 2018/19. In two cases, culture from one tubular reactor was used to inoculate another tubular reactor. The scale-up processes took between 28 and 73 days, depending on the growth of *Skeletonema* sp. in FP PBRs. Also, the time of production in the tubular PBR differed. The cultivation in a reactor was cancelled, when a strong contamination or slow growth were observed. Contaminants can be other microalgae species or aquatic microorganisms (figure 4.17). The production time was in one case as short as 12 days, another PBR could be operated for 33 days.

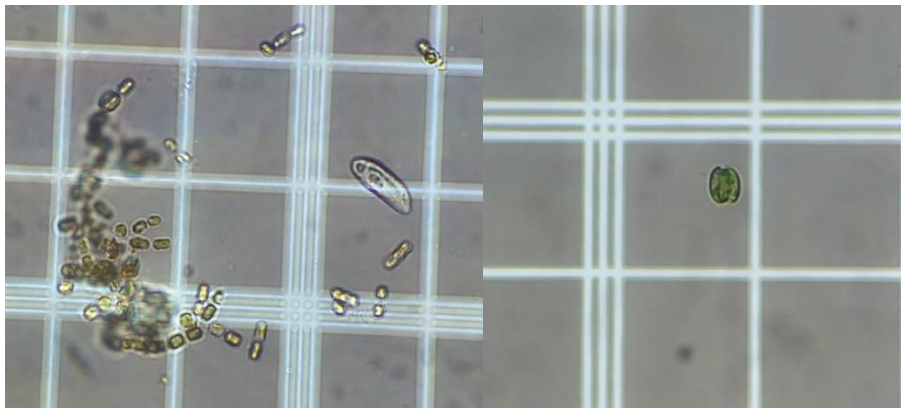


Figure 4.17 Left: a Ciliophora and right: Tetraselmis sp. found as contaminants in a *Skeletonema* sp. culture.

During the operated time, the PBRs were harvested irregularly (table 4.2), according to the OD. If the OD was at least 1.5 or the DW close to 1.0 g L^{-1} , culture volume was harvested. In the present case, no PBR was harvested more than two times, during the operated time. At the last day of each PBR, the complete remaining culture was harvested, and the biomass considered for the yield.

Table 4.2 Summary of the scale-up processes and harvests of *Skeletonema* sp. SKC0218 during the season 2018/29. Dates of the scale-up process as well as duration of the production in the tubular system are included. The harvested volume is the volume extracted during the production time and the final volume of the reactor.

Sequential number	Scale-up [days]	Inoculation	Production time [days]	Harvested volumes [summarized]	Biomass harvested [kg]
#1	31	20.12.2019	33	8000 L; final 15000 L	20.81
#2.1	28	10.01.2019	21	9000 L; final 15000 L	13.77
#2.2		25.01.2019	18	9000 L; final 15000 L	24.41
#2.3		1.02.2019	20	8000 L; final 15000	18.34
#3	62	12.02. 2019	29	9000 L; final 15000 L	16.95
#4	31 and 38	28.02.2019	20	3000 L; final 15000 L	11.72
#5	68 and 44	12.03.2019	14	5000 L; final 19000 L	11.22
#6		3.04.2019	12	5000 L; final 12000 L	15.16
#7	33 and 73	9.04.2019	18	2000 L; final 10000 L	8.96
Minimum	28		12		
Maximum	73		33		
Average	45 ± 17		21 ± 6		

The different PBRs yielded a different amount of biomass. The amount depends on the concentration of the culture, therefore, harvests and the operated time of the reactor.

4.2.4 Conclusion for scale-up processes of *Skeletonema* sp. cultures

Skeletonema sp. was successfully scaled up from indoor cultures to tubular PBRs, applying the given practices and facilities. The climatic conditions at the present place of production supported the growth of the species. The steady transfer of the culture to FP PBRs of increasing volume was a suitable strategy to cultivate biomass for the inoculum of PBRs with a production volume of several thousand litres. The duration of the scale-up took a different amount of time, depending on the weather conditions accelerating or inhibiting the growth of microalgae. The production time in the tubular PBRs varied distinctly and was strongly influenced by the weather conditions as well as by biological influences.

4.3 Large-scale production of *Skeletonema* sp. in tubular PBRs

The large-scale production of *Skeletonema* sp. was accomplished in outdoor tubular PBRs. The complete production period during the season 2018/19 lasted about five months (figure 4.18). The tubular PBRs had a volume of 10000 to 19000 L.

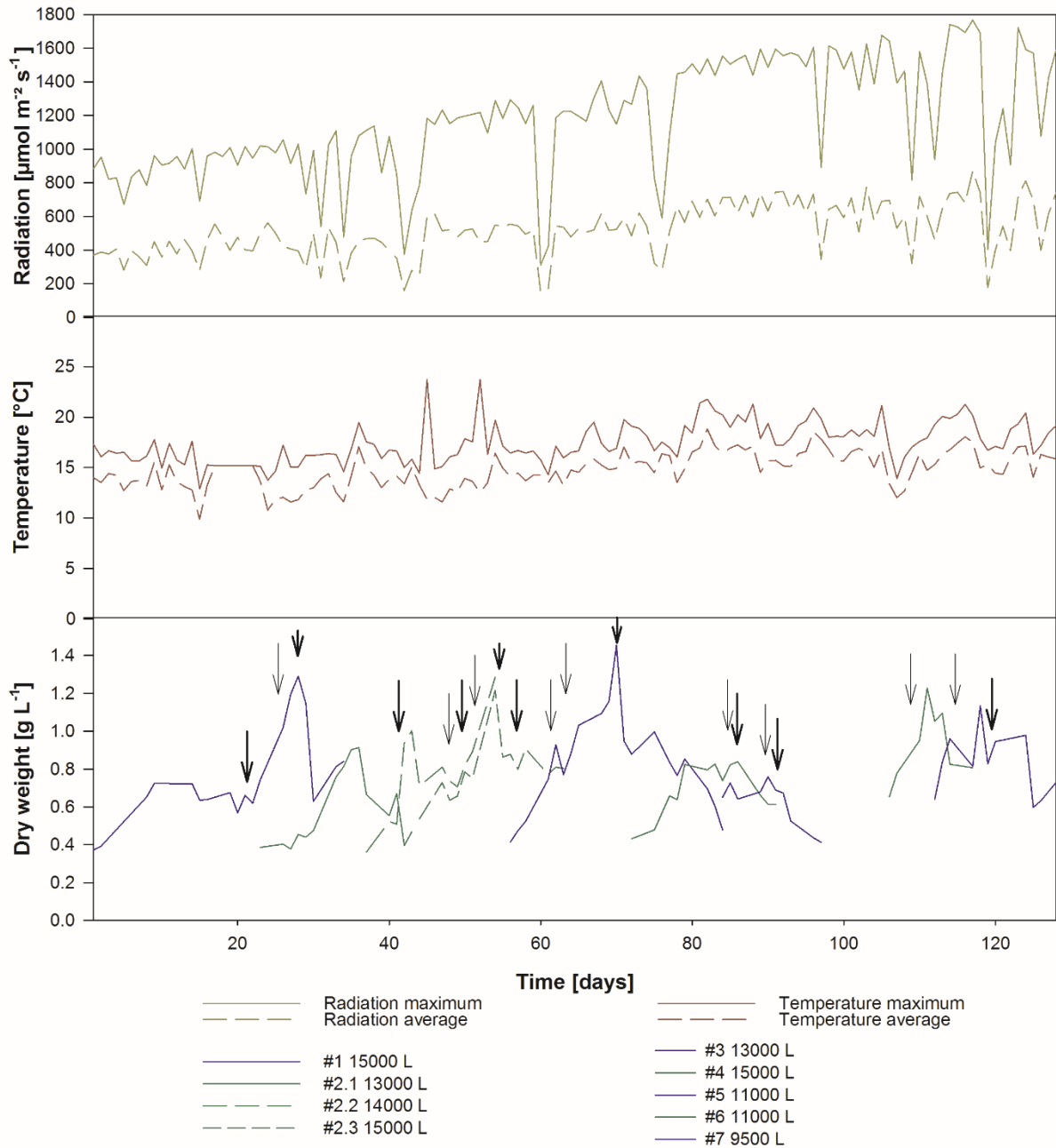


Figure 4.18 Overview of the large-scale production of *Skeletonema sp. SKC0218* in tubular photobioreactors. Timespan: 20.12.2018-26.04.2019. Thick arrows indicate culture harvest, thin arrows indicate addition of medium, explanation can be read in the additional data in table 7.3. Augmentation of reaction volume and volume renewal was always done with sterilized seawater and medium in the same ratio as used for inoculation. Meteorological data is shown in parallel.

4.3.1 Productivity evaluation

The growth rate in the reactors ranged from 0.129 to 0.331 d⁻¹, with an overall average of 0.217 d⁻¹ (table 4.3). The total volumetric and areal productivity were calculated based on the amount of harvested biomass. The maximal values were derived from a conversion of the continuous growth observation.

Table 4.3 Specific growth rate and productivity of all operated tubular photobioreactors with *Skeletonema sp. SKC0218* and average values of for the season 2018/19. The volume indicates the maximum volume of an operated reactor.

	Volume [L]	Specific growth rate [d ⁻¹]	Volumetric productivity [g L ⁻¹ d ⁻¹]		Areal productivity [g m ⁻² d ⁻¹]	
			Total / Maximal		Total / Maximal	
#1	15000	0.169 ± 0.056	0.031	0.176	1.355	7.756
#2.1	15000	0.129 ± 0.075	0.028	0.117	1.225	4.805
#2.2	15000	0.286 ± 0.281	0.072	1.283	3.160	14.787
#2.3	15000	0.208 ± 0.042	0.034	0.155	1.512	6.842
#3	15000	0.206 ± 0.068	0.039	0.297	1.719	13.103
#4	15000	0.260 ± 0.089	0.017	0.186	0.749	8.224
#5	19000	0.159 ± 0.002	0.015	0.329	0.853	17.418
#6	12000	0.220 ± 0.097	0.055	0.277	1.953	9.788
#7	10000	0.331 ± 0.108	0.017	0.320	0.496	9.405
Maximum		0.331	0.072	1.283	3.160	17.418
Minimum		0.129	0.015	0.117	0.497	4.805
Average		0.217 ± 0.059	0.034 ± 0.018	0.348 ± 0.338	1.447 ± 0.750	10.236 ± 3.839

A much higher maximum growth rate, than observed in the present production of *Skeletonema sp.* of 0.69 d⁻¹ was observed for *S. menzeli* (Jiang et al. 2015) or *S. marinoi* of 0.88 d⁻¹ in laboratory trials (Lauritano et al. 2015). In another work a division rate of 2.0 d⁻¹ was mentioned as close to the optimal value of 2.5 d⁻¹ (Kumar and Prabu 2014; Sakshaug and Andresen 1986). In the present laboratory results testing the same species in the Algem[®] system, growth rates between 0.15 and 0.40 were observed, the maximal value was higher than the maximum observed in the outdoor production. The Algem[®] PBRs had an initial cellular concentration of about 6·10⁵ cells mL⁻¹. The tubular PBRs had initial cellular concentrations between 1·10⁶ to 5·10⁶ cells mL⁻¹, an order of magnitude higher. Generally, a denser culture was desired to increase efficiency. Comparing *S. costatum* growth in different cultivation vessels and media, a maximum cellular density of 1.23·10⁶ cells mL⁻¹ was reported (Uddin and Zafar 2007). In the present study, the maximum cellular density in a tubular PBR with the strain SKC0118 was 1.89·10⁷ cells mL⁻¹ (data not presented), an order of magnitude higher than in the mentioned study. In the comparison of the average specific growth rate, the large-scale production stayed behind the laboratory trials. It was concluded, that *Skeletonema sp.* in the outdoor cultivation grew under suboptimal conditions. In the laboratory trials, lower inoculum concentrations led to higher growth rates. For all experiments and production PBRs, the initial cellular densities were in the range of 10⁵ - 10⁶ cells mL⁻¹. As a cellular concentration in a natural habitat, 10⁴ cells mL⁻¹ were given

(Saravanan and Godhe 2010). Another group started their experiments with $2.5 \cdot 10^4$ cells, two orders of magnitude lower than in the presented trials (Bertozzini et al. 2013). In a study with a comparable production scale, 10 % culture was used as inoculum concentration, but the group measured the OD at wavelength of 680 nm, which does not allow comparison to the present data (Pérez et al. 2017). A lower inoculum concentration could be tested. It must be considered, that the culture needed an adaption time to the outdoor conditions and that the lag-phase might be prolonged, since diluted cultures were strongly affected by irradiation. Also, the *Skeletonema* culture must compete with possible contaminants, in this sense a lower inoculum concentration might be disadvantageous.

The total volumetric productivity between the reactors ranged between 0.015 and 0.072 g L⁻¹ d⁻¹ (table 4.3). In a pilot-scale setup comparing two diatoms, volumetric productivities of *Skeletonema* sp. and *Chaetoceros* sp. of 0.028 and 0.032 g L⁻¹ d⁻¹ were achieved, which was similar to the average data of the present study (Pérez et al. 2017). Experiments growing another diatom, *Phaeodactylum* sp., in indoor PBRs showed an areal productivity of 21.0 g m⁻² d⁻¹ (Buono et al. 2016). These values were twice as high as the achieved maximal areal productivity. *Phaeodactylum* was produced in pilot-scale in open ponds and tubular PBR, achieving a slightly higher areal productivity of 13.1 g m⁻² d⁻¹ in the tubular system (Silva Benavides et al. 2013). Like in the own production of *Skeletonema* sp., DW densities of over 1 g L⁻¹ were achieved. In a study growing *S. costatum* in laboratory scale, extraordinary high biomass concentrations of up to 3.26 g L⁻¹ were presented, resulting in biomass productivities of up to 0.6 g L⁻¹ d⁻¹ (Sasireka and Muthuvelayudham 2015). Considering the highest value of the maximal productivity of 1.283 g L⁻¹ d⁻¹, *Skeletonema* sp. in the current outdoor cultivation even higher values could be achieved, whereas the average of the maximal productivity with 0.349 g L⁻¹ d⁻¹ is still half of the value presented by Sasireka and Muthuvelayudham (2015). Due to non-sterile conditions and lack of control of weather conditions, productivity in outdoor PBRs will always stay behind of a laboratory cultivation. The variation in productivity between the observed reactors could be due to various factors: the adaption of the strain to the outdoor conditions and the season, the present meteorological influences, contamination and aging of the culture and culture maintenance, respecting regulation of the pH value and nutrient level. The areal productivity had a high variation: if the reactor was filled completely, the area was more efficiently used and the value

increases. It can be noted, that the two first reactors showed rather low growth rates and productivities and were all under the average value. The conditions of spring might have been more favourable for the growth of *Skeletonema* sp. than during the winter. This was in line with the observation, that natural blooms of *Skeletonema* are strongest during spring (Saravanan and Godhe 2010). During the production season, the strain adapted to the weather condition. At the same time, the production performance was continuously optimised regarding scale-up process in the FP PBRs, sterility and nutrient control. All these factors in the large-scale cultivation need to be optimised and the culture maintained in ideal conditions to increase the productivity rates.

4.3.2 Conclusion for *Skeletonema* sp. in large-scale production

Skeletonema sp. was cultivated outdoors in large-scale with slightly lower growth rates compared to the own laboratory experiments. The productivity between the evaluated PBRs differed a lot, due to different weather conditions. Still, there were unknown influence factors and a stabilisation of the production is desirable.

4.4 Fluorometry evaluation of the large-scale production

4.4.1 Observation of a 100 L flat panel photobioreactor, scaled up to 1000 L of *Skeletonema* sp. SKC0119

Skeletonema sp. SKC0119 was cultivated outdoors in a 100 L FP PBR. In the observed period between the 18.03. and the 18.04.2019, the average radiation and temperature were $625 \mu\text{mol m}^{-2} \text{s}^{-1}$ and $15.79 \text{ }^\circ\text{C}$ (Figure 4.19). Some drops in radiation were noticed and the maximum values up to $1767 \mu\text{mol m}^{-2} \text{s}^{-1}$ and regarding the temperature $21.26 \text{ }^\circ\text{C}$ were measured at the end of the observed timespan, between the 12. and the 17.04.2019.

The pH during the described time was well regulated between 8.3 and 8.9, precluding an impairment of the culture growth by this factor.

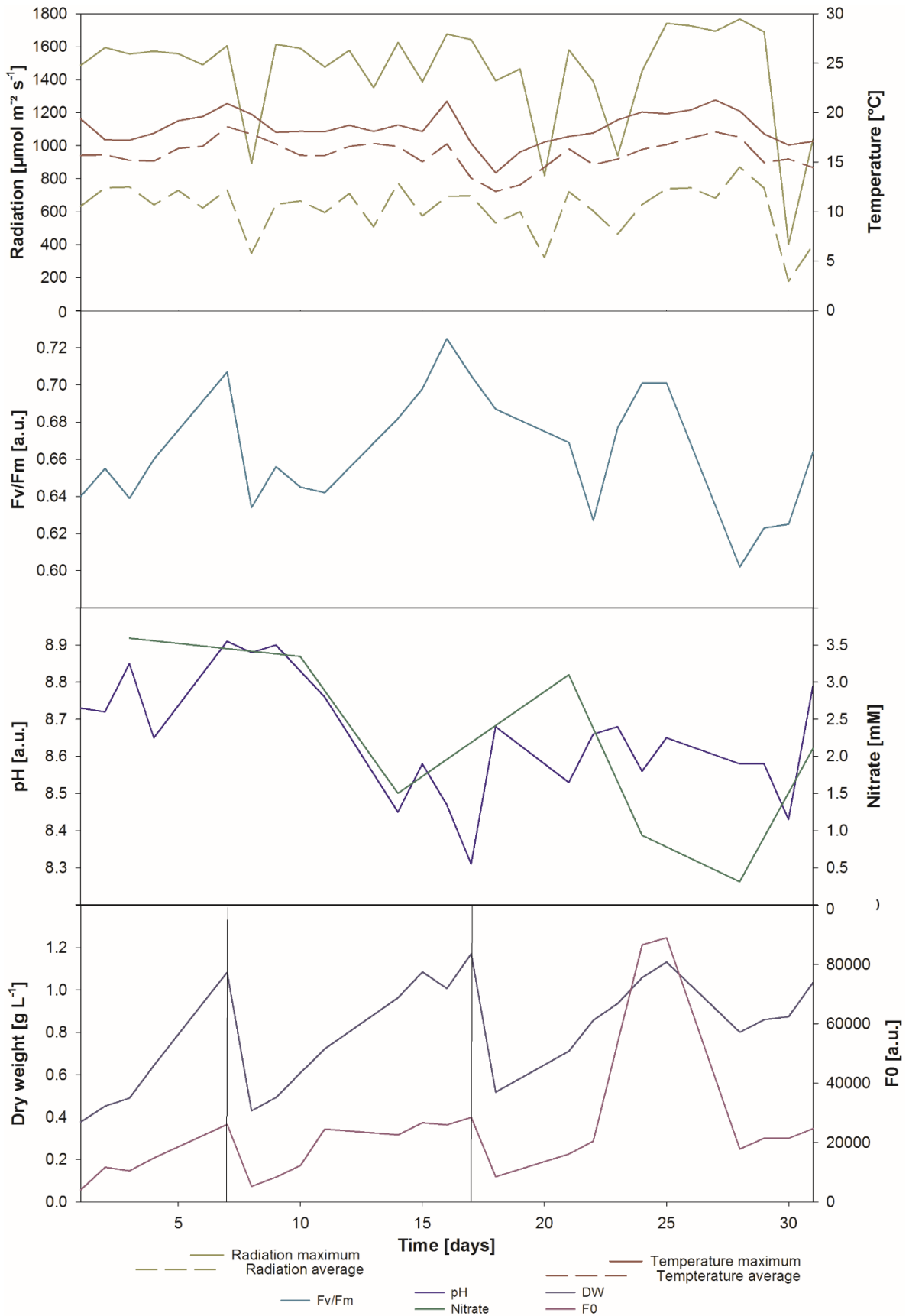


Figure 4.19 Flat panel photobioreactor, inoculated from laboratory culture at the 18.03.2019, volume 100 L. Transfer to 1000 L photobioreactor after seven days. At the seventeenth day, volume for the inoculation of another photobioreactor was used and renewed. Meteorological and fluorometry data are shown parallel with culture parameters and growth. Timespan: 18.03.-18.04.2019; Strain: *Skeletonema sp.* SKC0119.

The culture grew steadily in the first cultivation stage until the seventh day, when it was transferred to a larger PBR. The observation was accompanied by F_v/F_m values between 0.63 and 0.71. After that, the culture was more diluted in the second cultivation stage, initially, the F_v/F_m lowered to 0.63. In other FP PBRs, values as low as 0.45 were observed in cultures newly transferred to another culture vessel (Figure 7.6). These decreasing values were generally an indicator of stress on the culture. The measured meteorological values impaired the growth of a culture that came straight from the laboratory but were favourable for the development of a culture already growing outdoors for almost two weeks.

Similar patterns were observed by other groups, that found that diluted cultures were more susceptible to photo inactivation, this means stress by a higher irradiance (Masojídek et al. 2011). One week after the transfer, the F_v/F_m again reached a value of 0.68, which was considered as a high value, the culture did not suffer from stress. At this time, the DW reached 0.9 g L^{-1} , comparable to the 1.08 g L^{-1} before the culture was transferred. The F_v/F_m dropped again down to 0.62, as culture was taken out to inoculate another PBR. As the culture was diluted to 0.52 g L^{-1} , comparable to 0.43 g L^{-1} , the initial value in the second PBR, it was not able to protect itself in a sufficient manner to the high irradiation. The given sunlight irradiation might have been to intense for an efficient growth of *Skeletonema* sp., Sakshaug observed by altered doubling rates, that lower irradiation is preferred (Sakshaug and Andresen 1986). The study by Guihéneuf identified $100\text{-}340 \text{ } \mu\text{mol m}^{-2} \text{ s}^{-1}$ as an optimal growth condition (Guihéneuf et al. 2008). An optimal irradiation in outdoor condition still needs to be defined for *Skeletonema* sp., keeping in mind the constraint, that not the weather conditions but culture density and cultivation practices such as shading or cooling can be adapted.

The low value for F_v/F_m of 0.62 was observed at the 22nd day, together with a local maximum of the irradiation, $1580 \text{ } \mu\text{mol m}^{-2} \text{ s}^{-1}$ and the concentration of the culture at 0.71 g L^{-1} at the previous day. A culture diluted like this, might not have the ability to develop well with such a high irradiation. The lowest F_v/F_m was 0.60 at the 28th day, probably due to nutrient stress. The nitrate concentration fell to 0.3 mM at the 28th day of the culture, this was after a weekend with intense radiation. Probably, the culture had a quick metabolism during this time to consume the nutrients. In the days of increased radiation, the F_0 was unusually high, not reflecting the DW concentration of the culture anymore. This might be explained by an

extraordinary photosynthetically active culture. A decrease in F_v/F_m from 0.73 to 0.68 was observed in another culture at nitrate levels of 0.58 and 0.28 mM, respectively (see *figure 7.5*).

In the present case, the F_v/F_m decreased at constant radiation due to a dilution of the culture, the concentration of the cells was in this case not sufficient to protect the culture from photoinhibition. The denser a culture is, the higher is the effect of self-shading by the cells itself, making the culture more robust towards an elevated radiation.

4.4.2 Fluorometer evaluation of *Skeletonema* cultivated in a tubular photobioreactor

Skeletonema sp. was cultivated in an outdoors tubular PBR from the 12.02.-13.03.2019, with an initial volume of 13000 L, which was filled up to 15000 L. During the observed timespan the average radiation and temperature were $521 \mu\text{mol m}^{-2} \text{s}^{-1}$ and $15.2 \text{ }^\circ\text{C}$, respectively (*Figure 4.20*). Maximum values of up to $1554 \mu\text{mol m}^{-2} \text{s}^{-1}$ and $21.76 \text{ }^\circ\text{C}$ were observed.

In the first 15 days, both the biomass developed well, as also the F_v/F_m increased from initially 0.54 to 0.66, which was a value considered to reflect a good physiological state of the culture.

At the 14th day of the observation the highest radiation was observed, after this the F_v/F_m decreases to 0.60, which was an indication for photoinhibition. A radiation of up to $1400 \mu\text{mol m}^{-2} \text{s}^{-1}$ was observed at this day. The F_v/F_m recovered after that to up to 0.68, and also the biomass was increasing, interestingly, at the same time F_0 declined, showing a reduced photosynthetic capacity. Other tubular PBRs (see *figure 7.6* and *figure 7.7*) were impaired by average values for the radiation and temperature of above $600 \mu\text{mol m}^{-2} \text{s}^{-1}$ and $16 \text{ }^\circ\text{C}$.

The pH was in a range 7.3 and 8.6, assumedly a range without impairment to the *Skeletonema* culture. Due to high irradiation at the 14th and 15th day, the culture grew and consumed a lot of CO_2 , which left the pH value increasing. The sudden increase of the pH might also have been a reason for a lowered F_v/F_m in that days. During the whole observation, the culture was well supplied with nutrients, since the nitrate concentration never dropped under 0.98 mM.

The PBR generally showed a well development with some restrictions at elevated radiation and temperature. At the end of its lifetime, the growth stagnated for reasons not to be explained by the measured parameters. In this case a contamination and aging of the cells need to be considered.

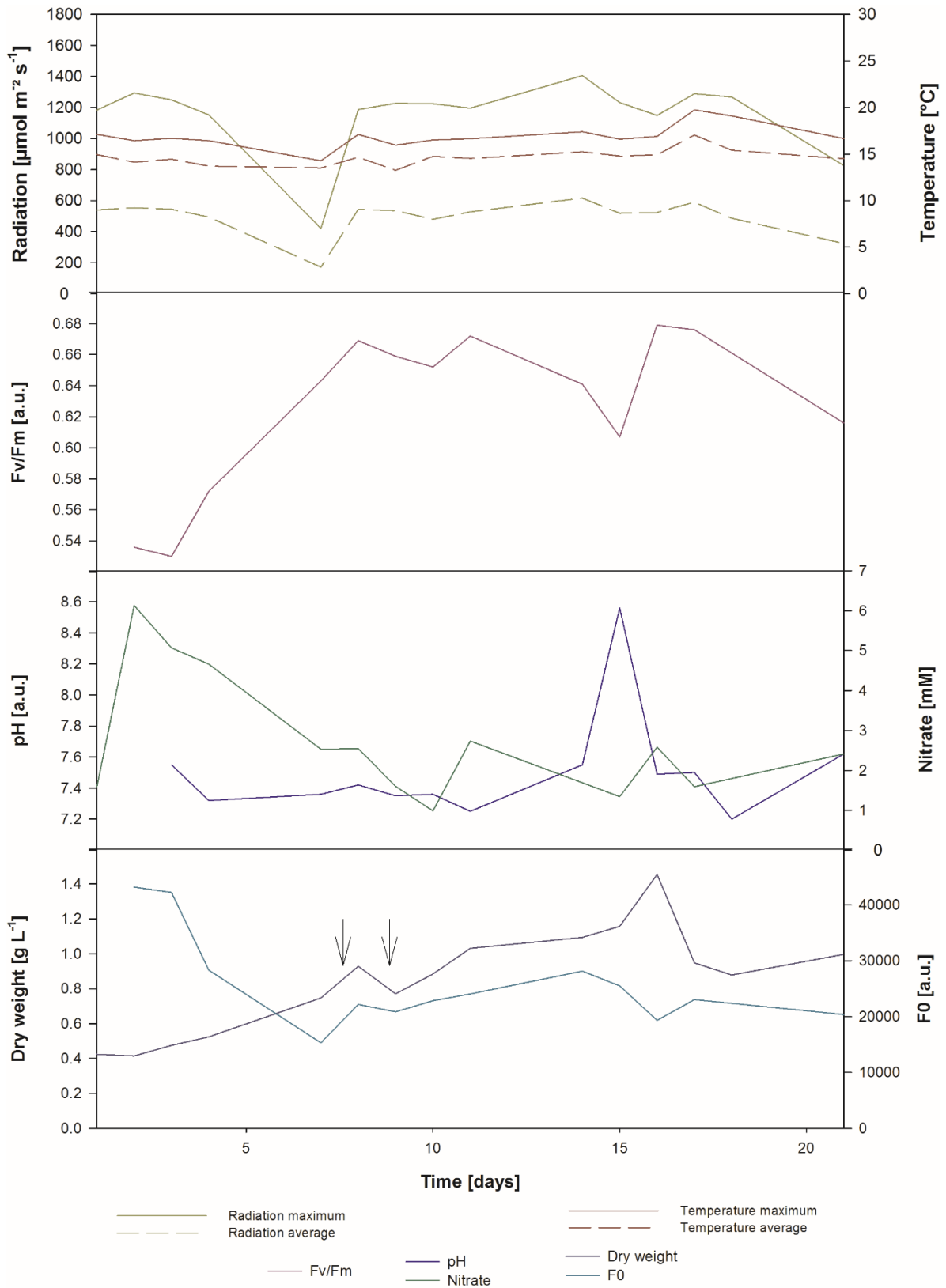


Figure 4.20 Growth development of *Skeletonema* sp. SKC0218 in relation to culture parameters and fluorometry evaluation, displayed with meteorological data. Tubular photobioreactor #3, 12.02.-13.03.2019, arrows indicate addition of 500 and 2500 L medium, respectively.

4.4.3 Conclusion for radiation effects *Skeletonema* growth

The observed growth and growth inhibitions during the production indicate that *Skeletonema* sp. growth was inhibited by an average radiation of $600 \mu\text{mol m}^{-2} \text{s}^{-1}$. It was reported, that an enzyme activity in *S. costatum* was enhanced at lower UV-radiation (Wu and Gao 2009). It must be considered, that *Skeletonema* might be more sensible to a high UV-radiation at a lower culture density as growth was inhibited in this case in combination with a high temperature. Still, a strict mechanism could not be defined, as the growth was influenced by more factors, such as media composition, adaption to the conditions, age of the culture and an eventual contamination or biological influence.

4.5 Biochemical evaluation of large-scale production

4.5.1 Average macronutrient composition of *Skeletonema* sp. biomass

The average carbohydrate, protein and lipid content in the sampled *Skeletonema* sp. biomass were 20.87, 31.52, 18.14 % of DW, with 33.66 % of DW of remaining ashes (table 4.4). The values of each samples are to be found in the additional data (Figure 7.8, figure 7.9, figure 7.10 and Figure 7.11).

Table 4.4 Macronutrient content in the biomass of *Skeletonema* sp. SKC0218, grown in large-scale. Average values and standard deviation from all collected samples during the season are calculated.

	Carbohydrate content [% DW]	Protein content [% DW]	Lipid content [% DW]	Total ashes [% DW]
Minimum	6.194	14.388	8.841	20.213
Maximum	36.375	53.536	66.355	46.542
Average	20.871 ± 14.106	31.523 ± 11.275	18.143 ± 11.139	33.656 ± 8.231

The carbohydrate content for *Skeletonema* sp. was given as 15-30 % of DW by another research group, where the present analysis revealed a value in the lower range of this (Olofsson et al. 2015). The same group found a protein content of 21-28 %, where in the present study a slightly higher value was measured. The lipid content was in the same range, namely 16-28 % as found by the mentioned group.

The high standard deviation of the macronutrient content in the biomass is striking. The different qualities of the biomass could be seen in a non-quantitative way in different colours of the lyophilized biomass (Figure 4.21).

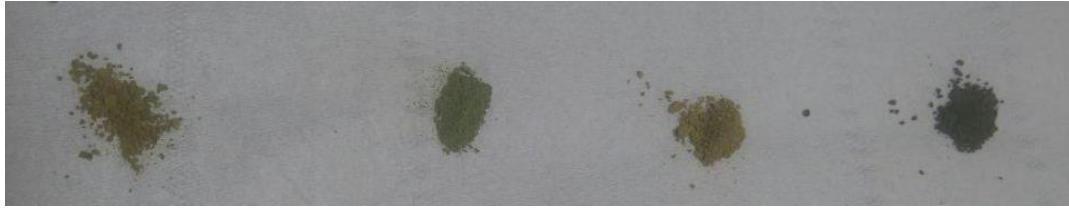


Figure 4.21 Lyophilized biomass from *Skeletonema* sp. SKC0218 in large scale production. All samples were harvested in March, stored and lyophilized under the same conditions.

The samples harvested on different days had a significant difference in the protein and total ashes content. In an early review, different culture conditions influencing the biochemical composition were identified as a constraint to microalgal biomass quality (De Pauw, Morales and Persoone 1984). The difference in lipid content could be explained by a different growth state of the culture, depending on the time already growing in one reactor (Schwenk et al. 2013). The mentioned study suggested that the growth stage has a stronger influence on the lipid content than salinity or temperature. A study examining the metabolome of *S. marinoi* confirmed the influence on growth stages on metabolites and revealed a diurnal difference during the exponential phase (Vidoudez and Pohnert 2012). In addition, it emphasized the dynamic of a metabolism, which alarms to always consider variations in the biomass constitution.

In the case of two samples, the harvested biomass was centrifuged in two batches on following days and samples were lyophilized in two batches (see Table 7.4). The samples centrifuged on different days differed in the carbohydrate and lipid contents. Regarding the protein content, one of the samples centrifuged first showed a significantly lower protein content than the sample lyophilized in another flask or samples centrifuged at the following day. The lyophilization process might have impaired the protein content in the sample, interestingly it was not different in the other two samples. The same sample that had a lower protein content, had a significantly less amount of total ashes.

There was no clear pattern to see, whether a sample harvested at a certain growth stage, had a different composition in any of the macronutrients. Also, regarding the season, it was not possible to tell that biomass harvested in a certain month had a different biochemical composition than in another month.

4.5.2 Valuable compounds in *Skeletonema* sp. biomass

Despite an unclear pattern of the macronutrient composition of *Skeletonema* sp. biomass from the present study, several studies showed that the biomass contains valuable functional

compounds. An oil content of up to 15% per DW was found for a locally isolated *Skeletonema* strain from the Bangladesh coast (Sharmin et al. 2016). In the same study, different extraction methods were compared, some of them only yielded as low as 2.49 % oil per DW. This pointed to the demand of a suitable and diligently performed extraction method. The extracted fatty acids were used in a skin anti-aging product (Widayati Putri et al. 2017). Here, a fatty acid content of up to 45.37 % of the lipid fraction was reported; major constituents were palmitic acid, palmitoleic acid, linoleic acid, oleic acid and stearic acid. Myristic acid was identified as the fatty acid with the highest percentage in another study; unsaturated fatty acids such as benzenedicarboxylic acid, arachidonic acid and eicosapentaenoic acid were also found in significant amounts (Sharmin et al. 2016). These findings were supported by the analysis of *S. marinoi* biomass applied in oyster feed (González-Araya et al. 2011). In addition, the ratio of saturated, monounsaturated and polyunsaturated fatty acids was given, the fatty acids fraction is constituted by 16.82, 15.46 and 65.73 % of the mentioned groups. A range of 38.26–50.48 % for polyunsaturated was found in *S. menzeli* (Jiang et al. 2015). The fatty acid methyl ester composition of *S. costatum* made the production of biodiesel with a high oxidation stability possible (Pérez et al. 2017). Up to 49 % fucoxanthin of total carotenoids were found in *S. costatum* (Pennington, Guillard and Liaaen-Jensen 1988). This anti-oxidant pigment has neuroprotective (Alghazwi et al. 2019) and anti-cancer activities (Chung et al. 2013). *Skeletonema* sp. was proven to inhibit the persistence of the pathogenic bacterium *Vibrio parahaemolyticus* (Olofsson et al. 2013). The biomass of the examined species found manifold and highly appreciated applications.

4.5.3 Conclusion from biochemical composition of *Skeletonema* biomass

Skeletonema sp. biomass contained compounds with highly appreciated applications. The content of carbohydrates, proteins and lipids was found to be very variable in the present study. A rigid control of growth parameters was demanded, to align the biochemical composition. The flexibility in the *Skeletonema* sp. metabolism could be used in the future, to direct the production of a desired compound by the manipulation of a culture parameter.

5. Conclusion and final remarks

5.1 Knowledge gain from laboratory trials

The laboratory trials, testing strains of *Skeletonema* sp., seasonal conditions, inoculum concentrations, silicate concentrations and pH setpoints revealed influences of the given parameters. *Skeletonema* sp. SKC0218 showed better growth than *Skeletonema* sp. SKM0118, the autumn condition was best for the examined species. Lower inoculum concentrations resulted in higher growth rates in the Algem[®] system. A culture provided with a silicate concentration of only 0.05 mM had a lower F_v/F_m value. This indicated stress, probably due to silicate starvation. pH values in the tested range from 7.0-8.5 did not impact the culture growth.

5.2 Experiences in outdoor production

In the season 2018/19, culture of *Skeletonema* sp. was successfully scaled up from 5 L glass balloons in the laboratory over 100-1000 L FP PBRs growing outside to tubular PBRs of up to 19000 L. The scale-up process lasted about one month. *Skeletonema* sp. culture was able to grow in tubular PBRs for 14-33 days. The maximum specific growth rate in tubular PBRs was 0.331 d^{-1} , an average volumetric productivity of $0.034 \text{ g L}^{-1} \text{ d}^{-1}$ was achieved, comparable to other diatoms.

The fluorometry evaluation registered a lowered F_v/F_m value under reduced nutrient levels as well as under high irradiation, indicating an impaired physiological state of the cultures. It was demonstrated that a high irradiation had a greater impact on diluted cultures. Also, cultures already growing for some days in a given PBR were adapted to the present weather conditions and were not as stressed by an increased irradiation as newly transferred cultures.

5.3 Value of *Skeletonema* sp. biomass

Skeletonema sp. has a balanced macronutrient profile, allowing it to serve as aquaculture feed. In addition, the presence of valuable compounds like unsaturated fatty acids and pigments frequently reported in the literature gave the species a potential use as nutraceutical.

5.4 Open questions

In the field of fluorometry, still a threshold of irradiation needs to be uncovered for *Skeletonema* sp. Probably, a maximum radiation must be defined for every dilution. The cells

ability to adapt to environmental conditions makes this issue more complex. Cultures of *Skeletonema* sp. could not be cultivated for a long time. Reasons could either be senescence or a biological contamination. Factors triggering the aging of the cells are not yet identified. As *Skeletonema* sp. shows a certain tolerance to salt concentration and pH value, it is thinkable to design culture conditions that allow growth of the cultivated microalgae but disfavour the spread of the contaminant.

5.5 Suggestions for future research

Further insight will improve the production of *Skeletonema* sp. Different *Skeletonema* sp. strains should be grown outdoors in pilot-scale, in order to find a strain well adapted to the given climatic conditions. In laboratory experiments, silicate concentrations between the insufficient 0.05 mM and saturating 0.11 mM can be tested, to optimise the medium composition and consecutive expenses for the cultivation. Outdoor trials with an inoculum concentration lower than 10^5 cells mL⁻¹ would reveal, if high growth rates can be achieved, as were observed in lab-scale, or other biological effects and contaminants impair the growth of a diluted culture. As production units are exposed to given climatic conditions, a cooling and protection of PBRs against extreme rises of irradiation should be developed and evaluated.

Regarding the macro-nutrient composition, the growth stage at the time of harvest must be observed. Depending on the desired application, the biochemical content can be manipulated, adjusting culture conditions and choosing specifically the time of harvest. Different extraction methods can be applied to the biomass in order to improve the accuracy of the analyses.

5.6 Summary

After conducting laboratory trials, the outdoor cultivation of *Skeletonema* sp. was optimised. The facilities of the production plant and climatic conditions at the location of Necton are suitable for the growth of this microalgae species. In the observed season, it was cultivated with different productivities. The biochemical analysis composition proofed the high value of this microalga. The scale-up procedure and large-scale production can continually be improved by providing optimal culture conditions and maintaining best production practices to rise the productivity.

6. References

- Alghazwi, M., Smid, S., Musgrave, I., Zhang, W. (2019) In vitro studies of the neuroprotective activities of astaxanthin and fucoxanthin against amyloid beta (A β 1-42) toxicity and aggregation. *Neurochemistry International* 124. <https://doi.org/https://doi.org/10.1016/j.neuint.2019.01.010>
- Arad, S.M., Yaron, A. (1992) Natural pigments from red microalgae for use in foods and cosmetics. *Trends in Food Science & Technology* 3: 92–97. [https://doi.org/https://doi.org/10.1016/0924-2244\(92\)90145-M](https://doi.org/https://doi.org/10.1016/0924-2244(92)90145-M)
- Balkos, K.D., Colman, B. (2007) Mechanism of CO₂ acquisition in an acid-tolerant *Chlamydomonas*. *Plant, Cell and Environment* 30 (6): 745–52. <https://doi.org/10.1111/j.1365-3040.2007.001662.x>
- Bertozzini, E., Galluzzi, L., Ricci, F., Penna, A., Magnani, M. (2013) Neutral Lipid Content and Biomass Production in *Skeletonema marinoi* (Bacillariophyceae) Culture in Response to Nitrate Limitation. *Applied Biochemistry and Biotechnology* 170 (7): 1624–36. <https://doi.org/10.1007/s12010-013-0290-3>
- Blanchemain, A., Grizeau, D., Guary, J. (1994) Effect of different organic buffers on the growth of *Skeletonema costatum* cultures; further evidence for an autoinhibitory effect. *Journal of Plankton Research* 16 (10): 1433–40
- Bligh, E.G., Dyer, W.J. (1959) A rapid method of total lipid extraction and purification. *Canadian Journal of Biochemistry and Physiology* 37 (8): 911–17
- Bouchard, J.N., Purdie, D.A. (2011) Effect of elevated temperature, darkness, and hydrogen peroxide treatment on oxidative stress and cell death in the bloom-forming toxic cyanobacterium *Microcystis aeruginosa*. *Journal of Phycology* 47 (6): 1316–25. <https://doi.org/10.1111/j.1529-8817.2011.01074.x>
- Boukhris, S., Athmouni, K., Hamza-Mnif, I., Siala-Elleuch, R., Ayadi, H., Nasri, M., Sellami-Kamoun, A. (2017) The Potential of a Brown Microalga Cultivated in High Salt Medium for the Production of High-Value Compounds. *BioMed Research International* 2017: 1–10. <https://doi.org/10.1155/2017/4018562>
- Brand, L.E. (1984) The salinity tolerance of forty-six marine phytoplankton isolates. *Estuarine, Coastal and Shelf Science* 18 (5): 543–56. [https://doi.org/10.1016/0272-7714\(84\)90089-1](https://doi.org/10.1016/0272-7714(84)90089-1)
- Brillatz, T., Lauritano, C., Jacmin, M., Khamma, S., Marcourt, L., Righi, D., Romano, G., et al. (2018) Zebrafish-based identification of the antiseizure nucleoside inosine from the marine diatom *Skeletonema marinoi*. *PLoS ONE* 13 (4): 1–15. <https://doi.org/10.1371/journal.pone.0196195>
- Brown, M.R., Jeffrey, S.W., Volkman, J.K., Dunstan, G.A. (1997) Nutritional properties of microalgae for mariculture. *Aquaculture* 151 (1): 315–31. [https://doi.org/https://doi.org/10.1016/S0044-8486\(96\)01501-3](https://doi.org/https://doi.org/10.1016/S0044-8486(96)01501-3)
- Buono, S., Colucci, A., Angelini, A., Langellotti, A.L., Massa, M., Martello, A., Fogliano, V., Dibenedetto, A. (2016) Productivity and biochemical composition of *Tetradesmus obliquus* and *Phaeodactylum tricorutum*: effects of different cultivation approaches. *Journal of Applied Phycology* 28 (6): 3179–92. <https://doi.org/10.1007/s10811-016-0876-6>
- Chini Zittelli, G., Rodolfi, L., Tredici, M.R. (2003) Mass cultivation of *Nannochloropsis* sp. in annular reactors. *Journal of Applied Phycology* 15 (2–3): 107–14. <https://doi.org/10.1023/A:1023830707022>
- Chung, T.W., Choi, H.J., Lee, J.Y., Jeong, H.S., Kim, C.H., Joo, M., Choi, J.Y., et al. (2013) Marine algal fucoxanthin inhibits the metastatic potential of cancer cells. *Biochemical and Biophysical Research Communications* 439 (4): 580–85. <https://doi.org/10.1016/j.bbrc.2013.09.019>

- Colman, B., Balkos, K.D. (2005) Mechanisms of inorganic carbon acquisition in two *Euglena* species. *Canadian Journal of Botany* 83 (7): 865–71. <https://doi.org/1139/B05-072>
- Colman, B., Rotatore, C. (1995) Photosynthetic inorganic carbon uptake and accumulation in two marine diatoms. *Plant, Cell & Environment* 18 (8): 919–24. <https://doi.org/10.1111/j.1365-3040.1995.tb00601.x>
- Cosgrove, J., Borowitzka, M.A. (2010) Chlorophyll Fluorescence Terminology: An Introduction. In *Chlorophyll a Fluorescence in Aquatic Sciences: Methods and Applications*, edited by Suggett, D.J., Prášil, O., and Borowitzka, M.A, 1–17. Dordrecht: Springer Netherlands. https://doi.org/10.1007/978-90-481-9268-7_1
- Croft, M.T., Lawrence, A.D., Raux-Deery, E., Warren, M.J., Smith, A.G. (2005) Algae acquire vitamin B₁₂ through a symbiotic relationship with bacteria. *Nature* 438 (7064): 90–93. <https://doi.org/10.1038/nature04056>
- Crowe, B., Attalah, S., Agrawal, S., Waller, P., Ryan, R., Wagenen, J. Van, Chavis, A., et al. (2012) A comparison of *Nannochloropsis salina* growth performance in two outdoor pond designs: Conventional raceways versus the arid pond with superior temperature management. *International Journal of Chemical Engineering* 2012: 1–9. <https://doi.org/10.1155/2012/920608>
- D'Souza, F.M.L., Loneragan, N.R. (1999) Effects of monospecific and mixed-algae diets on survival, development and fatty acid composition of penaeid prawn (*Penaeus* spp.) larvae. *Marine Biology* 133 (4): 621–33. <https://doi.org/10.1007/s002270050502>
- Fabregas, J., Herrero, C. (1986) Marine microalgae as a potential source of minerals in fish diets. *Aquaculture* 151 (3): 237–43. [https://doi.org/https://doi.org/10.1016/0044-8486\(86\)90315-7](https://doi.org/https://doi.org/10.1016/0044-8486(86)90315-7)
- Farias Silva, C.E. de, Bertucco, A. (2016) Bioethanol from microalgae and cyanobacteria: A review and technological outlook. *Process Biochemistry* 51 (11): 1833–42. <https://doi.org/10.1016/j.procbio.2016.02.016>
- Fouqueray, M., Mouget, J.-L., Morant-Manceau, A., Tremblin, G. (2007) Dynamics of short-term acclimation to UV radiation in marine diatoms. *Journal of Photochemistry and Photobiology B: Biology* 89 (1): 1–8. <https://doi.org/https://doi.org/10.1016/j.jphotobiol.2007.07.004>
- Galbraith, H., Miller, T.B. (1973) Physicochemical Effects of Long Chain Fatty Acids on Bacterial Cells and their Protoplasts. *Journal of Applied Bacteriology* 36 (4): 647–58. <https://doi.org/10.1111/j.1365-2672.1973.tb04150.x>
- Gao, G., Xia, J., Yu, J., Zeng, X. (2018) Physiological response of a red tide alga (*Skeletonema costatum*) to nitrate enrichment, with special reference to inorganic carbon acquisition. *Marine Environmental Research* 133 (2018): 15–23. <https://doi.org/10.1016/j.marenvres.2017.11.003>
- Gill, I., Valivety, R. (1997) Polyunsaturated fatty acids, part 1: Occurrence, biological activities and applications. *Trends in Biotechnology* 15 (10): 401–9. [https://doi.org/https://doi.org/10.1016/S0167-7799\(97\)01076-7](https://doi.org/https://doi.org/10.1016/S0167-7799(97)01076-7)
- Gilstad, M., Johnsen, G., Sakshaug, E. (1993) Photosynthetic parameters, pigment composition and respiration rates of the marine diatom *Skeletonema costatum* grown in continuous light and a 12:12 h light-dark cycle. *Journal of Plankton Research* 15 (8): 939–51. <https://doi.org/10.1093/plankt/15.8.939>
- Godhe, A., Kremp, A., Montresor, M. (2014) Genetic and Microscopic Evidence for Sexual Reproduction in the Centric Diatom *Skeletonema marinoi*. *Annals of Anatomy* 165 (4): 401–16. <https://doi.org/10.1016/j.prodis.2014.04.006>

- Goiris, K., Colen, W. Van, Wilches, I., León-Tamariz, F., Cooman, L. De, Muylaert, K. (2015) Impact of nutrient stress on antioxidant production in three species of microalgae. *Algal Research* 7 (2015): 51–57. <https://doi.org/10.1016/j.algal.2014.12.002>
- Goldman, J.C. (1999) Inorganic carbon availability and the growth of large marine diatoms. *Marine Ecology Progress Series* 180: 81–91. <https://doi.org/10.3354/meps180081>
- González-Araya, R., Quéau, I., Quéré, C., Moal, J., Robert, R. (2011) A physiological and biochemical approach to selecting the ideal diet for *Ostrea edulis* (L.) broodstock conditioning (part A). *Aquaculture Research* 42 (5): 710–26. <https://doi.org/10.1111/j.1365-2109.2010.02731.x>
- Guihéneuf, F., Mimouni, V., Ulmann, L., Tremblin, G. (2008) Environmental factors affecting growth and omega 3 fatty acid composition in *Skeletonema costatum*. The influences of irradiance and carbon source. *Diatom Research* 23 (1): 93–103. <https://doi.org/10.1080/0269249X.2008.9705739>
- Guillard, R.R.L., Ryther, J.H. (1962) Studies of Marine Planktonic Diatoms. *Canadian Journal of Microbiology* 8 (1140): 229–39. <https://doi.org/10.1139/m62-029>
- Hannah, C., Mani, M., Ramasamy, R. (2013) Evaluation of the Biochemical Composition of Four Marine Algae and Its Nutritional Value for Brine Shrimp. *Journal of Pharmacy and Boiological Sciences* 6 (3): 47–51. <https://doi.org/10.9790/3008-0634751>
- Harrison, P.J., Waters, R.E., Taylor, F.J.R. (1980) A broad spectrum artificial sea water medium for coastal and open ocean phytoplankton. *Journal of Phycology* 16 (1): 28–35. <https://doi.org/10.1111/j.0022-3646.1980.00028.x>
- Hasle, G.R., Evensen, D.L. (1976) Brackish Water and Freshwater Species of the Diatom Genus *Skeletonema* II. *Skeletonema potamos* comb. nov. *Journal of Phycology* 12 (1): 73–82. <https://doi.org/10.1111/j.1529-8817.1976.tb02829.x>
- Herawati, V.E., Hutabarat, J., Radjasa, O.K. (2015) Nutritional Content of *Artemia* sp. Fed with *Chaetoceros calcitrans* and *Skeletonema costatum*. *HAYATI Journal of Biosciences* 21 (4): 166–72. <https://doi.org/10.4308/hjb.21.4.166>
- Herbert, D., Phipps, P.J., Strange, R.E. (1971) Determination of protein with the Folin-Ciocalteu reagent. In *Methods in Microbiology*, edited by Norris, J.R. and Ribbons, D.W., 5B:249–52. London: Academic Press. [https://doi.org/10.1016/S0580-9517\(08\)70641-X](https://doi.org/10.1016/S0580-9517(08)70641-X)
- Hevia-Orube, J., Orive, E., David, H., Laza-Martinez, A., Seoane, S. (2016) *Skeletonema* species in a temperate estuary: a morphological, molecular and physiological approach. *Diatom Research* 31 (3): 185–97. <https://doi.org/10.1080/0269249X.2016.1228548>
- Hoek, C. Van Den, Mann, D.G., Jahns, H. (1995) *Algae. An Introduction to Phycology*. Cambridge University Press
- Houcke, J. Van, Medina, I., Maehre, H.K., Cornet, J., Cardinal, M., Linsen, J., Luten, J. (2017) The effect of algae diets (*Skeletonema costatum* and *Rhodomonas baltica*) on the biochemical composition and sensory characteristics of Pacific cupped oysters (*Crassostrea gigas*) during land-based refinement. *Food Research International* 100 (2017): 151–60. <https://doi.org/10.1016/j.foodres.2017.06.041>
- Jiang, X., Han, Q., Gao, X., Gao, G. (2015) Conditions optimising on the yield of biomass, total lipid, and valuable fatty acids in two strains of *Skeletonema menzeli*. *Food Chemistry* 194: 723–32. <https://doi.org/10.1016/j.foodchem.2015.08.073>
- Jorquera, O., Kiperstok, A., Sales, E.A., Embiruçu, M., Ghirardi, M.L. (2010) Comparative energy life-cycle analyses of microalgal biomass production in open ponds and photobioreactors. *Bioresource Technology* 101 (4): 1406–13. <https://doi.org/10.1016/j.biortech.2009.09.038>

- Kang, L.-K., Tsui, F.-H., Chang, J. (2012) Quantification of Diatom Gene Expression in the Sea by Selecting Uniformly Transcribed mRNA as the Basis for Normalization. *Applied and Environmental Microbiology* 78 (17): 6051–58. <https://doi.org/10.1128/aem.00935-12>
- Kaspar, H.F., Keys, E.F., King, N., Smith, K.F., Kesarcodi-Watson, A., Miller, M.R. (2014) Continuous production of *Chaetoceros calcitrans* in a system suitable for commercial hatcheries. *Aquaculture* 420–421: 1–9. <https://doi.org/10.1016/j.aquaculture.2013.10.021>
- Kooistra, W.H.C.F., Sarno, D., Balzano, S., Gu, H., Andersen, R.A., Zingone, A. (2008) Global Diversity and Biogeography of *Skeletonema* Species (Bacillariophyta). *Protist* 159 (2): 177–93. <https://doi.org/10.1016/j.protis.2007.09.004>
- Kumar, C.S., Prabu, V.A. (2014) Culture of the phytoplankton *Skeletonema costatum*, Cleve, 1873. *International Journal of Current Microbiology and Applied Sciences* 3 (11): 129–36
- Lai, J., Yu, Z., Song, X., Cao, X., Han, X. (2011) Responses of the growth and biochemical composition of *Prorocentrum donghaiense* to different nitrogen and phosphorus concentrations. *Journal of Experimental Marine Biology and Ecology* 405 (1–2): 6–17. <https://doi.org/10.1016/j.jembe.2011.05.010>
- Laing, I. (1985) Factors affecting the large-scale production of four species of commercially important marine algae. *Aquaculture* 44 (2): 161–66. [https://doi.org/10.1016/0044-8486\(85\)90019-5](https://doi.org/10.1016/0044-8486(85)90019-5)
- Latała, A., Marcin, N., Stepnowski, P. (2009) Toxicity of imidazolium and pyridinium based ionic liquids towards algae. *Chlorella vulgaris*, *Oocystis submarina* (green algae) and *Cyclotella meneghiniana*, *Skeletonema marinoi* (diatoms), 580–88. <https://doi.org/10.1039/b821140j>
- Lauritano, C., Martín, J., La Cruz, M. De, Reyes, F., Romano, G., Ianora, A. (2018) First identification of marine diatoms with anti-tuberculosis activity. *Scientific Reports* 8 (1): 1–10. <https://doi.org/10.1038/s41598-018-20611-x>
- Lauritano, C., Orefice, I., Procaccini, G., Romano, G., Ianora, A. (2015) Key genes as stress indicators in the ubiquitous diatom *Skeletonema marinoi*. *BMC Genomics* 16 (411): 1–10. <https://doi.org/10.1186/s12864-015-1574-5>
- Lee, E.T.-Y., Bazin, M.J. (1990) A laboratory scale air-lift helical photobioreactor to increase biomass output rate of photosynthetic algal cultures. *New Phytologist* 116 (2): 331–35. <https://doi.org/10.1111/j.1469-8137.1990.tb04722.x>
- Leonardos, N., Lucas, I.A.N. (2000) The nutritional value of algae grown under different culture conditions for *Mytilus edulis* L. larvae. *Aquaculture* 182 (3–4): 301–15. [https://doi.org/10.1016/S0044-8486\(99\)00269-0](https://doi.org/10.1016/S0044-8486(99)00269-0)
- Liang, Y., Zhao, X., Chi, Z., Rover, M., Johnston, P., Brown, R., Jarboe, L., Wen, Z. (2013) Utilization of acetic acid-rich pyrolytic bio-oil by microalga *Chlamydomonas reinhardtii*: Reducing bio-oil toxicity and enhancing algal toxicity tolerance. *Bioresour Technol* 133: 500–506. <https://doi.org/10.1016/j.biortech.2013.01.134>
- Lim, S.L., Chu, W.L., Phang, S.M. (2010) Use of *Chlorella vulgaris* for bioremediation of textile wastewater. *Bioresour Technol* 101 (19): 7314–22. <https://doi.org/10.1016/j.biortech.2010.04.092>
- Lorenz, R.T., Cysewski, G.R. (2000) Commercial potential for *Haematococcus* microalgae as a natural source of astaxanthin. *Trends in Biotechnology* 18 (4): 160–67. [https://doi.org/https://doi.org/10.1016/S0167-7799\(00\)01433-5](https://doi.org/https://doi.org/10.1016/S0167-7799(00)01433-5)
- Lowry, O.H., Rosebrough, N.J., Farr, A.L., Randall, R.J. (1951) Protein measurement with the folin

- Phenol Reagent. *Journal of Biological Chemistry* 193 (1): 256–75
- Maier, R.M. (2009) Bacterial Growth. In *Environmental Microbiology*, edited by Pepper, I.L. and Gerba, C.P., 37–54. Elsevier. <https://doi.org/10.1016/B978-0-12-370519-8.00003-1>
- Makarova, I. V, Proshkina-Lavrenko, A.I. (1964) New Diatoms in the Plankton of the Caspian Sea. *Novitates Systematicae Plantarum Non Vascularium (Academia Scientiarum URSS Institutum Botanicum Nomine V.L. Komarovii)* 1 (1964): 34–43
- Malapascua, J.R.F., Jerez, C.G., Sergejevová, M., Figueroa, F.L., Masojídek, J. (2014) Photosynthesis monitoring to optimize growth of microalgal mass cultures: Application of chlorophyll fluorescence techniques. *Aquatic Biology* 22: 123–40. <https://doi.org/10.3354/ab00597>
- Masojídek, J., Kopecký, J., Giannelli, L., Torzillo, G. (2011) Productivity correlated to photobiochemical performance of *Chlorella* mass cultures grown outdoors in thin-layer cascades. *Journal of Industrial Microbiology and Biotechnology* 38 (2): 307–17. <https://doi.org/10.1007/s10295-010-0774-x>
- Masojídek, J., Vonshak, A., Torzillo, G. (2010) Chlorophyll Fluorescence Applications in Microalgal Mass Cultures. In *Chlorophyll a Fluorescence in Aquatic Sciences: Methods and Applications*, edited by Suggett, D.J., Prášil, O., and Borowitzka, M.A., 277–92. Dordrecht: Springer Netherlands. https://doi.org/10.1007/978-90-481-9268-7_13
- Naviner, M., Bergé, J.P., Durand, P., Bris, H. Le (1999) Antibacterial activity of the marine diatom *Skeletonema costatum* against aquacultural pathogens. *Aquaculture* 174 (1–2): 15–24. [https://doi.org/10.1016/S0044-8486\(98\)00513-4](https://doi.org/10.1016/S0044-8486(98)00513-4)
- Olenina, I., Hajdu, S., Edler, L., Andersson, A., Wasmund, N., Busch, S., Göbel, J., Gromisz, S., Huseby, S., Huttunen, M., Jaanus, A., Kokkonen, P., Ledaine, I., Niemkiewicz, E. (2006) Biovolumes and Size-Classes of Phytoplankton in the Baltic Sea. *Baltic Sea Environment Proceedings* 106: 144
- Olofsson, M., Asplund, M.E., Karunasagar, I., Rehnstam-Holm, A.S., Godhe, A. (2013) *Prorocentrum micans* promote and *Skeletonema tropicum* disfavours persistence of the pathogenic bacteria *Vibrio parahaemolyticus*. *Indian Journal of Marine Sciences* 42 (6): 729–33
- Olofsson, M., Lindehoff, E., Frick, B., Svensson, F., Legrand, C. (2015) Baltic Sea microalgae transform cement flue gas into valuable biomass. *Algal Research* 11 (2015): 227–33. <https://doi.org/10.1016/j.algal.2015.07.001>
- Ono, E., Cuello, J.L. (2006) Feasibility Assessment of Microalgal Carbon Dioxide Sequestration Technology with Photobioreactor and Solar Collector. *Biosystems Engineering* 95 (4): 597–606. <https://doi.org/10.1016/j.biosystemseng.2006.08.005>
- Orefice, I., Chandrasekaran, R., Smerilli, A., Corato, F., Caruso, T., Casillo, A., Corsaro, M.M., Piaz, F.D., Ruban, A. V., Brunet, C. (2016) Light-induced changes in the photosynthetic physiology and biochemistry in the diatom *Skeletonema marinoi*. *Algal Research* 17 (2016): 1–13. <https://doi.org/10.1016/j.algal.2016.04.013>
- Pauw, N. De, Morales, J., Persoone, G. (1984) Mass culture of microalgae in aquaculture systems: Progress and constraints. *Hydrobiologia* 116 (1): 121–34. <https://doi.org/10.1007/BF00027650>
- Pauw, N. De, Verboven, J., Claus, C. (1983) Large-scale microalgae production for nursery rearing of marine bivalves. *Aquacultural Engineering* 2 (1): 27–47. [https://doi.org/10.1016/0144-8609\(83\)90004-3](https://doi.org/10.1016/0144-8609(83)90004-3)
- Pennarun, A.L., Prost, C., Haure, J., Demaimay, M. (2003) Comparison of two microalgal diets. 2. Influence on odorant composition and organoleptic qualities of raw oysters (*Crassostrea gigas*).

- Journal of Agricultural and Food Chemistry* 51 (7): 2011–18. <https://doi.org/10.1021/jf020549c>
- Pennington, F., Guillard, R.R.L., Liaaen-Jensen, S. (1988) Carotenoid Distribution Patterns in Bacillariophyceae (Diatoms). *Biochemical Systematics and Ecology* 16 (7–8): 589–92. [https://doi.org/10.1016/0305-1978\(88\)90067-1](https://doi.org/10.1016/0305-1978(88)90067-1)
- Pérez, L., Salgueiro, J.L., González, J., Parralejo, A.I., Maceiras, R., Cancela, Á. (2017) Scaled up from indoor to outdoor cultures of *Chaetoceros gracilis* and *Skeletonema costatum* microalgae for biomass and oil production. *Biochemical Engineering Journal* 127 (October): 180–87. <https://doi.org/10.1016/j.bej.2017.08.016>
- Pleonsil, P., Soogarun, S., Suwanwong, Y. (2013) Anti-oxidant activity of holo- and apo-c-phycoyanin and their protective effects on human erythrocytes. *International Journal of Biological Macromolecules* 60: 393–98. <https://doi.org/10.1016/j.ijbiomac.2013.06.016>
- Sakshaug, E., Andresen, K. (1986) Effect of light regime upon growth rate and chemical composition of a clone of *Skeletonema costatum* from the Trondheimsfjord, Norway . *Journal of Plankton Research* 8 (4): 619–37. <https://doi.org/10.1093/plankt/8.4.619>
- Saravanan, V., Godhe, A. (2010) Genetic heterogeneity and physiological variation among seasonally separated clones of *Skeletonema marinoi* (Bacillariophyceae) in the Gullmar Fjord, Sweden. *European Journal of Phycology* 45 (2): 177–90. <https://doi.org/10.1080/09670260903445146>
- Sarno, D., Kooistra, W.H.C.F., Balzano, S., Hargraves, P.E., Zingone, A. (2007) Diversity in the genus *Skeletonema* (Bacillariophyceae): III. Phylogenetic position and morphological variability of *Skeletonema costatum* and *Skeletonema grevillei*, with the description of *Skeletonema ardens* sp. nov. *Journal of Phycology* 43 (1): 156–70. <https://doi.org/10.1111/j.1529-8817.2006.00305.x>
- Sarno, D., Kooistra, W.H.C.F., Medlin, L.K., Percopo, I., Zingone, A. (2005) Diversity in the genus *Skeletonema* (Bacillariophyceae). II. An assessment of the taxonomy of *S. costatum*-like species with the description of four new species. *Journal of Phycology* 41 (1): 151–76. <https://doi.org/10.1111/j.1529-8817.2005.04067.x>
- Sasireka, G., Muthuvelayudham, R. (2015) Effect of Salinity and Iron Stressed on Growth and Lipid Accumulation In *Skeletonema costatum* for Biodiesel Production. *Research Journal of Chemical Sciences* 5 (5): 69–72
- Sathyendranath, S., Lazzara, L., Prieur, L. (1987) Variations in the spectral values of specific absorption of phytoplankton. *Limnology and Oceanography* 32 (2): 403–15. <https://doi.org/10.4319/lo.1987.32.2.0403>
- Schwenk, D., Seppälä, J., Spilling, K., Virkki, A., Tamminen, T., Oksman-Caldentey, K.M., Rischer, H. (2013) Lipid content in 19 brackish and marine microalgae: Influence of growth phase, salinity and temperature. *Aquatic Ecology* 47 (4): 415–24. <https://doi.org/10.1007/s10452-013-9454-z>
- Servel, M.-O., Claire, C., Derrien, A., Coiffard, L., Roeck-Holtzhauer, Y. De (1994) Fatty acid composition of some marine microalgae. *Phytochemistry* 36 (3): 691–93. [https://doi.org/https://doi.org/10.1016/S0031-9422\(00\)89798-8](https://doi.org/https://doi.org/10.1016/S0031-9422(00)89798-8)
- Sharmin, T., Monirul Hasan, C.M., Aftabuddin, S., Rahman, M.A., Khan, M. (2016) Growth, Fatty Acid, and Lipid Composition of Marine Microalgae *Skeletonema costatum* Available in Bangladesh Coast: Consideration as Biodiesel Feedstock . *Journal of Marine Biology* 2016: 1–8. <https://doi.org/10.1155/2016/6832847>
- Shih, S.-R., Tsai, K.-N., Li, Y.-S., Chueh, C.-C., Chan, E.-C. (2003) Inhibition of enterovirus 71-induced apoptosis by allophycoyanin isolated from a blue-green alga *Spirulina platensis*. *Journal of Medical Virology* 70 (1): 119–25. <https://doi.org/10.1002/jmv.10363>

- Sijtsma, L., Swaaf, M.E. De (2004) Biotechnological production and applications of the ω -3 polyunsaturated fatty acid docosahexaenoic acid. *Applied Microbiology and Biotechnology* 64 (2): 146–53. <https://doi.org/10.1007/s00253-003-1525-y>
- Silva Benavides, A.M., Torzillo, G., Kopecký, J., Masojídek, J. (2013) Productivity and biochemical composition of *Phaeodactylum tricornutum* (Bacillariophyceae) cultures grown outdoors in tubular photobioreactors and open ponds. *Biomass and Bioenergy* 54 (0): 115–22. <https://doi.org/10.1016/j.biombioe.2013.03.016>
- Slocombe, S.P., Zhang, Q., Ross, M., Anderson, A., Thomas, N.J., Lapresa, Á., Rad-Menéndez, C., et al. (2015) Unlocking nature's treasure-chest: Screening for oleaginous algae. *Scientific Reports* 5: 1–17. <https://doi.org/10.1038/srep09844>
- Smith, G.J., Zimmerman, R.C., Alberte, R.S. (1992) Molecular and physiological responses of diatoms to variable levels of irradiance and nitrogen availability: Growth of *Skeletonema costatum* in simulated upwelling conditions. *Limnology and Oceanography* 37 (5): 989–1007. <https://doi.org/10.4319/lo.1992.37.5.0989>
- Soletchnik, P., Moine, O. Le, Gouilletquer, P., Geairon, P., Razet, D., Faury, N., Fouché, D., Robert, S. (2001) Optimisation of the traditional pacific cupped oyster (*Crassostrea gigas* thunberg) culture on the french atlantic coastline: Autumnal fattening in semi-closed ponds. *Aquaculture* 199 (1–2): 73–91. [https://doi.org/10.1016/S0044-8486\(01\)00554-3](https://doi.org/10.1016/S0044-8486(01)00554-3)
- Song, N.Q., Wang, N., Lu, Y., Zhang, J.R. (2016) Temporal and spatial characteristics of harmful algal blooms in the Bohai Sea during 1952–2014. *Continental Shelf Research* 122: 77–84. <https://doi.org/10.1016/j.csr.2016.04.006>
- Stoermer, E.F., Julius, M.L. (2003) Centric Diatoms. In *Freshwater Algae of North America*, edited by Wehr, J.D. and Sheath, R.G. 559–94. Aquatic Ecology. Burlington: Academic Press. <https://doi.org/https://doi.org/10.1016/B978-012741550-5/50016-7>
- Stolz, P., Obermayer, B. (2005) Manufacturing Microalgae for Skin Care. *The International Magazine of Cosmetic Technology* 120 (3): 6
- Strasser, R.J., Tsimilli-Michael, M., Srivastava, A. (2004) Analysis of the Chlorophyll a Fluorescence Transient. In *Chlorophyll a Fluorescence: A Signature of Photosynthesis*, edited by Papageorgiou, G.C. and Govindjee, G: 321–62. https://doi.org/10.1007/978-1-4020-3218-9_12
- Taraldsvik, M., Myklestad, S. (2000) The effect of pH on growth rate, biochemical composition and extracellular carbohydrate production of the marine diatom *Skeletonema costatum*. *European Journal of Phycology* 35 (2): 189–94. <https://doi.org/10.1080/09670260010001735781>
- Tian, Y., Mingjiang, Z., Peiyuan, Q. (2002) Combined effects of temperature, irradiance and salinity on growth of diatom *Skeletonema costatum*. *Chinese Journal of Oceanology and Limnology* 20 (3): 237–43. <https://doi.org/10.1007/BF02848852>
- Tredici, M.R. (2007) Mass Production of Microalgae: Photobioreactors. In *Handbook of Microalgal Culture: Biotechnology and Applied Phycology*, edited by Richmond, A. 178–214. John Wiley & Sons, Ltd. <https://doi.org/10.1002/9780470995280.ch9>
- Tredici, M.R. (2010) Photobiology of microalgae mass cultures: Understanding the tools for the next green revolution. *Biofuels* 1 (1): 143–62. <https://doi.org/10.4155/bfs.09.10>
- Tredici, M.R., Rodolfi, L., Biondi, N., Bassi, N., Sampietro, G. (2016) Techno-economic analysis of microalgal biomass production in a 1-ha Green Wall Panel (GWP®) plant. *Algal Research* 19: 253–63. <https://doi.org/10.1016/j.algal.2016.09.005>

- Uddin, S.A., Zafar, M. (2007) Mass Culture of Marine Diatom *Skeletonema costatum* (Greville) Cleve Collected From the Bay of Bengal. *Pakistan Journal of Marine Sciences* 16 (1): 3338
- Vejrazka, C., Janssen, M., Streefland, M., Wijffels, R.H. (2012) Photosynthetic efficiency of *Chlamydomonas reinhardtii* in attenuated, flashing light. *Biotechnology and Bioengineering* 109 (10): 2567–74. <https://doi.org/10.1002/bit.24525>
- Vidoudez, C., Pohnert, G. (2012) Comparative metabolomics of the diatom *Skeletonema marinoi* in different growth phases. *Metabolomics* 8 (4): 654–69. <https://doi.org/10.1007/s11306-011-0356-6>
- Wang, H., Mi, T., Zhen, Y., Jing, X., Liu, Q., Yu, Z. (2017) Metacaspases and programmed cell death in *Skeletonema marinoi* in response to silicate limitation. *Journal of Plankton Research* 39 (4): 729–43. <https://doi.org/10.1093/plankt/fbw090>
- Watanabe, Y., Hall, D.O. (1996) Photosynthetic CO₂ conversion technologies using a photobioreactor incorporating microalgae - energy and material balances. *Energy Conversion and Management* 37 (6–8): 1321–26. [https://doi.org/10.1016/0196-8904\(95\)00340-1](https://doi.org/10.1016/0196-8904(95)00340-1)
- White, S., Anandraj, A., Bux, F. (2011) PAM fluorometry as a tool to assess microalgal nutrient stress and monitor cellular neutral lipids. *Bioresource Technology* 102 (2): 1675–82. <https://doi.org/10.1016/j.biortech.2010.09.097>
- Widayati Putri, T., Raya, I., Natsir, H., Mayasari, E. (2017) Fatty Acid Extraction of *Skeletonema costatum* by using Avocado Oil as Solvent and its Application as an Anti-Aging Cream. *Oriental Journal of Chemistry* 33: 2848–57. <https://doi.org/10.13005/ojc/330618>
- Wu, H., Gao, K. (2009) Ultraviolet radiation stimulated activity of extracellular carbonic anhydrase in the marine diatom *Skeletonema costatum*. *Functional Plant Biology* 36 (2): 137–43. <https://doi.org/10.1071/FP08172>
- Wu, H., Gao, K., Wu, H. (2009) Responses of a marine red tide alga *Skeletonema costatum* (Bacillariophyceae) to long-term UV radiation exposures. *Journal of Photochemistry and Photobiology B: Biology* 94 (2): 82–86. <https://doi.org/10.1016/j.jphotobiol.2008.10.005>
- Yamada, M., Otsubo, M., Tsutsumi, Y., Mizota, C., Iida, N., Okamura, K., Kodama, M., Umehara, A. (2013) Species diversity of the marine diatom genus *Skeletonema* in Japanese brackish water areas. *Fisheries Science* 79 (6): 923–34. <https://doi.org/10.1007/s12562-013-0671-0>
- Yongmanitchai, W., Ward, O.P. (1991) Growth of and omega-3 fatty acid production by *Phaeodactylum tricornutum* under different culture conditions. *Applied and Environmental Microbiology* 57 (2): 419–25. <https://doi.org/http://dx.doi.org/>

7. Additional data

7.1 Chapter 4.1 Results Algem[®] trials

7.1.1 Inoculum concentration

Growth parameters recorded during the duplicate of Algem[®] trial, testing inoculum concentration (Figure 7.1). The second trial lasted only seven days. The decline in nutrients showed a constant growth of the cultures. The F_0 value increased for all of the samples but the one with the highest inoculum concentration. It might be, that a cell concentration was reached by this culture, that is too dense and impairs the development of the culture.

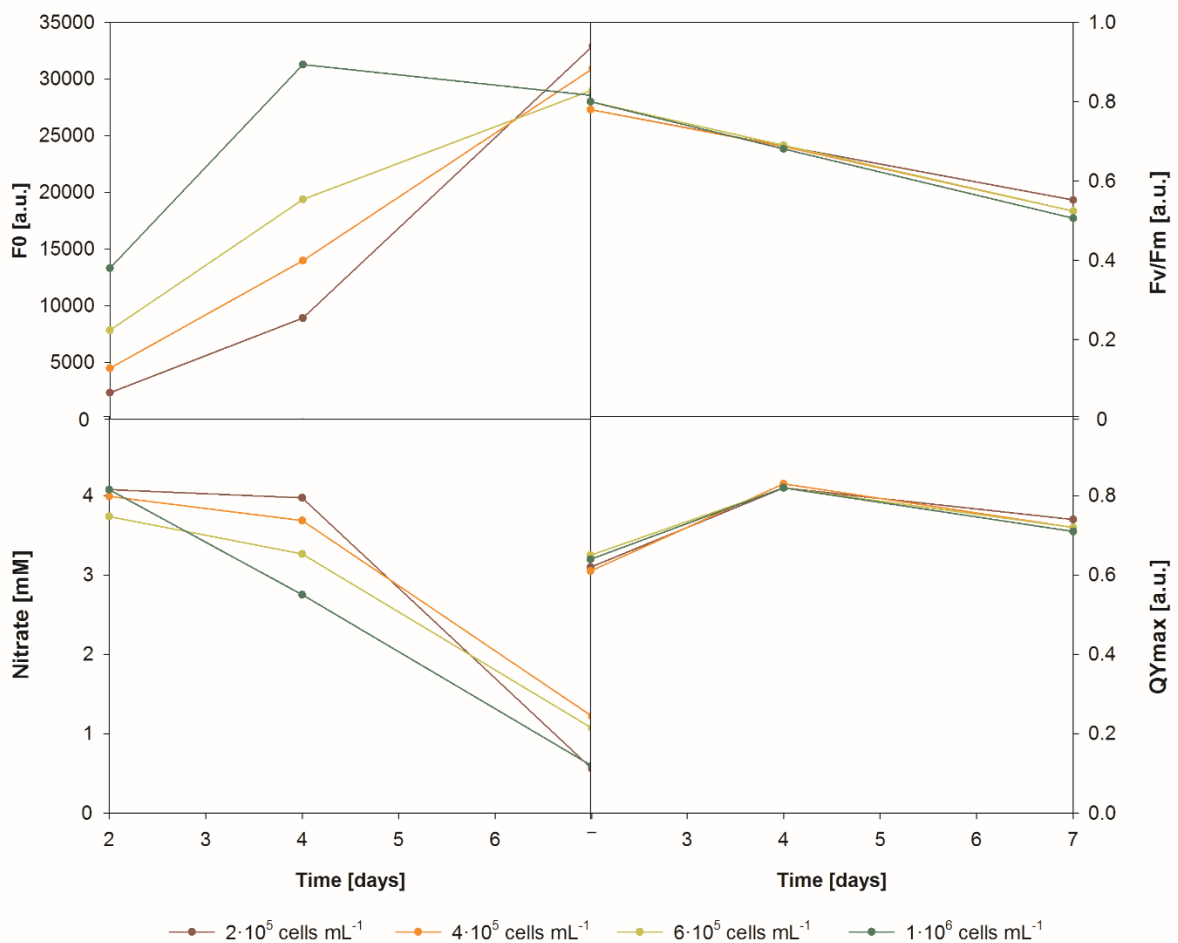


Figure 7.1 Overview of different fluorometry values and nitrate concentration in the medium in the second trial regarding the inoculum concentration. Analyses were done at the second, fourth and seventh day, at the end of the experiment. Species: *Skeletonema sp. SKC0218*.

7.1.2 pH setpoint

The recorded nitrate concentration declined similar for all four cultures, indicating a growth unaffected by the different pH setpoints (Figure 7.2). The same was observed for the photosynthetic efficiency. The F_0 values of the two cultures with pH 8.0 and 8.5 decline from the fourth to the sixth day, whereas the values of the cultures at pH 7.0 and 7.5 still increase.

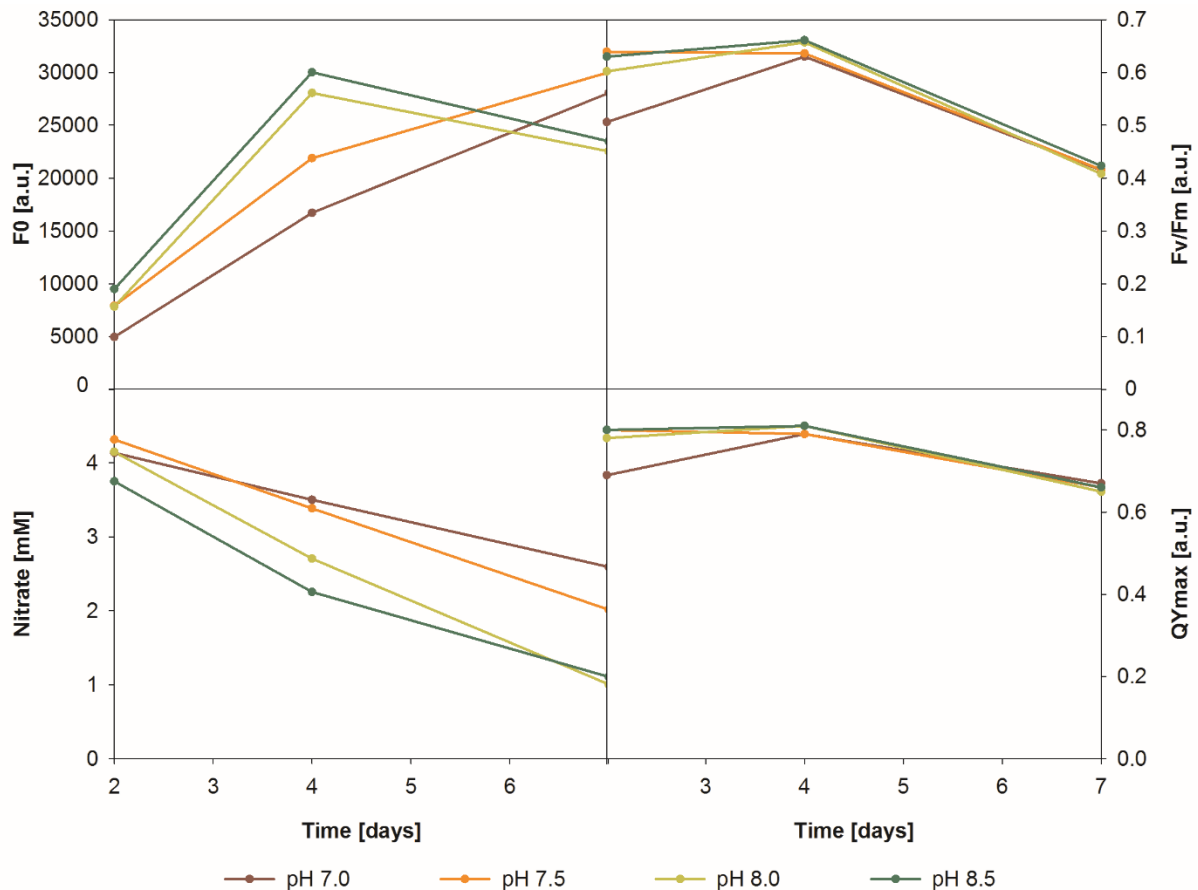


Figure 7.2 Different parameters recorded at the second, fourth, and eighth day (the end) of the second experiment testing different pH setpoints on the growth of *Skeletonema sp. SKC0218*.

7.2 Chapter 4.2 *Skeletonema sp.* in outdoor cultivation

7.2.1 Growth development flat panel photobioreactors in relation to meteorological data

The first inoculated outdoor PBRs in the season 2018/19 were 100 L FP PBR, meteorological conditions during the time of cultivation and growth of the cultures is shown in Figure 7.3. The cells of *Skeletonema sp. SKM0116* (FP 1B), died after 8 days. The culture of *Skeletonema sp. SKM0118* (FP 1A) showed poor growth and the cells developed weakly, after 14 days dead cells dominated the culture. The apparent DW rose between day eleven and 13, as it was calculated from the OD, also cell residues might have attributed to this value.

The average and maximum radiation during the observed timespan were $658 \mu\text{mol m}^{-2} \text{s}^{-1}$ and $1563 \mu\text{mol m}^{-2} \text{s}^{-1}$. The average temperature during this time was $25.16 \text{ }^\circ\text{C}$, with a maximum value of $30.78 \text{ }^\circ\text{C}$, which might have affected the growth of the *Skeletonema* culture. Under similar meteorological conditions, *Skeletonema* was cultivated outdoors in 80 L PBRs. The group measured radiation values of approximately $1294 \mu\text{mol m}^{-2} \text{s}^{-1}$ and average temperatures of $25 \pm 9 \text{ }^\circ\text{C}$ (Pérez et al. 2017).

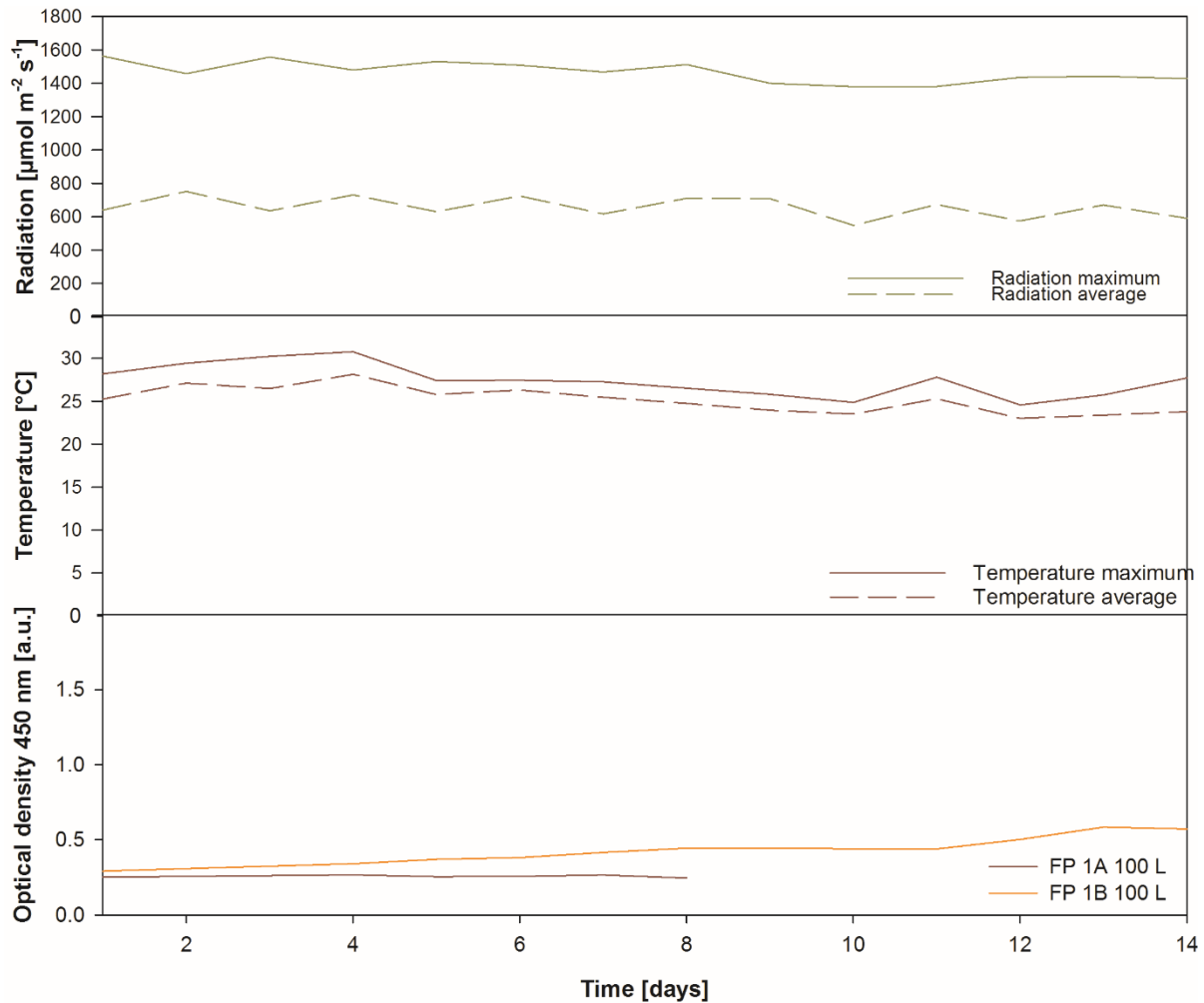


Figure 7.3 Meteorological data and growth of *Skeletonema* sp. in flat panel photobioreactors with 100 L volume. Timespan: 21.09.-4.10.2019, strains of *Skeletonema* sp: FP 1A: SKM0118, FP 1B: SKM0116.

The cultures came from controlled laboratory conditions to an outdoor environment. The cells had to adapt immediately to the changed light and radiation conditions. The cells might have suffered from the high sunlight intensity and did not grow in this case, as the same species is able to grow under comparable weather conditions. Still, another strain might be more suitable for the given weather conditions.

7.2.2 Scale up process of the tubular photobioreactor #2

Figure 7.4 shows another example of a scale-up process carried out for the inoculation of a tubular PBR. At the 14.12.2018 a 100 L FP was inoculated and after six days transferred to a 1000 L FP. After one week this FP was split into two 800 L FPs, growing for another seven days. One was split into two FPs of 1000 L, the other to two 800 L FPs. Thereafter, 900 L from a FP and the complete culture of the other three (in the sum 3500 L) were used to inoculate the tubular reactor at the 10.01.2019, after a scale-up process of 28 days in total. During the

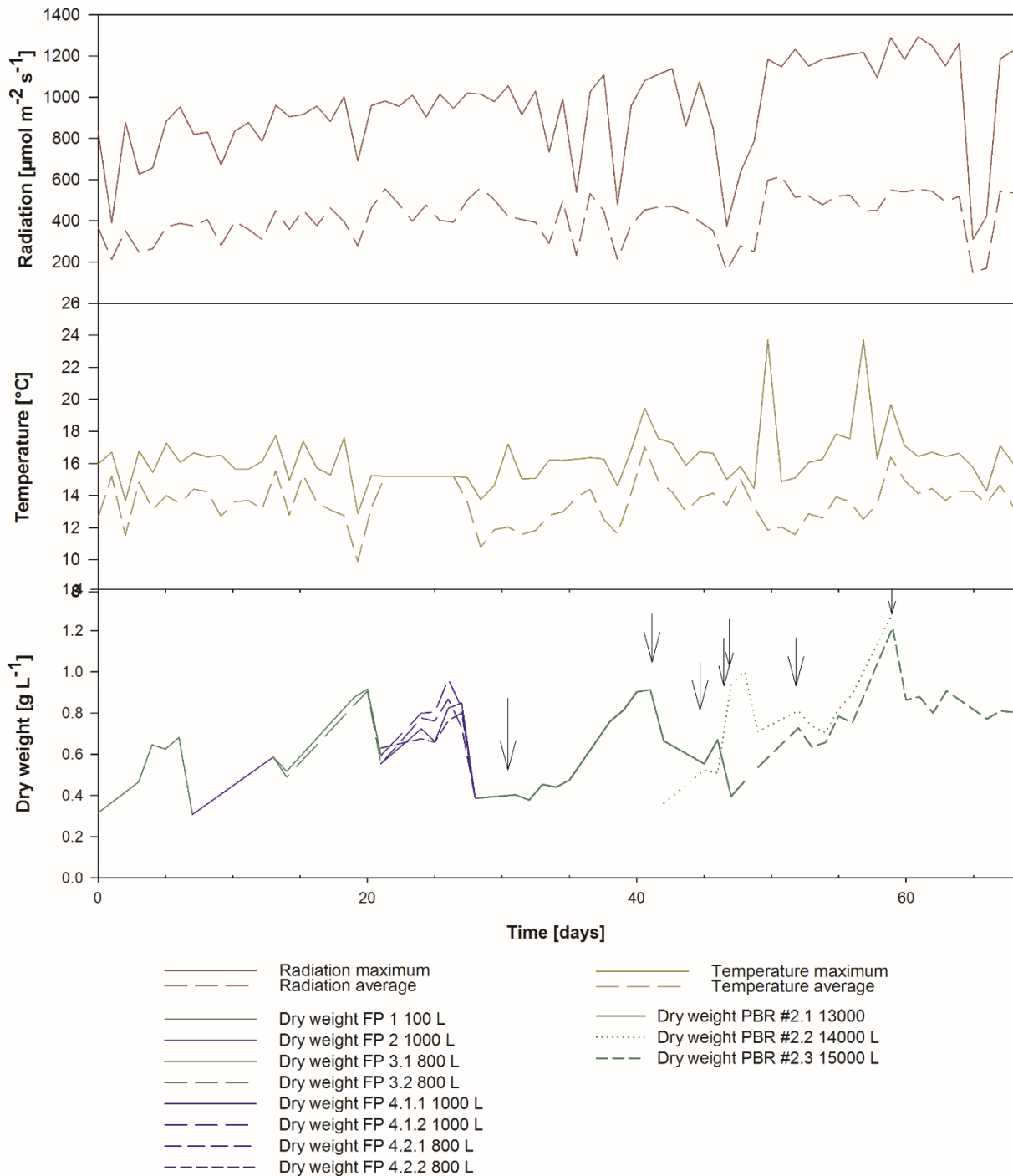


Figure 7.4 Scale-up process of *Skeletonema* sp. SKC0218 in a tubular photobioreactor. Growth of flat panel and tubular photobioreactors in dry weight, meteorological observations are displayed in parallel. Timespan: 14.12.2018-21.02.2019. Arrows refer to operational changes and are listed in Table 7.3.

production, culture volume from the first two tubular PBRs was used to inoculate each one other tubular PBR. Culture renewal and addition is indicated in the graph by arrows and explained in Table 7.3. The lifetime of the three reactors were 21, 18 and 20 days, respectively.

Table 7.1 Operations in production management of tubular photobioreactor #2.

Day	Date	Reactor	Operation
31	14.01.2019	#2.1	+2000 L
41	30.01.2019	#2.1	4000 L renewed, inoculum for #2.2
46	4.02.2019	#2.1	5000 L renewed
48	6.02.2019	#2.2	6500 L renewed, inoculum for #2.3
49	7.02.2019	#2.2	+2000 L
53	11.02.2019	#2.2	2000 L renewed
53	11.02.2019	#2.3	3000 L renewed
61	13.02.2019	#2.3	5000 L renewed

The average radiation and temperature in the observed period were $415 \mu\text{mol m}^{-2} \text{s}^{-1}$ and $13.60 \text{ }^\circ\text{C}$, respectively, as maximum values $1293 \mu\text{mol m}^{-2} \text{s}^{-1}$ and $23.17 \text{ }^\circ\text{C}$ were respectively observed.

From every tubular PBR of the fourth generation, culture was harvested and also used for the inoculation of another reactor, after that the same volume was always replaced by water and medium. At the end of the lifetime the complete culture volume was harvested. Biomass harvested from #4.2 ET03, after 18 days in the respective reactor, was biochemically analysed and the properties can be found in the section below.

Table 7.2 Yielded biomass, specific growth rate and productivity parameters from the a tubular photobioreactor. The productivity parameters were calculated from the harvest yield in the production period. Species: *Skeletonema sp. SKC0218*

Parameter	PBR #2.2	PBR #2.2	PBR #2.3
Reactor volume [L]	13000-15000	13000-15000	15000
Sum produced biomass [kg]	10.12	19.44	18.34
Average growth rate [d^{-1}]	0.062 ± 0.038	0.120 ± 0.128	0.076 ± 0.055
Maximum growth rate [d^{-1}]	0.117	0.426	0.155
Total volumetric productivity [$\text{g L}^{-1} \text{d}^{-1}$]	0.028	0.072	0.034
Total areal productivity [$\text{g m}^{-2} \text{d}^{-1}$]	1.225	3.160	1.512

The maximal growth rates of the three reactors are in the same range as the average values observed in the Algem[®] experiment; ranging from 0.12 to 0.43 d^{-1} . The average values match the average values estimated for the complete production season of 0.217 d^{-1} . Even tough growing consecutively in a short time frame of one month, the values between the three reactors differ a lot. Reactor #2.2 seems to be the most productive of the three. This indicates other influences impairing the other reactors, such as nutrient level and contamination, which might have influenced the growth of *Skeletonema sp.* in the given production.

7.3 Chapter 4.3 Large-scale production of *Skeletonema sp.* in tubular photobioreactors

7.3.1 Overview over large-scale production during the season 2018/19

The table contains the changes in production management, operated in the tubular PBRs for *Skeletonema sp.* production (graph in figure 4.18).

Table 7.3 Changes in operation management in tubular photobioreactors, referring to arrows in figure 4.18.

Day	Date	Reactor	Operation
21	9.01.2019	#1	2000 L renewed
26	14.01.2019	#2.1	+2000 L
29	17.01.2019	#1	6000 L renewed
42	30.01.2019	#2.1	4000 L renewed, inoculum for #2.2
47	4.02.2019	#2.1	5000 L renewed
49	6.02.2019	#2.2	7000 L renewed, inoculum for #2.3
50	7.02.2019	#2.2	+2000 L
54	11.02.2019	#2.2	2000 L renewed
54	11.02.2019	#2.3	3000 L renewed
56	13.02.2019	#2.3	5000 L renewed
61	18.02.2019	#3	+500 L
63	20.02.2019	#3	+2500 L
70	27.02.2019	#3	5000 L renewed
85	13.03.2019	#5	+7000 L
86	15.03.2019	#4	3000 L renewed
90	19.03.2019	#5	+1000 L
92	21.03.2019	#5	4500 L renewed
110	8.04.2019	#6	+1000 L
115	13.04.2019	#7	+500 L
120	18.04.2019	#7	2000 L renewed

7.4 Chapter 4.4 Fluorometer evaluation of the large-scale production

7.4.1 Fluorometer evaluation in a 1000 L flat panel photobioreactor

Figure 7.5 describes the growth of a FP PBR and gives meteorological data, cultivation parameters and measures fluorometry data in parallel. During the 5. and 16.04. the radiation and temperature are constantly increasing, with local minima at the 7. and 10.04., the third and sixth day of the observation. The overall average values were $638 \mu\text{mol m}^{-2} \text{s}^{-1}$ and $15.55 \text{ }^\circ\text{C}$, for radiation and temperature respectively.

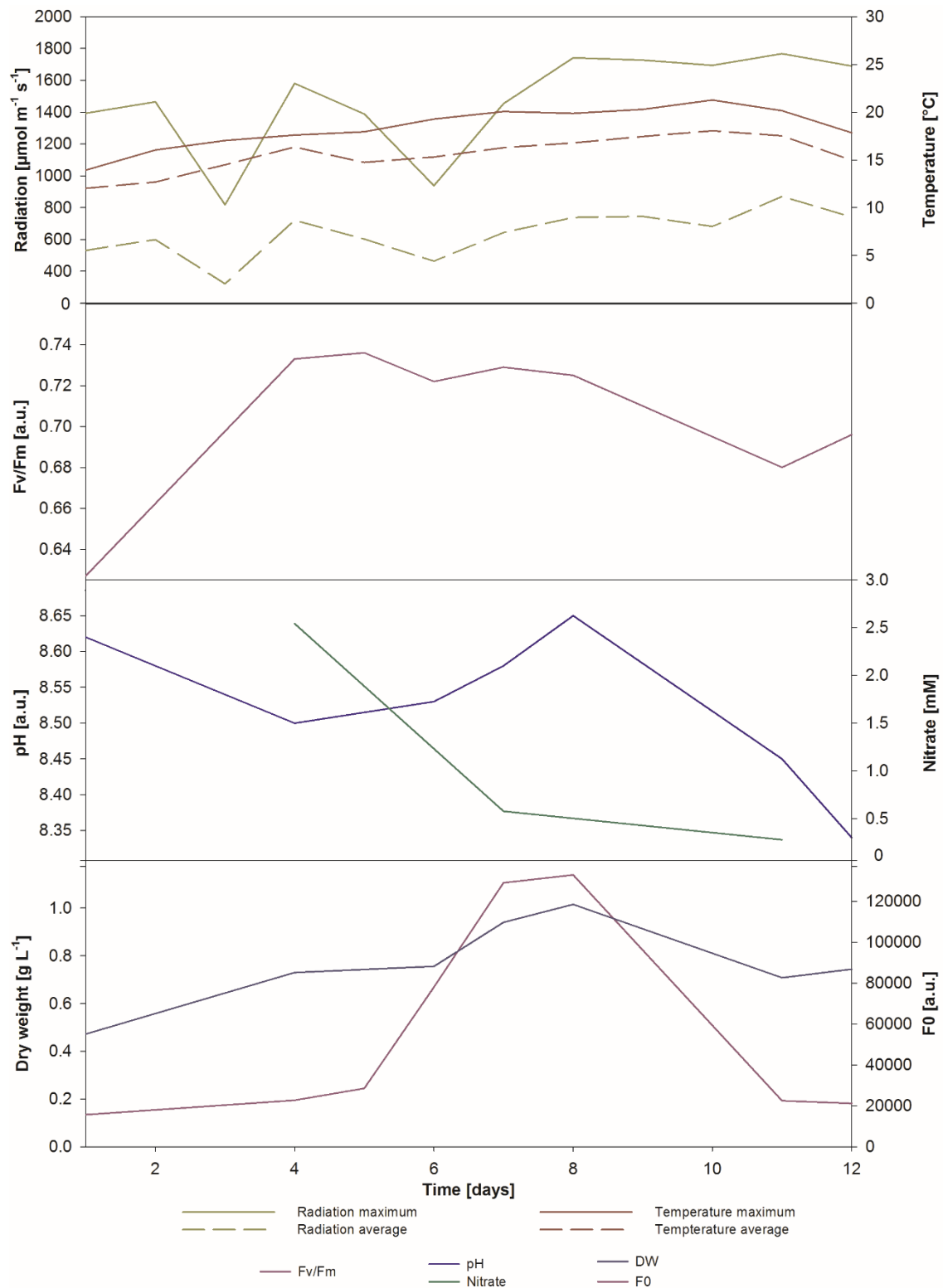


Figure 7.5 Growth and culture parameters of *Skeletonema* sp. SKC0119 between 5. and 16.04.2019 in a 1000 L flat panel photobioreactors. Meteorological and fluorometry values are shown in parallel.

The biomass is constantly increasing until the eighth day of the cultivation, especially the F_0 value drops considerably at this day. At the same time, the F_v/F_m shows a slight decrease, indicating stress on the culture. The stress might derive from a badly regulated nutrient supply. On the 11.4. and 15.4., the nitrate concentration was only 0.58 and 0.28 mM, respectively. After measuring the nitrate concentration, the culture was again supplied with nutrients to achieve a theoretical nitrate

concentration of 4 mM. But the lack of nutrients might have impaired the culture within a short time. The unexpected high nutrient demand might be due to increasing radiation and temperature from the 11.4. on. As the F_v/F_m still is above 0.68, it is assumed, that no photoinhibition was observed, but a lack of nutrients slowed the growth of the culture. The lowest F_v/F_m in the present observation was the first measured value with 0.63. The culture was only transferred a day before to the PBR, so it can be said that the culture was in a period of adaption. Also, the culture was most diluted in the beginning of the observation and less capable for photoprotection.

7.4.2 Fluorometer evaluation of a 100 L and a 1000 L flat panel photobioreactor

In figure 7.6 the growth development of two FP PBR are shown. The 100 L PBR GW 13B was inoculated at the 17.4.2019 with 25 L volume from culture grown in the laboratory. The 1000 L PBR GW 12 was inoculated at the 16.4.2019 with 100 L volume of a 12-day old culture. The overall average values of the meteorological data were $599 \mu\text{mol m}^{-2} \text{s}^{-1}$ and $16.43 \text{ }^\circ\text{C}$ for radiation and temperature, respectively.

The smaller PBR started with a biomass concentration of 0.28 g L^{-1} , which can be considered as diluted. The culture didn't grow fast, which is reflected by low nutrient consume, the nitrate value never fell under 2.22 mM. The value of F_v/F_m fell from 0.69, a value in a range representing a well physiological state, to 0.45 at the 23.4.2019. The sunlight might have affected the culture, as coming from indoor conditions not already adapted to the higher irradiation. Within the observed timespan, the F_v/F_m does not surpass 0.55, which is still considered as a stressed culture. It is assumed, that the meteorological values in the given period are not suitable for a diluted culture.

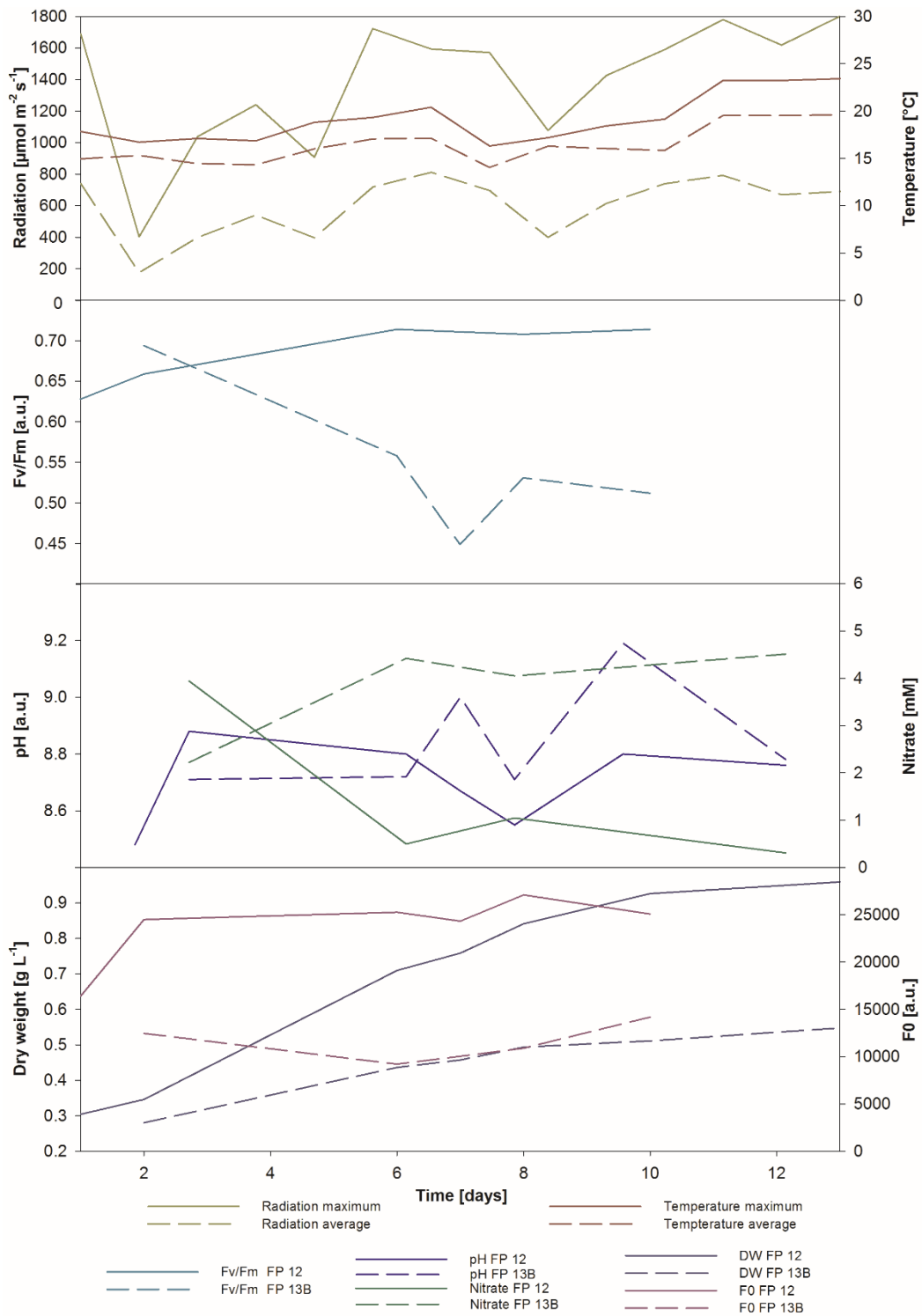


Figure 7.6 Growth observations, culture parameters and fluorometry results shown in parallel with meteorological data. In both flat panel photobioreactors *Skeletonema sp. SKC0119* was grown. Timespan: 16.-29.04.2019. FP 12: 1000 L flat panel photobioreactor, inoculated with culture of another outdoor photobioreactor. FP 13B: 100 L flat panel photobioreactor, inoculated with laboratory culture.

The culture in the 1000 L FP PBR was inoculated from a culture, already growing outdoors for 12 days. The initial biomass concentration was 0.30 g L^{-1} , only slightly higher than in the newly inoculated smaller PBR. Despite the similar biomass concentration, the F_v/F_m value is with 0.63 much higher and in a range not considered as severely impaired. F_v/F_m increases after the first day constantly to a value of up to 0.71. The culture showed a quick growth, doubled the biomass concentration after six days by

reaching 0.71 g L^{-1} and at the end of the observation after thirteen days 0.96 g L^{-1} . The nutrient consume was strong, as the nitrate concentration fell from 3.94 to 0.50 mM within four days. The nutrients were supplied after each measurement to a nitrate concentration of up to 4 mM . The nutrients were consumed, leaving 1.05 mM nitrate after two days, accompanied by an increasing biomass concentration.

7.4.3 Fluorometer evaluation of culture in a tubular photobioreactor

The tubular reactor was maintained from the 28.2. to 20.3.2019, whereas the fluorometry evaluation considers the 11.-20.3.2019 (figure 7.7). In this timespan, the average radiation and temperature were $679 \mu\text{mol m}^{-2} \text{ s}^{-1}$ and $16.63 \text{ }^\circ\text{C}$, which are the highest average values for the observation of one reactor, maximum values were recorded as $1596 \mu\text{mol m}^{-2} \text{ s}^{-1}$ and $21.76 \text{ }^\circ\text{C}$.

The culture didn't develop well, considering the biomass development. This is supported by the of the F_v/F_m value, that from initially 0.67 is constantly decreasing to 0.51 . Also the F_0 value decreased notably from day seven, showing a reduced amount of biomass with good photosynthetic properties. The stress on the culture cannot be explained by the given pH value and nutrient supply, as both were regulated in a suitable range. The constant elevated temperatures as well as aging might have influenced the cultures physiological state and growth.

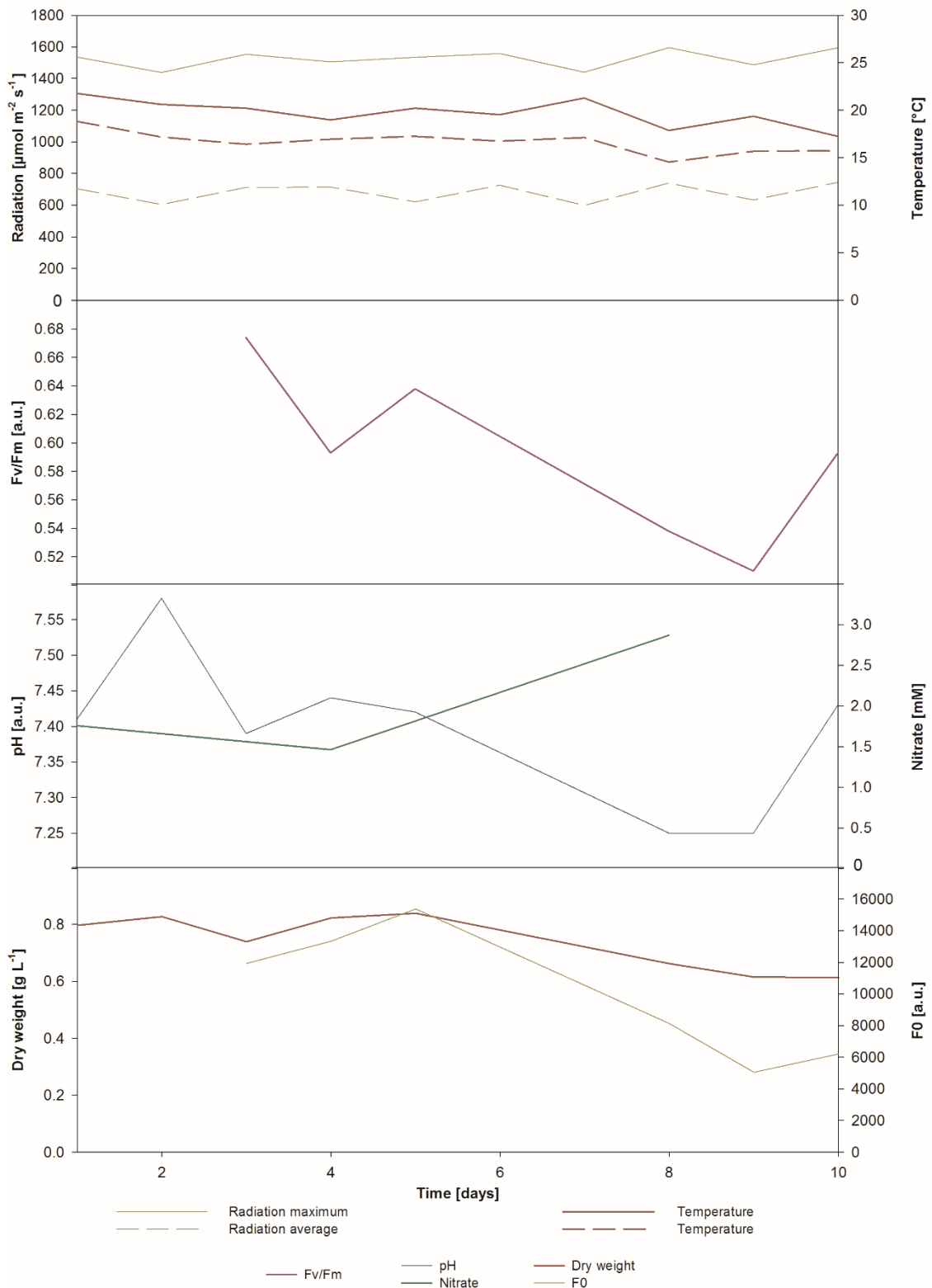


Figure 7.7 Growth development of *Skeletonema sp. SKC0218* in a tubular photobioreactor. Culture growth and fluorometer parameters are shown as well as meteorological data. Timespan: 11.-20.3.2019

7.5 Chapter: biochemical analysis

A biochemical analysis was done for samples from the large-scale production, listed in Table 7.4. The separate results of the carbohydrate, protein, lipid and total ash analysis for each sample is given in Figure 7.8, Figure 7.9, Figure 7.10 and Figure 7.11

7.5.1 Origin of samples

Table 7.4 Origin of *Skeletonema sp. SKC0218* biomass samples in biochemical analysis. A consecutive number was given to the samples, the date of harvest and originating photobioreactor are given, the growth stage of the culture at the time of harvest was estimated according to growth development.

Label	Date of sampling	Reactor	Growth phase
1	11.02.2019	#2.1	exponential
2	12.02.2019	#2.3	decline
3	27.02.2019	#3	exponential
4	04.03.2019	#3	stationary
5	13.03.2019	#3	decline
6	15.03.2019	#4	stationary
7.1	20.03.2019	#4	decline
7.2	20.03.2019	#4	decline
8	25.03.2019	#5	decline
FP	28.03.2019	FP	
9.1	15.04.2019	#6	decline
9.2	15.04.2019	#6	decline
10	18.04.2019	#7	exponential
11	26.04.2019	#7	decline

7.5.2 Carbohydrate content of *Skeletonema sp. biomass*

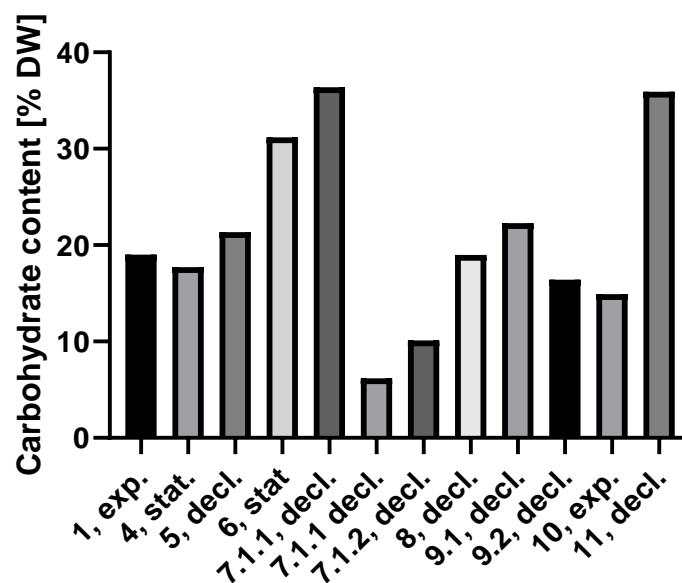


Figure 7.8 Carbohydrate content in *Skeletonema sp. SKC0218* biomass expressed as percentage of dry weight. The samples were all collected from tubular photobioreactors during the season 2018/19, kept under the same culture conditions. The label indicates a sequential number of the sample, a second number refers to the batch of centrifugation, a third number to the batch of lyophilization. The growth stage of the culture in the moment of sampling is indicated: exp.: exponential phase, stat.: stationary phase, decl.: decline phase.

7.5.3 Protein content of *Skeletonema sp.* biomass

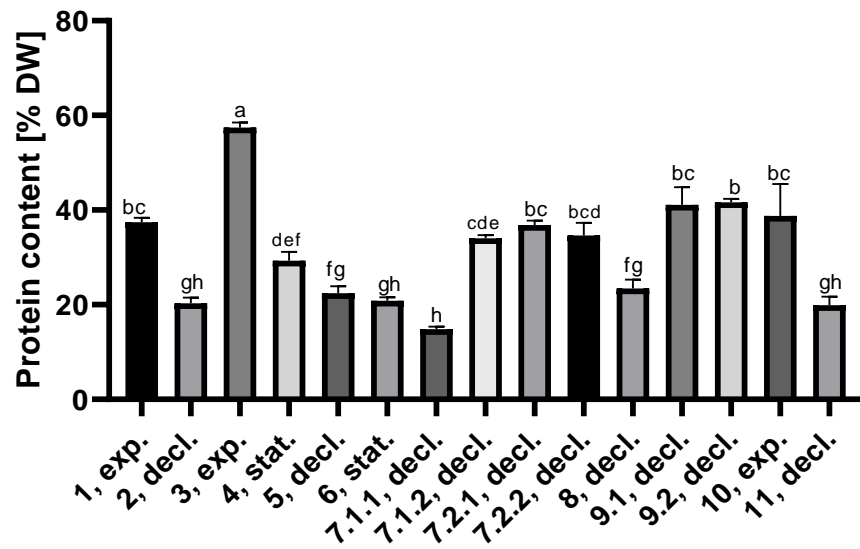


Figure 7.9 Protein content in percentage of dry weight in *Skeletonema sp.* SKC0218 biomass. Significant differences are expressed with different letters. The label indicates a sequential number of the sample, a second number refers to the batch of centrifugation, a third number to the batch of lyophilization. The growth stage of the culture in the moment of sampling is indicated: exp.: exponential phase, stat.: stationary phase, decl.: decline phase.

7.5.4 Lipid content of *Skeletonema sp.* biomass

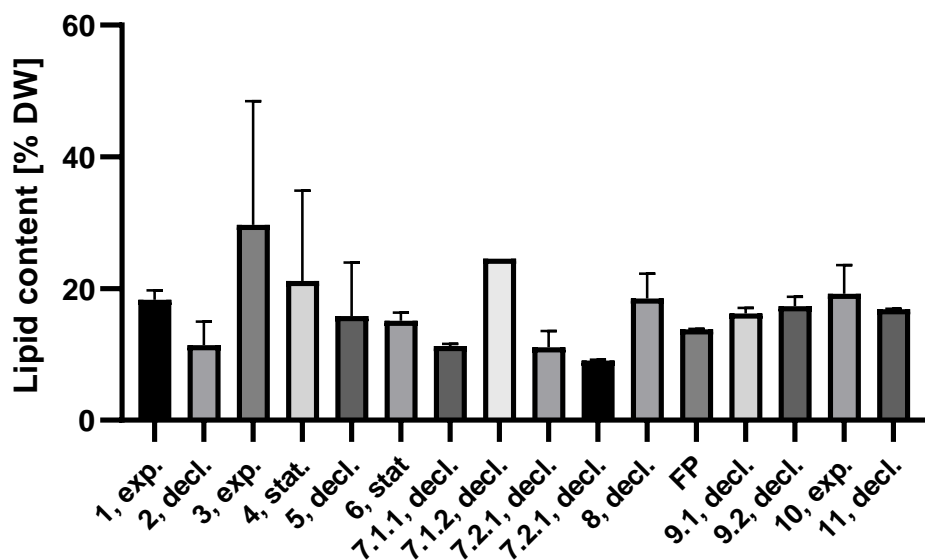


Figure 7.10 Lipid content in *Skeletonema sp.* SKC0218 biomass, harvested from cultures in outdoor production. The label indicates a sequential number of the sample, a second number refers to the batch of centrifugation, a third number to the batch of lyophilization. The growth stage of the culture in the moment of sampling is indicated: exp.: exponential phase, stat.: stationary phase, decl.: decline phase. FP: the sample derives from flat panel photobioreactors. There are no significant differences between the values.

7.5.5 Ash content of *Skeletonema sp. biomass*

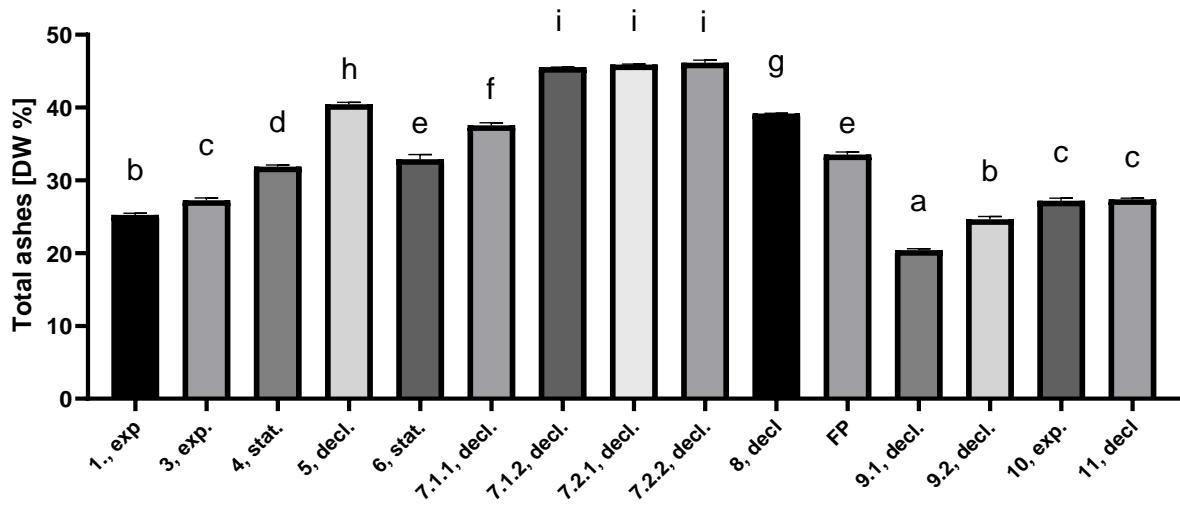


Figure 7.11 The total ashes (inorganic matter) in the biomass of *Skeletonema sp. SKC0218* is expressed in percentage of dry weight. The label indicates a sequential number of the sample, a second number refers to the batch of centrifugation, a third number to the batch of lyophilization. The growth stage of the culture in the moment of sampling is indicated: exp.: exponential phase, stat.: stationary phase, decl.: decline phase. FP: the sample derives from flat panel photobioreactors. There are no significant differences between the values.